

# TECHNICAL SPECIFICATION



**Metallic communication cable test methods –  
Part 4-1: Electromagnetic compatibility (EMC) – Introduction to electromagnetic  
screening measurements**

IECNORM.COM : Click to view the full PDF of IEC TS 62153-4-1:2014



## THIS PUBLICATION IS COPYRIGHT PROTECTED

Copyright © 2014 IEC, Geneva, Switzerland

All rights reserved. Unless otherwise specified, no part of this publication may be reproduced or utilized in any form or by any means, electronic or mechanical, including photocopying and microfilm, without permission in writing from either IEC or IEC's member National Committee in the country of the requester. If you have any questions about IEC copyright or have an enquiry about obtaining additional rights to this publication, please contact the address below or your local IEC member National Committee for further information.

IEC Central Office  
3, rue de Varembe  
CH-1211 Geneva 20  
Switzerland

Tel.: +41 22 919 02 11  
Fax: +41 22 919 03 00  
[info@iec.ch](mailto:info@iec.ch)  
[www.iec.ch](http://www.iec.ch)

### About the IEC

The International Electrotechnical Commission (IEC) is the leading global organization that prepares and publishes International Standards for all electrical, electronic and related technologies.

### About IEC publications

The technical content of IEC publications is kept under constant review by the IEC. Please make sure that you have the latest edition, a corrigenda or an amendment might have been published.

#### IEC Catalogue - [webstore.iec.ch/catalogue](http://webstore.iec.ch/catalogue)

The stand-alone application for consulting the entire bibliographical information on IEC International Standards, Technical Specifications, Technical Reports and other documents. Available for PC, Mac OS, Android Tablets and iPad.

#### IEC publications search - [www.iec.ch/searchpub](http://www.iec.ch/searchpub)

The advanced search enables to find IEC publications by a variety of criteria (reference number, text, technical committee,...). It also gives information on projects, replaced and withdrawn publications.

#### IEC Just Published - [webstore.iec.ch/justpublished](http://webstore.iec.ch/justpublished)

Stay up to date on all new IEC publications. Just Published details all new publications released. Available online and also once a month by email.

#### Electropedia - [www.electropedia.org](http://www.electropedia.org)

The world's leading online dictionary of electronic and electrical terms containing more than 30 000 terms and definitions in English and French, with equivalent terms in 14 additional languages. Also known as the International Electrotechnical Vocabulary (IEV) online.

#### IEC Glossary - [std.iec.ch/glossary](http://std.iec.ch/glossary)

More than 55 000 electrotechnical terminology entries in English and French extracted from the Terms and Definitions clause of IEC publications issued since 2002. Some entries have been collected from earlier publications of IEC TC 37, 77, 86 and CISPR.

#### IEC Customer Service Centre - [webstore.iec.ch/csc](http://webstore.iec.ch/csc)

If you wish to give us your feedback on this publication or need further assistance, please contact the Customer Service Centre: [csc@iec.ch](mailto:csc@iec.ch).

IECNORM.COM : Click to view the full text IEC 1534-1:2014

# TECHNICAL SPECIFICATION



---

**Metallic communication cable test methods –  
Part 4-1: Electromagnetic compatibility (EMC) – Introduction to electromagnetic  
screening measurements**

INTERNATIONAL  
ELECTROTECHNICAL  
COMMISSION

PRICE CODE

**XD**

ICS 33.100

ISBN 978-2-8322-1311-7

**Warning! Make sure that you obtained this publication from an authorized distributor.**

## CONTENTS

FOREWORD.....	7
1 Scope.....	9
2 Normative references .....	9
3 Symbols interpretation.....	10
4 Electromagnetic phenomena.....	12
5 The intrinsic screening parameters of short cables .....	14
5.1 General.....	14
5.2 Surface transfer impedance, $Z_T$ .....	14
5.3 Capacitive coupling admittance, $Y_C$ .....	14
5.4 Injecting with arbitrary cross-sections .....	16
5.5 Reciprocity and symmetry.....	16
5.6 Arbitrary load conditions .....	16
6 Long cables – coupled transmission lines.....	16
7 Transfer impedance of a braided wire outer conductor or screen .....	24
8 Test possibilities.....	30
8.1 General.....	30
8.2 Measuring the transfer impedance of coaxial cables .....	30
8.3 Measuring the transfer impedance of cable assemblies.....	31
8.4 Measuring the transfer impedance of connectors .....	31
8.5 Calculated maximum screening level .....	31
9 Comparison of the frequency response of different triaxial test set-ups to measure the transfer impedance of cable screens .....	36
9.1 General.....	36
9.2 Physical basics .....	36
9.2.1 Triaxial set-up.....	36
9.2.2 Coupling equations.....	38
9.3 Simulations.....	40
9.3.1 General .....	40
9.3.2 Simulation of the standard and simplified methods according to EN 50289-1-6, IEC 61196-1 (method 1 and 2) and IEC 62153-4-3 (method A).....	40
9.3.3 Simulation of the double short circuited methods .....	46
9.4 Conclusion.....	54
10 Background of the shielded screening attenuation test method (IEC 62153-4-4).....	54
10.1 General.....	54
10.2 Objectives.....	55
10.3 Theory of the triaxial measuring method .....	55
10.4 Screening attenuation .....	60
10.5 Normalised screening attenuation .....	62
10.6 Measured results .....	63
10.7 Comparison with absorbing clamp method .....	65
10.8 Practical design of the test set-up .....	66
10.9 Influence of mismatches .....	67
10.9.1 Mismatch in the outer circuit .....	67
10.9.2 Mismatch in the inner circuit .....	69

11	Background of the shielded screening attenuation test method for measuring the screening effectiveness of feed-throughs and electromagnetic gaskets (IEC 62153-4-10).....	72
11.1	General.....	72
11.2	Theoretical background of the test Fixtures and their equivalent circuit.....	73
11.3	Pictures and measurement results .....	76
11.3.1	Characteristic impedance uniformity .....	76
11.3.2	Measurements of shielding effectiveness.....	78
11.3.3	Calculation of transfer impedance.....	80
11.4	Calculation of screening attenuation for feed-through when the transfer impedance $Z_T$ is known .....	82
12	Background of the shielded screening attenuation test method for measuring the screening effectiveness of RF connectors and assemblies (IEC 62153-4-7).....	83
12.1	Physical basics .....	83
12.1.1	Surface transfer impedance $Z_T$ .....	83
12.1.2	Screening attenuation $a_S$ .....	84
12.1.3	Coupling attenuation $a_C$ .....	84
12.1.4	Coupling transfer function.....	84
12.1.5	Relationship between length and screening measurements .....	85
12.2	Tube in tube set-up (IEC 62153-4-7).....	86
12.2.1	General .....	86
12.2.2	Procedure.....	86
12.2.3	Measurements and simulations.....	88
12.2.4	Influence of contact resistances.....	89
	Bibliography.....	91
	Figure 1 – Total electromagnetic field $(\vec{E}_t, \vec{H}_t)$ .....	12
	Figure 2 – Defining and measuring screening parameters – A triaxial set-up.....	13
	Figure 3 – Equivalent circuit for the testing of $Z_T$ .....	15
	Figure 4 – Equivalent circuit for the testing of $Y_C = j \omega C_T$ .....	15
	Figure 5 – Electrical quantities in a set-up that is matched at both ends .....	16
	Figure 6 – The summing function $S\{L \cdot f\}$ for near and far end coupling .....	20
	Figure 7 – Transfer impedance of a typical single braid screen .....	20
	Figure 8 – The effect of the summing function on the coupling transfer function of a typical single braid screen cable .....	21
	Figure 9 – Calculated coupling transfer functions $T_n$ and $T_f$ for a single braid – $Z_F = 0$ .....	21
	Figure 10 – Calculated coupling transfer functions $T_n$ and $T_f$ for a single braid – $\text{Im}(Z_T)$ is positive and $Z_F = +0,5 \times \text{Im}(Z_T)$ at high frequencies.....	22
	Figure 11 – Calculated coupling transfer functions $T_n$ and $T_f$ for a single braid – $\text{Im}(Z_T)$ is negative and $Z_F = -0,5 \times \text{Im}(Z_T)$ at high frequencies.....	23
	Figure 12 – $L \cdot S$ : the complete length dependent factor in the coupling function $T$ .....	24
	Figure 13 – Transfer impedance of typical cables .....	25
	Figure 14 – Magnetic coupling in the braid – Complete flux.....	26
	Figure 15 – Magnetic coupling in the braid – Left-hand lay contribution .....	26
	Figure 16 – Magnetic coupling in the braid – Right-hand lay contribution .....	26
	Figure 17 – Complex plane, $Z_T = \text{Re } Z_T + j \text{Im } Z_T$ , frequency $f$ as parameter.....	27
	Figure 18 – Magnitude (amplitude), $ Z_T(f) $ .....	27

Figure 19 – Typical $Z_T$ (time) step response of an overbraided and underbraided single braided outer conductor of a coaxial cable .....	28
Figure 20 – $Z_T$ equivalent circuits of a braided wire screen .....	29
Figure 21 – Comparison of signal levels in a generic test setup .....	32
Figure 22 – Triaxial set-up for the measurement of the transfer impedance $Z_T$ .....	36
Figure 23 – Equivalent circuit of the triaxial set-up .....	37
Figure 24 – Simulation of the frequency response for $g$ .....	41
Figure 25 – Simulation of the frequency response for $g$ .....	41
Figure 26 – Simulation of the frequency response for $g$ .....	42
Figure 27 – Simulation of the frequency response for $g$ .....	42
Figure 28 – Simulation of the 3 dB cut off wavelength ( $L/\lambda_1$ ) .....	43
Figure 29 – Interpolation of the simulated 3 dB cut off wavelength ( $L/\lambda_1$ ) .....	43
Figure 30 – 3 dB cut-off frequency length product as a function of the dielectric permittivity of the inner circuit (cable) .....	44
Figure 31 – Measurement result of the normalised voltage drop of a single braid screen on a solid PE dielectric in the triaxial set-up .....	45
Figure 32 – Measurement result of the normalised voltage drop of a single braid screen on a foam PE dielectric in the triaxial set-up .....	46
Figure 33 – Triaxial set-up (measuring tube), double short circuited method .....	47
Figure 34 – Simulation of the frequency response for $g$ of a cable having solid PE dielectric ( $\epsilon_{r1}=2,3$ ) .....	48
Figure 35 – Simulation of the frequency response for $g$ of a cable having foamed PE dielectric ( $\epsilon_{r1}=1,6$ ) .....	48
Figure 36 – Simulation of the frequency response for $g$ of a cable having foamed PE dielectric ( $\epsilon_{r1}=1,3$ ) .....	49
Figure 37 – Simulation of the frequency response for $g$ of a cable having PVC dielectric ( $\epsilon_{r1}=5$ ) .....	49
Figure 38 – Interpolation of the simulated 3 dB cut off wavelength ( $L/\lambda_1$ ) .....	50
Figure 39 – 3 dB cut-off frequency length product as a function of the dielectric permittivity of the inner circuit (cable) .....	51
Figure 40 – Simulation of the frequency response for $g$ .....	52
Figure 41 – Interpolation of the simulated 3 dB cut off wavelength ( $L/\lambda_1$ ) .....	53
Figure 42 – 3 dB cut-off frequency length product as a function of the dielectric permittivity of the inner circuit (cable) .....	53
Figure 43 – Definition of transfer impedance .....	55
Figure 44 – Definition of coupling admittance .....	55
Figure 45 – Triaxial measuring set-up for screening attenuation .....	56
Figure 46 – Equivalent circuit of the triaxial measuring set-up .....	56
Figure 47 – Calculated voltage ratio for a typical braided cable screen .....	58
Figure 48 – Calculated periodic functions for $\epsilon_{r1} = 2,3$ and $\epsilon_{r2} = 1,1$ .....	59
Figure 49 – Calculated voltage ratio-typical braided cable screen .....	59
Figure 50 – Equivalent circuit for an electrical short part of the length $\Delta l$ and negligible capacitive coupling .....	61
Figure 51 – $a_s$ of single braid screen, cable type RG 58, $L = 2$ m .....	63
Figure 52 – $a_s$ of single braid screen, cable type RG 58, $L = 0,5$ m .....	64
Figure 53 – $a_s$ of cable type HF 75 0,7/4,8 2YCY (solid PE dielectric) .....	64

Figure 54 – $a_s$ of cable type HF 75 1,0/4,8 02YCY (foam PE dielectric) .....	65
Figure 55 – $a_s$ of double braid screen, cable type RG 223 .....	65
Figure 56 – Schematic for the measurement of the screening attenuation $a_s$ .....	67
Figure 57 – Short circuit between tube and cable screen of the CUT .....	67
Figure 58 – Triaxial set-up, impedance mismatches .....	68
Figure 59 – Calculated voltage ratio including multiple reflections caused by the screening case .....	69
Figure 60 – Calculated voltage ratio including multiple reflections caused by the screening case .....	69
Figure 61 – Attenuation and return loss of a self-made 50 $\Omega$ to 5 $\Omega$ impedance matching adapter .....	70
Figure 62 – equivalent circuit of a load resistance connected to a source .....	71
Figure 63 – Cross-sectional sketch of a typical feed-through configuration .....	72
Figure 64 – Cross-sectional sketch of the test fixture with a feed-through connector (a) and EMI gasket (b) under test .....	73
Figure 65 – Equivalent circuit of the test fixture .....	74
Figure 66 – Two-port network .....	74
Figure 67 – TDR measurement of the test-fixture with inserted “Teflon-through” sample .....	76
Figure 68 – TDR step response from A (Input)-port of test fixture with inserted “Teflon-through” sample .....	77
Figure 69 – TDR step response from B (Output)-port of test fixture with inserted “Teflon-through” sample .....	77
Figure 70 – S-parameter measurement (linear sweep): “Teflon-through” sample .....	78
Figure 71 – S-parameter measurement (logarithmic sweep): “Teflon-through” sample .....	78
Figure 72 – S parameter test setup .....	79
Figure 73 – TDR test setup .....	79
Figure 74 – Test fixture assembled .....	79
Figure 75 – Detailed views of the contact area the test fixture and the secondary side of side opened .....	80
Figure 76 – $S_{21}$ measurements .....	80
Figure 77 – $S_{21}$ measurements of “Teflon-through” and “Sonnenscheibe” feed-through .....	81
Figure 78 – Transfer impedance $Z_T$ of a “Sonnenscheibe” feed-through based on the $S_{21}$ measurement in Figure 77 .....	81
Figure 79 – measurements of a conducting plastic gasket .....	82
Figure 80 – $Z_T$ of the conducting plastic gasket based on the $S_{21}$ measurement in Figure 79 .....	82
Figure 81 – equivalent circuit of the set-up without DUT .....	82
Figure 82 – equivalent circuit of the set-up with inserted DUT .....	83
Figure 83 – Definition of $Z_T$ .....	84
Figure 84 – Calculated coupling transfer function .....	85
Figure 85 – Principle test set-up for measuring the screening attenuation of a connector with the tube in tube procedure .....	86
Figure 86 – Principle test set-up for measuring the coupling attenuation of screened balanced or multipin connectors .....	87
Figure 87 – Principle preparation of balanced or multiconductor connectors for coupling attenuation .....	87

Figure 88 – Comparison of simulation and measurement, linear frequency scale ..... 88

Figure 89 – Comparison of simulation and measurement, logarithmic frequency scale ..... 89

Figure 90 – Measurement of the coupling attenuation of a CAT6 connector ..... 89

Figure 91 – Contact resistances of the test set-up ..... 90

Figure 92 – Equivalent circuit of the test set-up with contact resistances ..... 90

Table 1 – The coupling transfer function  $T$  (coupling function)<sup>a</sup> ..... 18

Table 2 – Screening effectiveness of cable test methods for surface transfer impedance  $Z_T$  ..... 34

Table 3 – Load conditions of the different set-ups ..... 38

Table 4 – Parameters of the different set-ups ..... 40

Table 5 – Cut-off frequency length product ..... 44

Table 6 – Typical values for the factor  $\nu$ , for an inner tube diameter of 40 mm and a generator output impedance of 50  $\Omega$  ..... 47

Table 7 – Cut-off frequency length product ..... 50

Table 8 – Material combinations and the factor  $n$  ..... 52

Table 9 – Cut-off frequency length product ..... 53

Table 10 – Cut-off frequency length product for some typical cables in the different set-ups ..... 54

Table 11 –  $\Delta a$  in dB for typical cable dielectrics ..... 63

Table 12 – Comparison of results of some coaxial cables ..... 66

Table 13 – Cable parameters used for simulation ..... 88

IECNORM.COM : Click to view the full PDF of IEC TS 62153-4-1:2014

## INTERNATIONAL ELECTROTECHNICAL COMMISSION

**METALLIC COMMUNICATION CABLE TEST METHODS –****Part 4-1: Electromagnetic compatibility (EMC) –  
Introduction to electromagnetic screening measurements**

## FOREWORD

- 1) The International Electrotechnical Commission (IEC) is a worldwide organization for standardization comprising all national electrotechnical committees (IEC National Committees). The object of IEC is to promote international co-operation on all questions concerning standardization in the electrical and electronic fields. To this end and in addition to other activities, IEC publishes International Standards, Technical Specifications, Technical Reports, Publicly Available Specifications (PAS) and Guides (hereafter referred to as “IEC Publication(s)”). Their preparation is entrusted to technical committees; any IEC National Committee interested in the subject dealt with may participate in this preparatory work. International, governmental and non-governmental organizations liaising with the IEC also participate in this preparation. IEC collaborates closely with the International Organization for Standardization (ISO) in accordance with conditions determined by agreement between the two organizations.
- 2) The formal decisions or agreements of IEC on technical matters express, as nearly as possible, an international consensus of opinion on the relevant subjects since each technical committee has representation from all interested IEC National Committees.
- 3) IEC Publications have the form of recommendations for international use and are accepted by IEC National Committees in that sense. While all reasonable efforts are made to ensure that the technical content of IEC Publications is accurate, IEC cannot be held responsible for the way in which they are used or for any misinterpretation by any end user.
- 4) In order to promote international uniformity, IEC National Committees undertake to apply IEC Publications transparently to the maximum extent possible in their national and regional publications. Any divergence between any IEC Publication and the corresponding national or regional publication shall be clearly indicated in the latter.
- 5) IEC itself does not provide any attestation of conformity. Independent certification bodies provide conformity assessment services and, in some areas, access to IEC marks of conformity. IEC is not responsible for any services carried out by independent certification bodies.
- 6) All users should ensure that they have the latest edition of this publication.
- 7) No liability shall attach to IEC or its directors, employees, servants or agents including individual experts and members of its technical committees and IEC National Committees for any personal injury, property damage or other damage of any nature whatsoever, whether direct or indirect, or for costs (including legal fees) and expenses arising out of the publication, use of, or reliance upon, this IEC Publication or any other IEC Publications.
- 8) Attention is drawn to the Normative references cited in this publication. Use of the referenced publications is indispensable for the correct application of this publication.
- 9) Attention is drawn to the possibility that some of the elements of this IEC Publication may be the subject of patent rights. IEC shall not be held responsible for identifying any or all such patent rights.

The main task of IEC technical committees is to prepare International Standards. In exceptional circumstances, a technical committee may propose the publication of a technical specification when

- the required support cannot be obtained for the publication of an International Standard, despite repeated efforts, or
- the subject is still under technical development or where, for any other reason, there is the future but no immediate possibility of an agreement on an International Standard.

Technical specifications are subject to review within three years of publication to decide whether they can be transformed into International Standards.

IEC/TS 62153-4-1, which is a technical specification, has been prepared by IEC technical committee 46: Cables, wires, waveguides, R.F. connectors, R.F. and microwave passive components and accessories.

This first edition of technical specification IEC/TS 62153-4-1 cancels and replaces the second edition of the technical report IEC/TR 62153-4-1 published in 2010. This edition constitutes a technical revision. This edition includes the following significant technical changes with respect to IEC/TR 62153-4-1:

- a) comparison of the frequency response of different triaxial test set-ups to measure the transfer impedance of cable screens;
- b) background of the shielded screening attenuation test method (IEC 62153-4-4);
- c) background of the shielded screening attenuation test method for measuring the screening effectiveness of feed-throughs and electromagnetic gaskets (IEC 62153-4-10);
- d) background of the shielded screening attenuation test method for measuring the screening effectiveness of RF connectors and assemblies (IEC 62153-4-7).

The text of this technical specification is based on the following documents:

Enquiry draft	Report on voting
46/465/DTS	46/492/RVC

Full information on the voting for the approval of this technical specification can be found in the report on voting indicated in the above table.

This publication has been drafted in accordance with the ISO/IEC Directives, Part 2.

A list of all parts of the IEC 62153 series, under the general title: *Metallic communication cable test methods*, can be found on the IEC website.

The committee has decided that the contents of this publication will remain unchanged until the stability date indicated on the IEC web site under "<http://webstore.iec.ch>" in the data related to the specific publication. At this date, the publication will be

- transformed into an International standard,
- reconfirmed,
- withdrawn,
- replaced by a revised edition, or
- amended.

A bilingual version of this publication may be issued at a later date.

**IMPORTANT – The 'colour inside' logo on the cover page of this publication indicates that it contains colours which are considered to be useful for the correct understanding of its contents. Users should therefore print this document using a colour printer.**

## METALLIC COMMUNICATION CABLE TEST METHODS –

### Part 4-1: Electromagnetic compatibility (EMC) – Introduction to electromagnetic (EMC) screening measurements

#### 1 Scope

This part of IEC 62153 deals with screening measurements. Screening (or shielding) is one basic way of achieving electromagnetic compatibility (EMC). However, a confusingly large number of methods and concepts is available to test for the screening quality of cables and related components, and for defining their quality. This technical specification gives a brief introduction to basic concepts and terms trying to reveal the common features of apparently different test methods. It is intended to assist in correct interpretation of test data, and in the better understanding of screening (or shielding) and related specifications and standards.

#### 2 Normative references

The following documents, in whole or in part, are normatively referenced in this document and are indispensable for its application. For dated references, only the edition cited applies. For undated references, the latest edition of the referenced document (including any amendments) applies.

IEC 60096-1:1986, *Radio-frequency cables – Part 1: General requirements and measuring methods*<sup>1</sup>

IEC 60096-4-1, *Radio-frequency cables – Part 4: Specification for superscreened cables – Section 1: General requirements and test methods*<sup>1</sup>

IEC 60169-1-3, *Radio-frequency connectors - Part 1: General requirements and measuring methods - Section Three: Electrical tests and measuring procedures: Screening effectiveness*

IEC 61196-1:2005, *Coaxial communication cables - Part 1: Generic specification - General, definitions and requirements*

IEC 61726, *Cable assemblies, cables, connectors and passive microwave components - Screening attenuation measurement by the reverberation chamber method*

IEC 62153-4-2, *Metallic communication cable test methods - Part 4-2: Electromagnetic compatibility (EMC) - Screening and coupling attenuation - Injection clamp method*

IEC 62153-4-3, *Metallic communication cable test methods - Part 4-3: Electromagnetic compatibility (EMC) - Surface transfer impedance - Triaxial method*

IEC 62153-4-4, *Metallic communication cable test methods - Part 4-4: Electromagnetic compatibility (EMC) - Shielded screening attenuation, test method for measuring of the screening attenuation as up to and above 3 GHz*

IEC 62153-4-5, *Metallic communication cables test methods - Part 4-5: Electromagnetic compatibility (EMC) - Coupling or screening attenuation - Absorbing clamp method*

---

<sup>1</sup> This publication has been withdrawn.

IEC 62153-4-6, *Metallic communication cable test methods - Part 4-6: Electromagnetic compatibility (EMC) - Surface transfer impedance - Line injection method*

IEC 62153-4-7, *Metallic communication cable test methods - Part 4-7: Electromagnetic compatibility (EMC) - Test method for measuring the transfer impedance and the screening - or the coupling attenuation - Tube in tube method*

IEC 62153-4-10, *Metallic communication cable test methods - Part 4-10: Electromagnetic compatibility (EMC) - Shielded screening attenuation test method for measuring the screening effectiveness of feed-throughs and electromagnetic gaskets double coaxial method*

IEC/TR 62152:2009, *Transmission properties of cascaded two-ports or quadripols – Background of terms and definitions*

EN 50289-1-6: 2002, *Communication cables – Specifications for test methods Part 1-6: Electrical test methods – Electromagnetic performance*

CISPR 25, *Vehicles, boats and internal combustion engines – Radio disturbance characteristics – Limits and methods of measurement for the protection of on-board receivers*

### 3 Symbols interpretation

This clause gives the interpretation of the symbols used throughout this specification.

$\alpha_1, \alpha_2$	attenuation constants of primary and secondary circuit
$a_s$	screening attenuation
$a_{sn}$	normalized screening attenuation with phase velocity difference not greater than 10 % and 150 $\Omega$ characteristic impedance of the injection line ( $Z_s=150 \Omega$ and $ \Delta v/v_1 =10\%$ or $\epsilon_{r1}/\epsilon_{r2n}=1,21$ )
$c_0$	velocity of light in free space $c_0 = 3 \times 10^8$ m/s
$C_T$	through capacitance of the braided cable
CUT	cable or component under test
$E$	e.m.f.
$f$	frequency
f	far end
$f_c$	cut-off frequency
$f_{cf}$	far end cut-off frequency
$f_{cn}$	near end cut-off frequency
$\Phi_1$	the total flux of the magnetic field induced by the disturbing current $I_1$
$\Phi'_{12}$	the direct leaking magnetic flux
$\Phi''_{12}$	complete magnetic flux in the braid
$I_1, U_1$	current and voltage in the primary circuit (feeding system)
$I_F$	current coupled by the feed through capacitance to the secondary system (measuring system)
$\epsilon_{r1}$	relative permittivity of the injection line (feeding system)
$\epsilon_{r2}$	relative permittivity of the cable (measuring system)

$L$	cable length, coupling length
$L_1$	(external) inductance of the outer circuit
$L_2$	(external) inductance of the inner circuit
$M'_{12}$	mutual inductance related to direct leakage of the magnetic flux $\Phi'_{12}$
$M''_{12}$	mutual inductance related to the magnetic flux $\Phi''_{12}$ (or $\frac{1}{2} \Phi''_{12}$ ) in the braid
	$M'_{12} = \frac{\Phi'_{12}}{j\omega I_1}$ and $M''_{12} = \frac{1}{2} \cdot \frac{\Phi''_{12}}{j\omega I_1}$
$M_T$	effective mutual inductance per unit length for braided screens
	$M_T = M'_{12} - M''_{12}$
	where $M'_{12}$ relates to the direct leakage of the magnetic flux and $M''_{12}$ relates to the magnetic flux in the braid [24]
$n$	near end
$P_1$	sending power
$P_{2f}$	far end measured power
$P_{2n}$	near end measured power
$P_r$	radiated power in the environment of the cable, which is comparable to $P_{2n} + P_{2f}$ of the absorbing clamp method of 12.4 of IEC 61196-1:1995
$P_s$	radiated power in the normalised environment of the cable under test ( $Z_s = 150 \Omega$ and $ \Delta v/v_1  = 10\%$ or $\varepsilon_{r1}/\varepsilon_{r2n} = 1,21$ )
$R$	load resistance of secondary circuit (input resistance of receiver)
$R_T$	screen resistance per unit length
$T$	coupling transfer function
$T_f$	far end transfer function
$T_n$	near end transfer function
$U'_{12}$	the disturbing voltage induced by $\Phi'_{12}$
$U''_{rh}$	the disturbing voltage induced by $\frac{1}{2} \Phi''_{12}$ of the right hand lay contribution
$U''_{lh}$	the disturbing voltage induced by $\frac{1}{2} \Phi''_{12}$ of the left hand lay contribution
$U''_{12}$	is equal to $U''_{rh}$ and $U''_{lh}$ (= the disturbing voltage induced by $\frac{1}{2} \Phi''_{12}$ )
$v$	phase velocity
$v_1$	phase velocity of the "primary" system (feeding system)
$v_2$	phase velocity of the "secondary" system (measuring system)
$v_{r1}$	relative phase velocity of the "primary" system (feeding system)
$v_{r2}$	relative phase velocity of the "secondary" system (measuring system)
$Z_1$	characteristic impedance of the "primary" system (feeding system or line (1))
$Z_2$	characteristic impedance of the cable under test (CUT) (measuring system or line (2))
$Z_{1f}$	terminating impedance of the line (1) in the far end
$Z_{2n}$	terminating impedance of the line (2) in the near end
$Z_{2f}$	terminating impedance of the line (2) in the far end (in a matched set-up
	$Z_{1f} = Z_1$ and $Z_{2n} = Z_{2f} = Z_2$ )
	$Z_{12} = \sqrt{Z_1 Z_2}$

- $Z_a$  surface impedance of the braided cable
- $Z_F$  capacitive coupling impedance per unit length
- $Z_f$  capacitive coupling impedance
- $Z_T$  surface transfer impedance per unit length
- $Z_{Th}$  transfer impedance of a tubular homogeneous screen per unit length
- $Z_t$  surface transfer impedance
- $Z_{TE_n}$  effective transfer impedance ( $= |Z_F + Z_T|$ ) per unit length in the near end
- $Z_{TE_f}$  effective transfer impedance ( $= |Z_F - Z_T|$ ) per unit length in the far end
- $Z_{TE_{n,f}}$  effective transfer impedance ( $= |Z_F \pm Z_T|$ ) per unit length in the near end or in the far end
- $Z_{TE}$  effective transfer impedance ( $= \max |Z_{TE_n}, Z_{TE_f}|$ ) per unit length
- $Z_{te}$  effective transfer impedance ( $= \max |Z_f \pm Z_t|$ )
- $Z_{ten}$  normalized effective transfer impedance of a cable  
 $(Z_1 = 150 \Omega \text{ and } |v_1 - v_2| / v_2 \leq 10 \% \text{ velocity difference in relation to velocity of CUT})$

#### 4 Electromagnetic phenomena

It is assumed that if an electromagnetic field is incident on a screened cable, there is only weak coupling between the external field and that inside, and that the cable diameter is very small compared with both the cable length and the wavelength of the incident field. The superposition of the external incident field and the field scattered by the cable yields the total electromagnetic field  $(\vec{E}_t, \vec{H}_t)$  in Figure 1. The total field at the screen's surface may be considered as the source of the coupling: electric field penetrates through apertures by electric or capacitive coupling; also magnetic fields penetrate through apertures by inductive or magnetic coupling. In addition, the induced current in the screen results in conductive or resistive coupling.

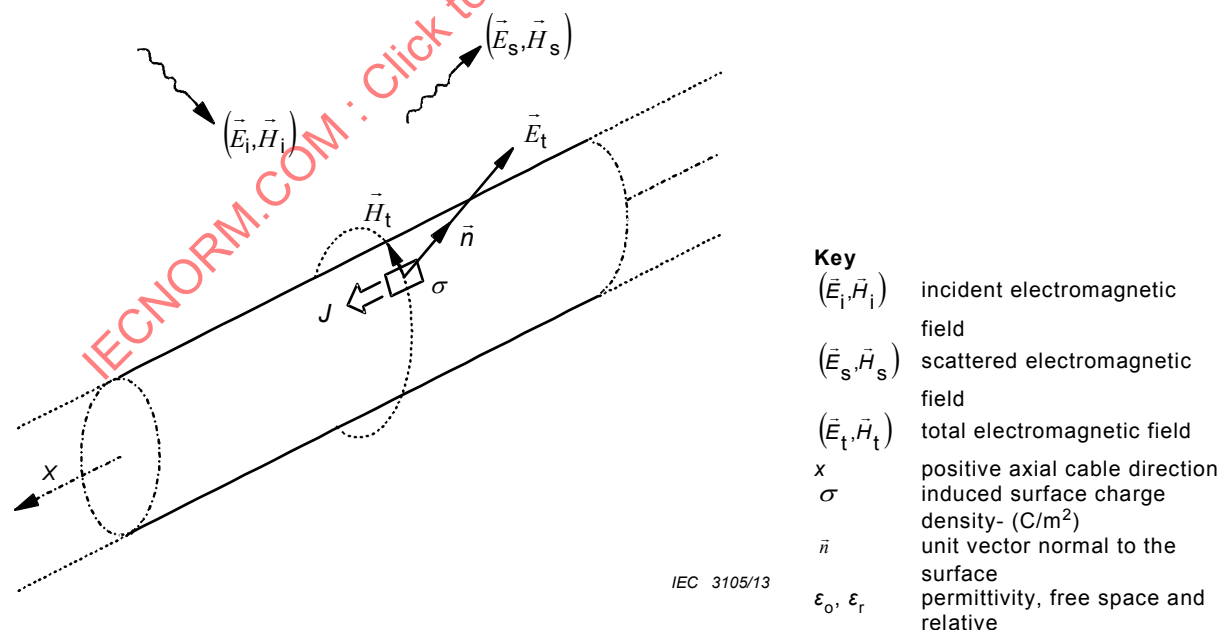


Figure 1 – Total electromagnetic field  $(\vec{E}_t, \vec{H}_t)$

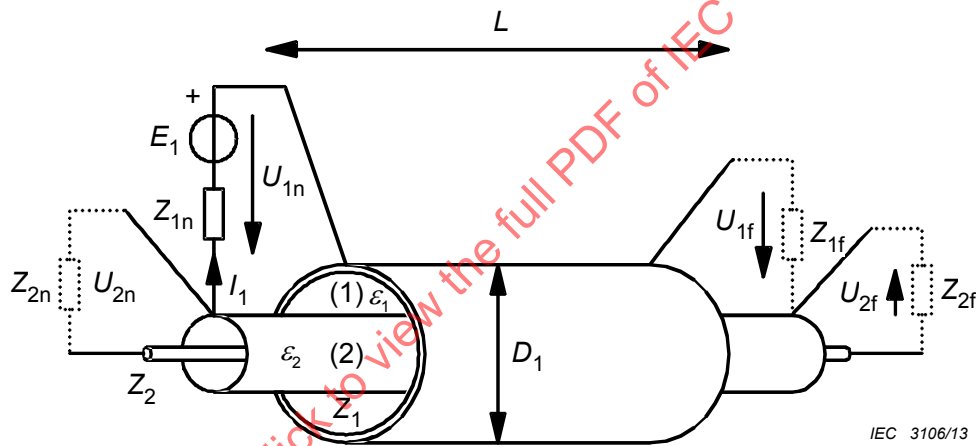
$$(\vec{E}_t, \vec{H}_t) = (\vec{E}_i, \vec{H}_i) + (\vec{E}_s, \vec{H}_s) \tag{1}$$

$$J = \vec{n} \cdot \vec{H}_t \tag{2}$$

$$\sigma = \vec{n} \cdot \vec{E}_t \epsilon_0 \epsilon_r \tag{3}$$

where the symbols are described in the key of Figure 1.

As the field at the surface of the screen is directly related to density of surface current and surface charge, the coupling may be assigned either to the total field  $(\vec{E}_t, \vec{H}_t)$  or to the surface current- and charge- densities ( $J$  and  $\sigma$ ). Consequently, the coupling into the cable may be simulated by reproducing, through any suitable means, the surface currents and charges on the screen. Because the cable diameter is assumed to be small, the higher modes may be neglected and it is possible to use an additional coaxial conductor as the injection structure, as shown in Figure 2.



IEC 3106/13

**Key (for Figures 2,3,4,5)**

- (1), (2) outer circuit (1), tube, respectively inner circuit (2), cable
- $Z_{1,2}$  characteristic impedance of the outer circuit (1), tube, respectively inner circuit (2), cable
- $\epsilon_{1,2}$  dielectric permittivity of the outer circuit (1), tube, respectively inner circuit (2), cable
- $\beta_{1,2}$  phase constant of the outer circuit (1), tube, respectively inner circuit (2), cable
- $\lambda_{1,2}$  wave length of the outer circuit (1), tube, respectively inner circuit (2), cable
- $L$  coupling length
- $D_1$  diameter of injection cylinder-tube
- $V$  voltmeter
- $A$  ammeter
- $Z_{1n}, Z_{1f}$  load resistance at the near end, respectively far end of the outer circuit (1), tube
- $Z_{2n}, Z_{2f}$  load resistance at the near end, respectively far end of the inner circuit (2), cable
- $E_1$  EMF of the generator
- $I_1, I_2$  current in the outer circuit (1), tube, respectively inner circuit (2), cable
- $U_{1n}, U_{1f}$  voltage at the near end, respectively far end of the outer circuit (1), tube
- $U_{2n}, U_{2f}$  voltage at the near end, respectively far end of the inner circuit (2), cable

**Figure 2 – Defining and measuring screening parameters – A triaxial set-up**

Figure 2 shows the concept of a triaxial set-up. The outer circuit (1) is formed by an injection cylinder-tube and the screen under test, with a characteristic impedance  $Z_1$ . The inner circuit (2) is formed by the screen under test, and centre conductor, with a characteristic impedance  $Z_2$ . The screening at the ends of circuit (2) is not shown. Observe the conditions  $Z_{1f}$ ,  $Z_{2n}$ ,  $Z_{2f}$  and  $\lambda$  in Figure 3 and Figure 4. Also note that diameter of the injection cylinder tube ( $D_1$ ) shall be much smaller than the coupling length ( $L$ ).

## 5 The intrinsic screening parameters of short cables

### 5.1 General

The intrinsic parameters refer to an infinitesimal length of cable, like the inductance or capacitance per unit length of transmission lines. Assuming electrically short cables, with  $L \ll \lambda$  which will always apply at low frequencies, the intrinsic screening parameters are defined and can be measured as indicated in the subclauses 5.2 and 5.3.

### 5.2 Surface transfer impedance, $Z_T$

As shown in Figure 3, where  $Z_{1f}$  and  $Z_{2f}$  are zero, the surface transfer impedance ( $Z_T$  in  $\Omega/m$ ) is given:

$$Z_T = \frac{U_{2n}}{I_1 \cdot L} \quad (4)$$

where

$Z_T$  is the transfer impedance,

$U_{2n}$  is the voltage at the near end of the inner circuit (2),

$L$  is the coupling length

$I_1$  is the current in the outer circuit (1).

The dependence of  $Z_T$  on frequency is not simple and is often shown by plotting  $\log Z_T$  against  $\log$  frequency. Note that the phase of  $Z_T$  may have any value, depending on braid construction and frequency range.

NOTE In circuit (2) of Figure 3, the voltmeter and short circuit may also be interchanged.

### 5.3 Capacitive coupling admittance, $Y_C$

As shown in Figure 4, where  $Z_{1f}$  and  $Z_{2f}$  are open circuit, the capacitive coupling admittance ( $Y_C$  in S/m) is given by:

$$Y_C = j \cdot \omega C_T = \frac{I_2}{U_{in} \cdot L} \quad (5)$$

where

$Y_C$  is the coupling admittance

$C_T$  is the through capacitance;

$\omega$  is the radian frequency;

$j$  is the imaginary operator

$L$  is the coupling length

$I_2$  is the current in the inner circuit (2).

The through capacitance  $C_T$  is a real capacitance and has usually a constant value up to 1 GHz and higher (with aperture  $a \ll \lambda$ ).

While  $Z_T$  is independent of the characteristics of the coaxial circuits (1) and (2),  $C_T$  is dependent on those characteristics. There are two ways of overcoming this dependence:

- a) The normalized through elastance  $K_T$  (with units of m/F) derived from  $C_T$  is independent of the size of the outer coaxial circuit (2), but it depends on its permittivity:

$$K_T = C_T / (C_1 \cdot C_2) \tag{6}$$

$$K_T \sim 1 / (\epsilon_{r1} + \epsilon_{r2}) \tag{7}$$

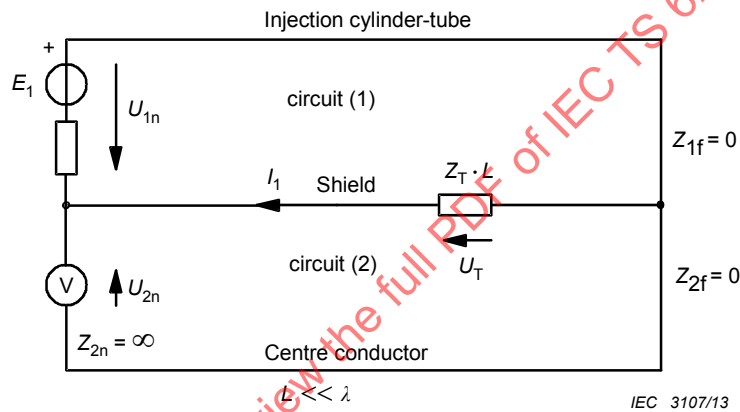
where  $C_1$  and  $C_2$  are the capacitance per unit length of the two coaxial circuits.

- b) The capacitive coupling impedance  $Z_F$  (with units of  $\Omega/m$ ) again derived from  $C_T$  is also independent of the size of the outer coaxial circuit (2) and, for practical values of  $\epsilon_{r1}$ , is only slightly dependent on its permittivity:

$$Z_F = Z_1 Z_2 Y_C = Z_1 Z_2 j \omega C_T \tag{8}$$

$$Z_F \sim \sqrt{(\epsilon_{r1} \cdot \epsilon_{r2})} / (\epsilon_{r1} + \epsilon_{r2}) \tag{9}$$

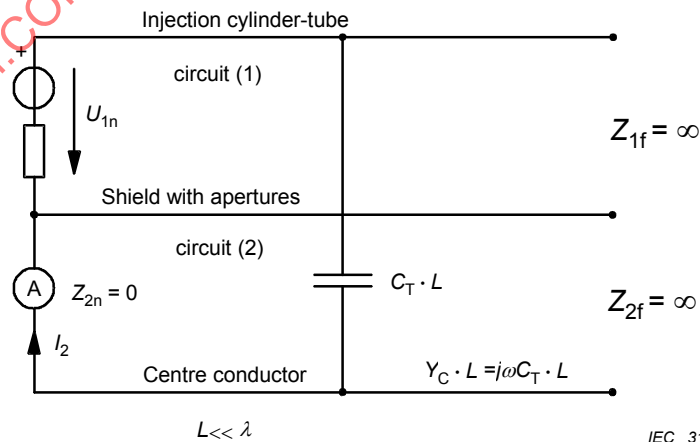
Compared with  $Z_T$ ,  $Z_F$  is usually negligible, except for open weave braids. It may, however, be significant when  $Z_{2n}$  and  $Z_{2f} \gg Z_2$  (audio circuits).



**Key**

See Figure 2.

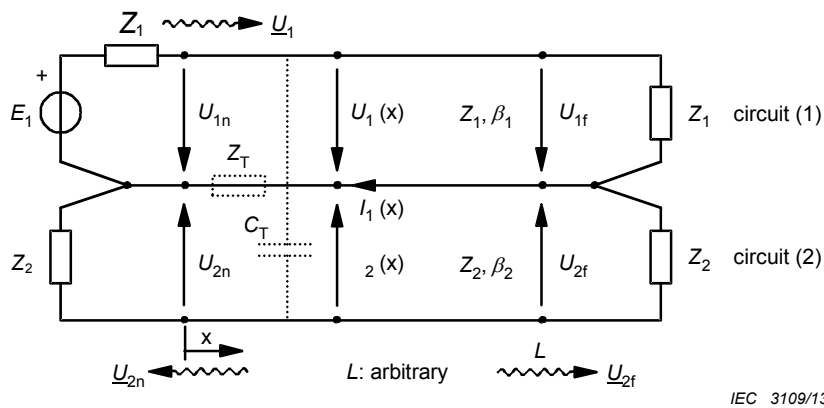
**Figure 3 – Equivalent circuit for the testing of  $Z_T$**



**Key**

See Figure 2.

**Figure 4 – Equivalent circuit for the testing of  $Y_c = j \omega C_T$**



**Key**

See Figure 2.

NOTE  $Z_T$  and  $C_T$  are distributed (not correctly shown here). The loads  $Z_1, Z_2$  at the ends may represent matched receivers.

**Figure 5 – Electrical quantities in a set-up that is matched at both ends**

**5.4 Injecting with arbitrary cross-sections**

A coaxial outer circuit (2) has been assumed so far in this report, but it is not essential because of the invariance of  $Z_T$  and  $Z_F$ . Using a wire in place of the outer cylinder, the injection circuit (2) becomes two-wire with the return via the screen of the cable under test. Obviously the charge and current distribution become non-uniform, but the results are equivalent to coaxial injection, especially if two injection lines are used opposite to each other, and may be justified for worst-case testing. Note that the IEC line injection test uses a wire.

**5.5 Reciprocity and symmetry**

Assuming linear shield materials, the measured  $Z_T$  and  $Z_F$  values will not change when interchanging the injection circuit (1) and the measuring circuit (2). Each of the two conductors of the two-line circuit can be interchanged, but in practice the set-up will have to take into account possible ground loops and coupling to the environment.

**5.6 Arbitrary load conditions**

When the circuit ends of Figure 3 and Figure 4 are not ideally a short or open circuit,  $Z_T$  and  $Z_F$  will act simultaneously. Their superposition is noticeable in the low frequency coupling of the matched circuit (1) and circuit (2) (see Figure 5 and Table 1).

**6 Long cables – coupled transmission lines**

The coupling over the whole length of the cable is obtained by summing up (integrating) the infinitesimal coupling contributions along the cable while observing the correct phase. The analysis utilizes the following assumptions and conventions:

- matched circuits considered with the voltage waves  $\underline{U}_1, \underline{U}_{2n}, \underline{U}_{2f}$ , see Figure 5,
- representation of the coupling, using the normalized wave amplitudes  $U/\sqrt{Z} [\sqrt{\text{Watt}}]$ , instead of voltage waves. i.e. the coupling transfer function, in the following denoted by "coupling function", will be defined as

$$T_n = \frac{U_{2n} / \sqrt{Z_2}}{U_1 / \sqrt{Z_1}} \quad (10)$$

$$T_f = \frac{U_{2f} / \sqrt{Z_2}}{U_1 / \sqrt{Z_1}} \quad (11)$$

The square of the coupling transfer function,  $|T|^2$ , is the ratio of the power waves travelling in circuits (2) and (1). Due to reciprocity and assuming linear screen (shield) materials,  $T$  is reciprocal, i.e. invariant with respect to the interchange of injection and measuring circuits (1) and (2). The quantity  $|1/T|^2$  or in logarithmic quantities

$$a_s = -20 \times \log_{10} |T| \quad (12)$$

may be considered as the "screening attenuation" of the cable, specific to the set-up.

Performing the straight forward calculations of coupled transmission line theory, the coupling function  $T$ , given in Table 1, is obtained. The term  $S\{L \cdot f\}$  is the "summing function"  $S$ , being dependent on  $L$  and  $f$ . (The wavy bracket just indicates that the product  $L \cdot f$  is the argument of the function  $S$  and not a factor to  $S$ ).  $S$  represents the phase effect, when summing up the infinitesimal couplings along the line, and is:

$$S_n \{L \cdot f\} = \frac{\sin \frac{\beta L \pm}{2}}{\frac{\beta L \pm}{2}} \exp\left(-j \cdot \frac{\beta L \pm}{2}\right) \quad (13)$$

$$\beta L + = (\beta_2 + \beta_1) \cdot L \quad (14)$$

$$\beta L \pm = (\beta_2 \pm \beta_1) \cdot L \quad (15)$$

$$\beta L \pm = 2\pi L f \cdot (1/v_2 \pm 1/v_1) \quad (16)$$

$$\beta L \pm = 2\pi L f \cdot (\sqrt{\varepsilon_{r2}} \pm \sqrt{\varepsilon_{r1}}) / c \quad (17)$$

subscript  $\pm$  refers to near/far end respectively; i.e. + indicates the near end and – indicates the far end;

+ refers to both near/far ends.

Note that weak coupling, i.e.  $T \ll 1$ , has been assumed. This case, including losses, is given in [1]<sup>2</sup>.

Equation (18) and the representation in Table 1 illustrate the contributions of the different parameters to the coupling function  $T$ :

$$T_n = (Z_F \pm Z_T) \cdot \frac{1}{\sqrt{Z_1 \cdot Z_2}} \cdot \frac{L}{2} \cdot S_n \{L \cdot f, \varepsilon_{r1}, \varepsilon_{r2}\} \quad (18)$$

<sup>2</sup> Figures in square brackets refer to the bibliography.

**Table 1 – The coupling transfer function  $T$  (coupling function)<sup>a</sup>**

Set-up parameters <sup>b</sup>	
$(Z_1), L, \epsilon_{r1}$	
$T_n = (Z_F \pm Z_T) \cdot \frac{1}{\sqrt{Z_1 \cdot Z_2}} \cdot \frac{L}{2} \cdot S_n \{L \cdot f, \epsilon_{r1}, \epsilon_{r2}\}$	
$\sqrt{\quad}$	$\sqrt{\quad}$
Intrinsic screen parameters	Cable parameters <sup>b</sup> $(Z_2, L), \epsilon_{r2}$
$\sqrt{\quad}$	$\sqrt{\quad}$
"Low-frequency coupling", short cables <sup>c</sup>	"HF-effect", cut-off $(L \cdot f)_c$
	$\sqrt{\quad}$
	Length + frequency effect
<p><sup>a</sup> <math>T^2</math> is the power coupling from circuit (1) to circuit (2). The stacked subscripts <math>_f^n</math> are associated to the stacked operation symbols <math>\pm</math> in the obvious way: upper subscript <math>\rightarrow</math> upper operation, lower subscript <math>\rightarrow</math> lower operation.</p> <p><sup>b</sup> <math>\epsilon_{r1}</math> and <math>\epsilon_{r2}</math> contained in <math>S</math> as parameters.</p> <p><sup>c</sup> for <math>L \ll \lambda</math>, <math>S\{L \cdot f\} \rightarrow 1</math>.</p>	

Note especially the following points.

- a) There may be a directional effect ( $T_n \neq T_f$ ) in the whole frequency range if  $Z_F$  is not negligible. (But  $Z_F$  is usually negligible except with loose, single braid shields.)
- b) Up to a constant factor,  $T$  is the quantity directly measured in a set-up.
- c) For low frequencies, i.e. for short cables ( $L \ll \lambda$ ), the trivial coupling formula is obtained that is directly proportional to  $L$ :

$$T_n = (Z_F \pm Z_T) \cdot \frac{1}{Z_{12}} \cdot \frac{L}{2} \tag{19}$$

where

$$Z_{12} = \sqrt{Z_1 \cdot Z_2}$$

- d) The summing function  $S\{L \cdot f\}$  is presented in Figure 6.
- e)  $S\{L \cdot f\}$  has a  $\sin(x)/x$  behaviour. A cut-off point may be defined as  $(L \cdot f)_c$ :

$$(L \cdot f)_{c_n} = \frac{c}{\pi \left| \sqrt{\epsilon_{r1}} \pm \sqrt{\epsilon_{r2}} \right|} \tag{20}$$

- f) The exact envelope of  $S\{L \cdot f\}$  is

$$\text{Env} \left| S_n \left\{ \frac{L \cdot f}{f} \right\} \right| = \frac{1}{\sqrt{1 + \frac{(L \cdot f)^2}{(L \cdot f)_{cn}^2}}} \quad (21)$$

g) The first minimum (zero) of  $S\{L \cdot f\}$  occurs at

$$(L \cdot f)_{\min} = \pi(L \cdot f)_c \quad (22)$$

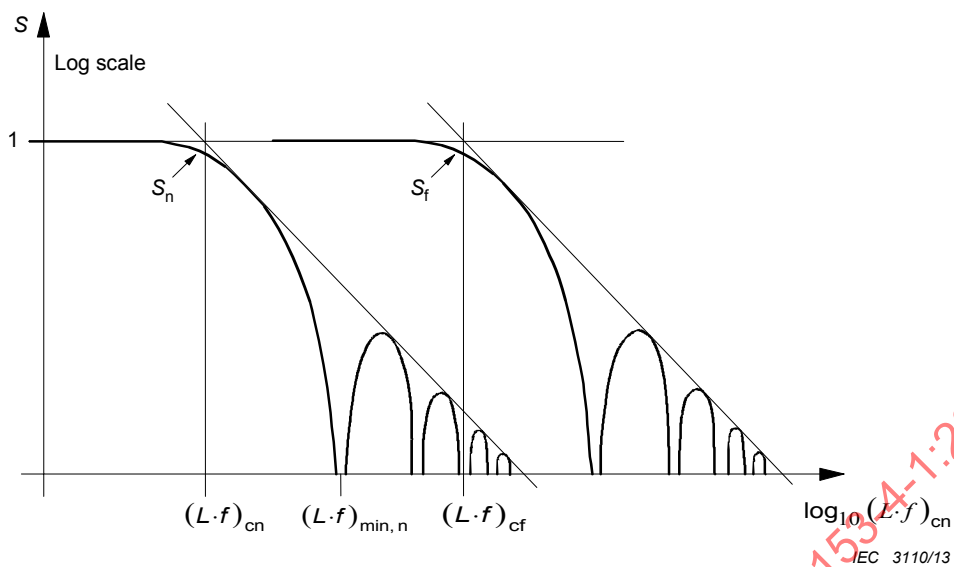
h) As seen from Equations (13) and (21), below the cut-off points  $(L \cdot f)_{cn}$  is  $S\{L \cdot f\} \approx 1$  and above them it starts to oscillate and its envelope drops asymptotically 20 dB/decade,

$$\text{Env} \left| S_n \left\{ \frac{L \cdot f}{f} \right\} \right| \approx \frac{(L \cdot f)_{cn}}{(L \cdot f)} \quad (23)$$

i)  $S$  is symmetrical in  $L$  and  $f$ , i.e.  $L$  and  $f$  are interchangeable. For a fixed length a cut-off frequency  $f_c$  and vice versa, for a fixed frequency a cut-off length  $L_c$  may be defined. Substituting  $c/\lambda_0$  for  $f$ , we obtain the cut-off length as

$$L_{cn} = \frac{\lambda_0}{\pi \left| \sqrt{\epsilon_{r1}} \pm \sqrt{\epsilon_{r2}} \right|} \quad (24)$$

- j) The effect of  $S$  in the frequency range ( $L = \text{constant}$ ) is illustrated in Figure 8. The coupling function is proportional to  $Z_T$ , only if  $f < f_c$ . Note also the typical values indicated for  $f_c$ .
- k) The minima and maxima of  $S$  are not resonances, they are due to cancelling and additive effects of the coupling along the line.
- l) The far end cut-off frequency is significantly influenced by the permittivity of the outer system ( $\epsilon_{r1}$ ). Selecting  $\epsilon_{r1} \rightarrow \epsilon_{r2}$  we obtain  $(L \cdot f)_{cf} \rightarrow \infty$ , i.e. no cut-off at the far end. Due to practical aspects (tolerances, homogeneity, etc.), an ideal phase matching ( $\epsilon_{r1} \equiv \epsilon_{r2}$ ) is not feasible.
- m) The effects of  $Z_T$  and  $Z_F$  on the coupling transfer functions  $T_n$  and  $T_f$  are shown in Figure 8.
- n) The total effect of  $L$  on the coupling is not contained in  $S$  alone, but in the product  $L \cdot S\{L \cdot f\}$ . The product  $L \cdot S$  is presented in Figure 12 for  $f = \text{constant}$ . The coupling function  $T$  which can be measured in a set-up is proportional to  $L$  if  $L < L_c$ . However, for appropriately long cables ( $L > L_c$ ), the maximum coupling is independent of  $L$  and we obtain a length independent shielding attenuation above the cut-off point  $(L \cdot f)_c$ . But we should remember that  $(L \cdot f)_c$  as well as  $A_s$  are still dependent on the set-up parameters ( $\epsilon_{r1}, Z_1$ ).

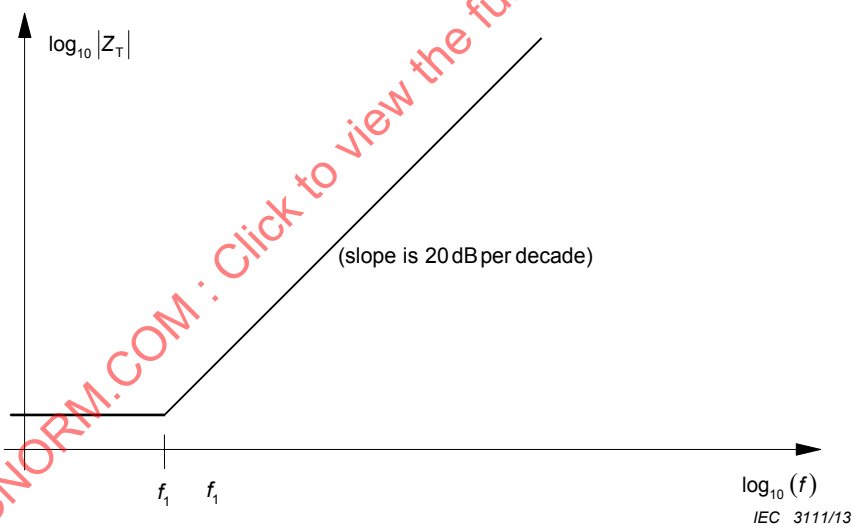


**Key**

- $(L \cdot f)_{cn,f}$  cut-off point at near (n) respectively far (f) end
- $S_{n,f}$  summing function at the (n) respectively far (f) end

NOTE  $S_f > S_n$  above near end cut-off, yielding a directive effect.

**Figure 6 – The summing function  $S(L \cdot f)$  for near and far end coupling**

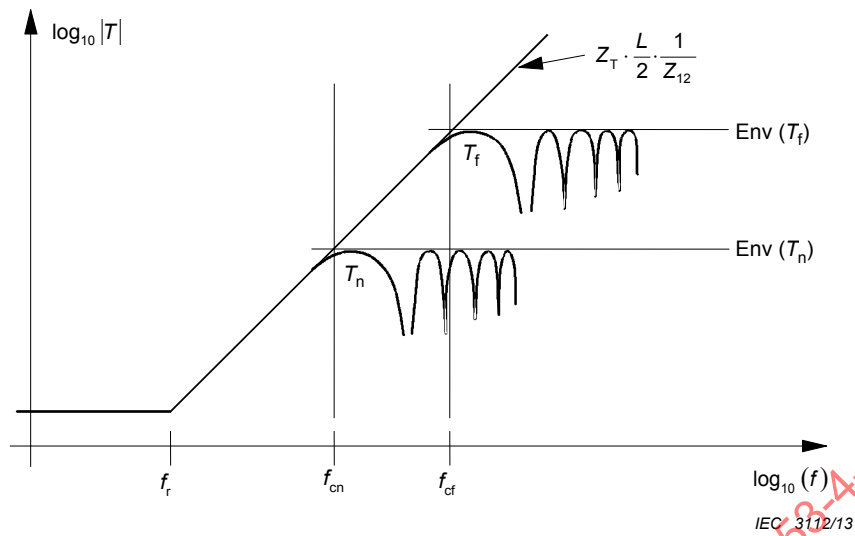


**Key**

- $\log_{10}|Z_T|$  magnitude of the transfer impedance drawn on a logarithmic scale
- $\log_{10}(f)$  frequency drawn on a logarithmic scale
- $f_1$  frequency of the intersection of the DC resistance of the screen and the 20dB slope at higher frequencies

**Figure 7 – Transfer impedance of a typical single braid screen**

Figure 8 gives the result of adding (on a log scale) the frequency responses from Figure 6 and Figure 7. It is assumed the cable has a negligible capacitive coupling impedance  $Z_F$  ( $Z_F \ll Z_T$ ).

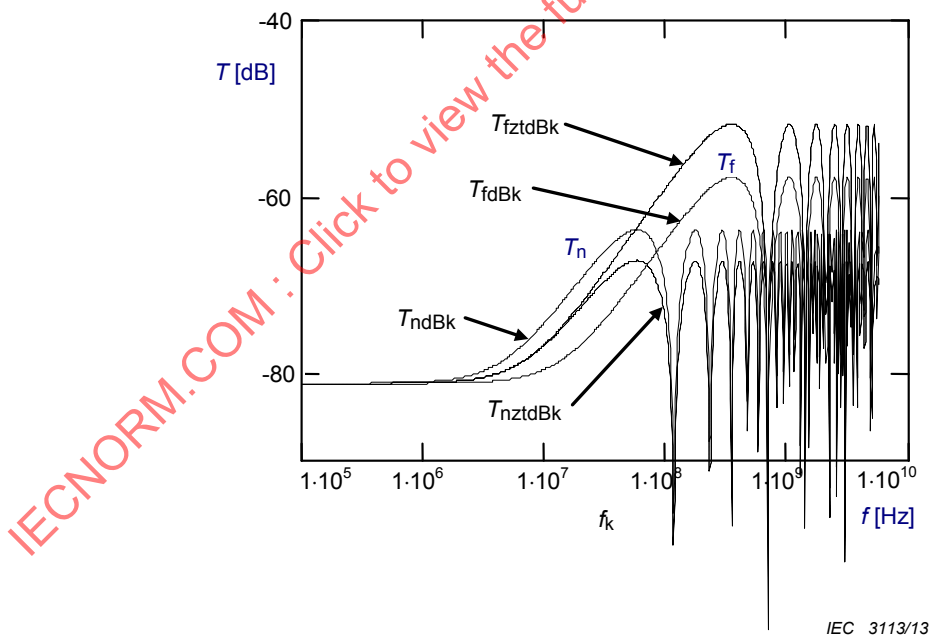


**Key**

- $T_{n,f}$  coupling transfer function at the (n) respectively far (f) end
- $Env(T_{n,f})$  envelope of the coupling transfer function at the (n) respectively far (f) end
- $f_{cn,f}$  cut-off frequency at the (n) respectively far (f) end

Example:  $\epsilon_{r1} = 1$  (set-up),  $\epsilon_{r2} = 2,2$  (cable),  $L = 1$  m; results in  $f_{cn} = 40$  MHz;  $f_{cf} = 200$  MHz

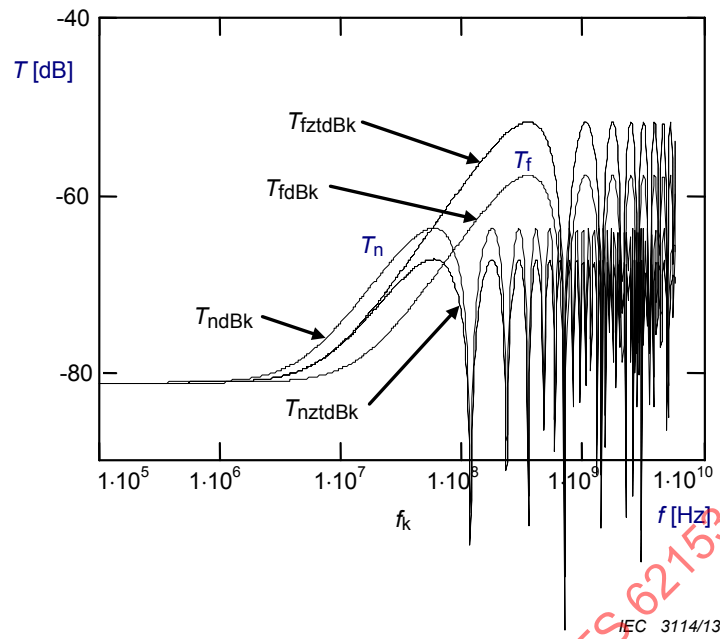
**Figure 8 – The effect of the summing function on the coupling transfer function of a typical single braid screen cable**



In calculations the following parameters are used:

$Z_T$  (d.c.) = 15 mΩ/m and  $Z_T$  (10 MHz) = 20 mΩ/m increasing 20 dB/decade (see Figure 7), cable length 1 m, and velocities of the outer and inner line:  $v_1 = 200$  Mm/s and  $v_2 = 280$  Mm/s corresponding to a velocity difference of 40 %.

**Figure 9 – Calculated coupling transfer functions  $T_n$  and  $T_f$  for a single braid –  $Z_F = 0$**



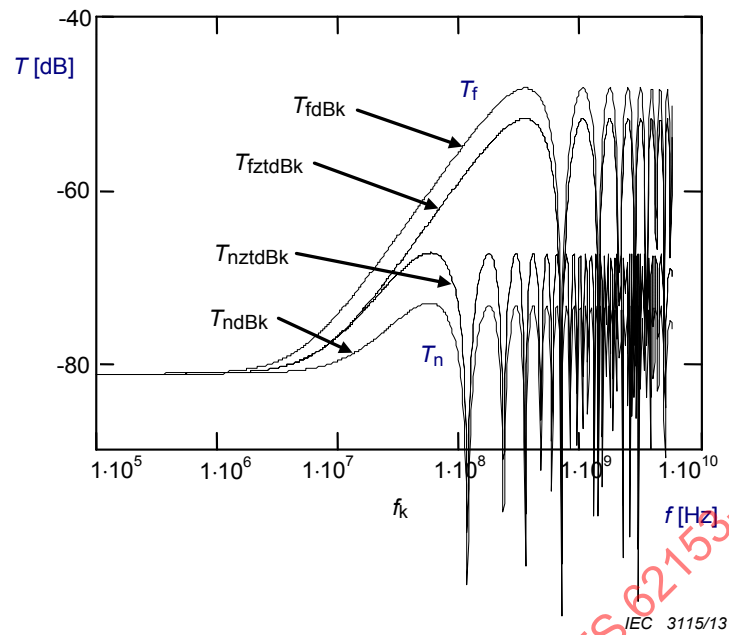
$T_n$  is 3,5 dB higher and  $T_f$  is 6 dB lower than in reference Figure 9 because

$$T_n \sim |Z_F + Z_T| = 1,5 \times Z_T \text{ and}$$

$$T_f \sim |Z_F - Z_T| = 0,5 \times Z_T$$

**Figure 10 – Calculated coupling transfer functions  $T_n$  and  $T_f$  for a single braid –  $\text{Im}(Z_T)$  is positive and  $Z_F = +0,5 \times \text{Im}(Z_T)$  at high frequencies**

IECNORM.COM : Click to view the full PDF of IEC TS 62153-4-1:2014



$T_f$  is 3,5 dB higher and  $T_n$  is 6 dB lower than in reference Figure 9 because

$$T_f \sim |Z_F - Z_T| = 1,5 \times |Z_T| \text{ and}$$

$$T_n \sim |Z_F + Z_T| = 0,5 \times |Z_T|$$

**Figure 11 – Calculated coupling transfer functions  $T_n$  and  $T_f$  for a single braid –  $\text{Im}(Z_T)$  is negative and  $Z_F = -0,5 \times \text{Im}(Z_T)$  at high frequencies**

In Figure 9,  $Z_F = 0$  and  $Z_T$  is positive.

In Figure 10 and Figure 11,  $Z_F$  is significant ( $Z_F = (1/2) \times Z_T$ ).

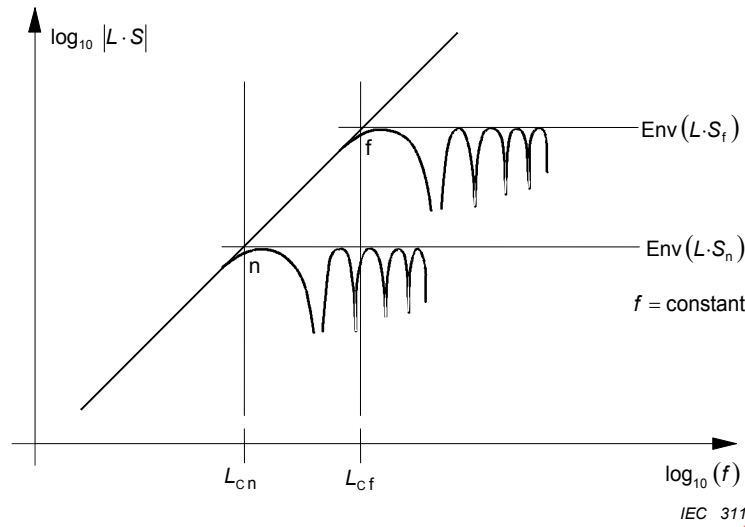
In Figure 11, the imaginary part of  $Z_T$  is negative at high frequencies.

The following notes apply to Figure 9 to Figure 11.

NOTE 1  $T_n$  for near-end,  $T_f$  for far-end and dB means that  $T_{n,f}$  are calculated in dB ( $20 \times \log_{10} |T_{n,f}|$ ).

NOTE 2  $T_n$  dB: near-end when  $Z_F = (1/2) \times Z_T$  and  $T_{nzt}$  dB: near-end when  $Z_F = 0$ .

NOTE 3  $T_f$  dB: far-end when  $Z_F = (1/2) \times Z_T$  and  $T_{fzt}$  dB: far-end when  $Z_F = 0$ .



NOTE 1 For  $L > L_c$ , the maximum value of  $T$  is attained, i.e. the maximum coupling (or the screening attenuation) is not dependent on  $L$ .

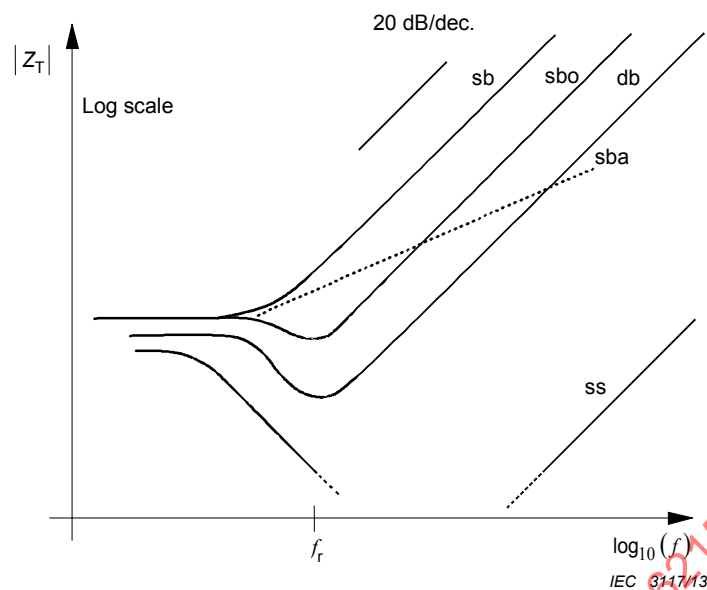
NOTE 2  $L_{cf}$  strongly depends on  $\epsilon_{r1}$ .

NOTE 3 See also Table 1 and list item n)

**Figure 12 –  $L \cdot S$ : the complete length dependent factor in the coupling function  $T$**

### 7 Transfer impedance of a braided wire outer conductor or screen

Typical transfer impedances of cables with braided wire screens are shown in Figure 13. The constant  $Z_T$  value at the low-frequency end is equal to the DC resistance of the screen, the 20 dB per decade rise at the high-frequency end is due to the inductive coupling through the screen and the dip at the middle frequencies is caused by eddy currents or skin effect of the braid. Some braided cables may behave anomalously having less than a 20 dB per decade rise at high frequencies. By using an extrapolation of 20 dB per decade we are in most cases on the conservative side. This extrapolation can be used up to several GHz.

**Key**

- $f_r$ : typically 1....10 MHz  
 sb: single braid  
 sbo: single braid optimized  
 sba: single braid 'anomalous'  
 db: double braid  
 ss: superscreen

**Figure 13 – Transfer impedance of typical cables**

An electrically short piece of braided coaxial cable (2) is considered to be placed in a triaxial arrangement as in Figure 2.

It is assumed that the outer circuit (1) is the disturbing one. As stated, a braided cable has a transfer impedance  $Z_T$  that increases proportionally to frequency at high frequencies, because of the leakage of the magnetic field through holes in the braid.

The total flux of the magnetic field induced by the disturbing current  $I_1$  is  $\Phi_1$ . A part of it,  $\Phi'_{12}$  leaks directly through the holes and includes a disturbing voltage  $U'_2$  in the inner circuit. However, a part  $\Phi''_{12}$  of  $\Phi_1$  flows in the braid and complicates the mechanism of the total magnetic leakage by the following additional phenomenon.

The braiding wires alternate between the outer and inner layer. It means that the inner and outer braid wires are likewise ingredients of both the inner (2) and outer (1) circuit of Figure 14.

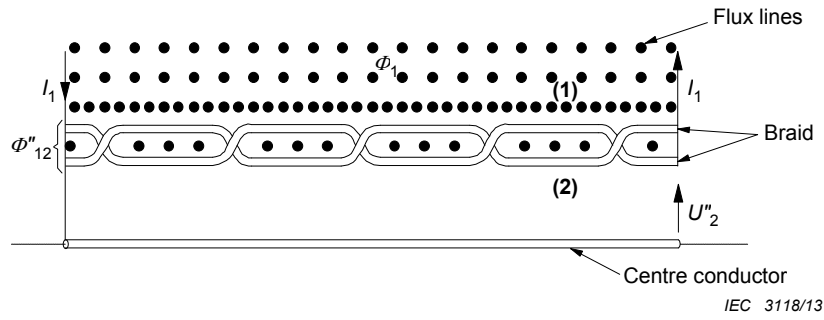


Figure 14 – Magnetic coupling in the braid – Complete flux

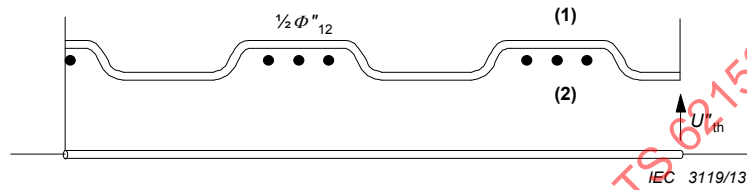


Figure 15 – Magnetic coupling in the braid – Left-hand lay contribution

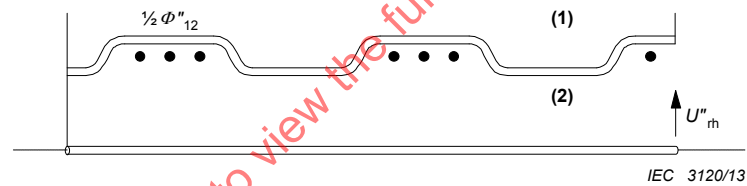


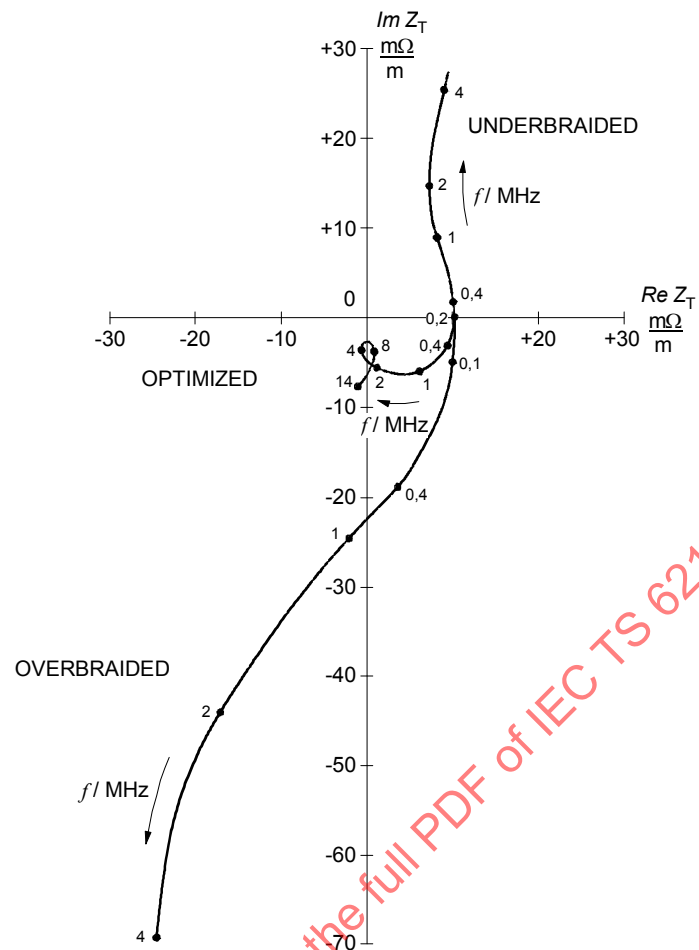
Figure 16 – Magnetic coupling in the braid – Right-hand lay contribution

Therefore it is necessary and unavoidable that  $\Phi''_{12}$  is partly also in the inner circuit (see Figure 14). Both the left hand (lh) (see Figure 15) and right hand (rh) lay (see Figure 16) of the braiding wires bring into the inner circuit (2) an equal disturbing voltage  $U''_2$  induced by  $\Phi''_{12} / 2$ . The voltages are in parallel:

$$U''_{rh} = U''_{lh} = U''_2 = \frac{1}{2} j \omega \Phi''_{12} \tag{25}$$

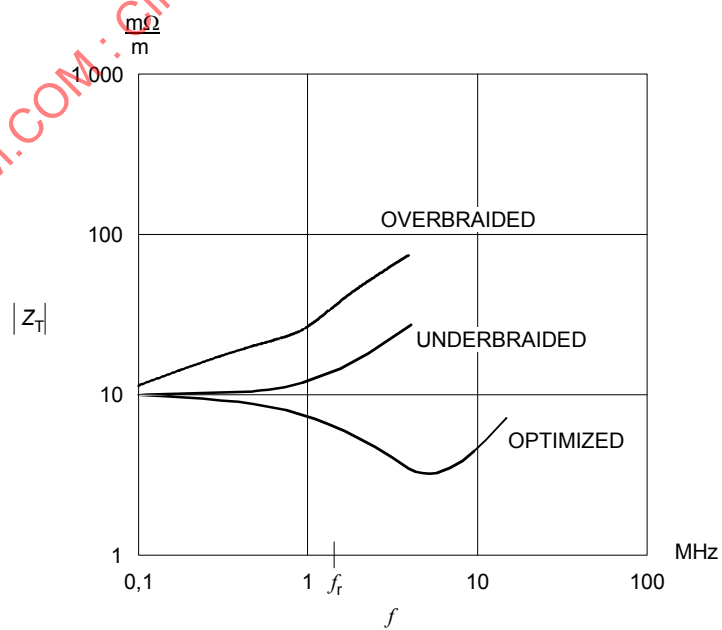
This phenomenon is similar to the "magnetic part" of the coupling through a homogeneous screen.

The two induced disturbing voltages oppose each other.



IEC 3121/13

Figure 17 – Complex plane,  $Z_T = Re Z_T + j Im Z_T$ , frequency  $f$  as parameter



IEC 3122/13

Figure 18 – Magnitude (amplitude),  $|Z_T(f)|$

In Figure 17 and Figure 18, the d.c., resistance  $Z_T$  (d.c.), is set to the value of 10 mΩ/m.

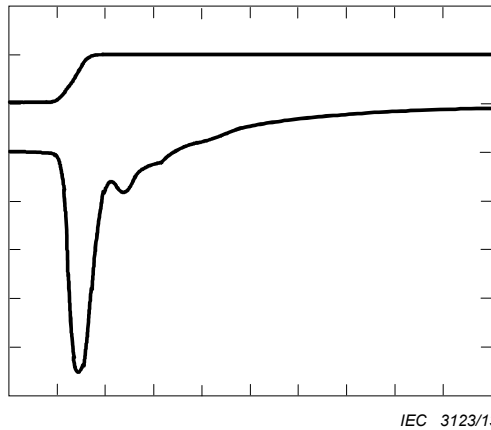


Figure 19a – Overbraided cable

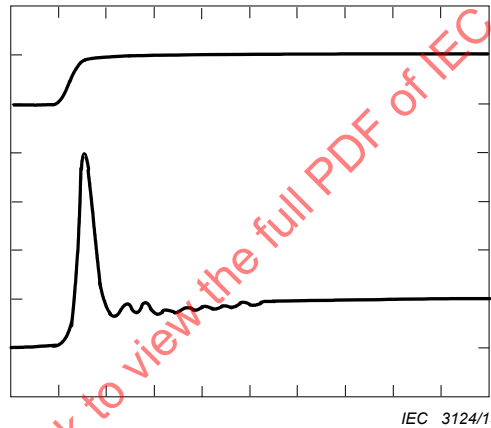


Figure 19b – Underbraided cable

Top trace: Injection step current (100 mA/div)

Time base: 50 ns/div

Amplifier gain: 30 dB, therefore  $Z_T$  (time) = 12,5 mΩ/m/div

Lower trace: The height of the spike corresponds to

a)  $-Z_T$  (3 MHz) =  $-4,7 \times 12,5 \text{ m}\Omega/\text{m} = -59 \text{ m}\Omega/\text{m}$ ;

b)  $-Z_T$  (3 MHz) =  $+4 \times 12,5 \text{ m}\Omega/\text{m} = +50 \text{ m}\Omega/\text{m}$ .

Figure 19 – Typical  $Z_T$  (time) step response of an overbraided and underbraided single braided outer conductor of a coaxial cable

Braid optimization is based on these important physical facts. Both leakage phenomena can be described by mutual inductances:

$$M'_{12} = \frac{\Phi_{12}}{j\omega I_1} \quad (26)$$

$$M''_{12} = \frac{1}{2} \times \frac{\Phi_{12}}{j\omega I_1} \tag{27}$$

Clearly it is possible to make braided-wire screens where either  $M'_{12}$  or  $M''_{12}$  are dominant or where they cancel each other. Therefore, underbraided, overbraided or optimized braids may be considered. Figure 17 shows measured transfer impedances in the complex plane of such screens and the main transfer impedance components of a braided screen can be observed. From the optimized case, it can be concluded that at low frequencies the braid behaves approximately as a homogeneous tubular screen. The same can be concluded from Figure 18 where the transfer impedance amplitudes are shown as a function of frequency, but from it cannot be seen directly if the screen is underbraided or overbraided.

The transfer impedance of a braided wire screen consists of the following three main components (mentioned above).

- a) At low and medium frequencies, the tubular screen coupling behaviour ( $Z_{Th}$ ) varies with eddy currents and decreasing  $Z_T$ . In [2] it is stated that a good approximation for  $Z_{Th}$  is a tubular homogeneous screen [3] with the thickness of one wire diameter and the same d.c. resistance as the braid.
- b) The mutual inductance  $M'_{12}$  is related to direct leakage of the magnetic flux  $\Phi'_{12}$ .
- c) The mutual inductance  $M''_{12}$  (negative) is related to the magnetic flux  $\Phi''_{12}$  in the braid.

By adding these components, a good approximation is obtained for the transfer impedance  $Z_T$  of a braided wire screen:

$$Z_T \approx Z_{Th} + j \omega (M'_{12} - M''_{12}) \tag{28}$$

and the first approximation of the equivalent circuit is shown in Figure 20a.

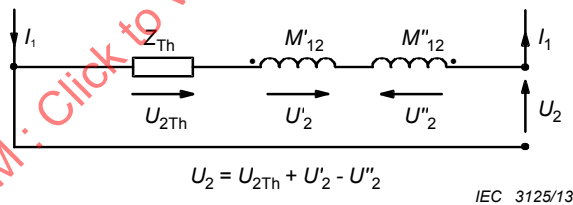


Figure 20a – Contributions to the transfer impedance

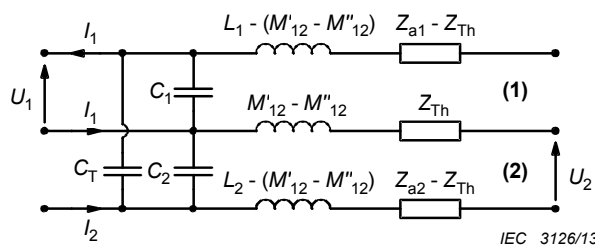


Figure 20b – Significant elements of circuits (1) and (2)

Figure 20 –  $Z_T$  equivalent circuits of a braided wire screen

A more complete equivalent circuit where the through capacitance  $C_T$  and surface impedances  $Z_a$  of the braided cable are incorporated is shown in Figure 20b.  $L_1$  and  $L_2$  are the (external) inductances of the outer and inner circuit.

Many attempts have been made to calculate the transfer impedance of a braided coaxial cable. Most of the literature ([2], [4], [5]) have concentrated on models of braided screens and calculation of direct leakage of the magnetic field induced by  $I_1$ , and of  $M'_{12}$ . Satisfactory results have been achieved.

There exists very little literature ([6], [7]) on  $M''_{12}$  but the matter has been studied by experts of standardization bodies. Especially the calculation and stability of  $M''_{12}$  have been shown to be very problematic because of so many uncertain and unstable parameters, e.g. the resistance of the crossover points of the wires, which have an effect on the magnetic field distribution in the braid. Also the pressure of the jacket has an effect on the small space between the right hand lay and left-hand lay of the braided wires. Not to mention the number of wire ends per carrier and the braid angle and the tightness and optical coverage of the braid.

After understanding the magnetic coupling mechanisms, it is not surprising that the transfer impedances of braided wire screens vary considerably and are unstable for many braid and cable constructions whether or not they are optimized. It is also clear that a perforated tube cannot be used as a model for a braided screen.

It is clear that a loose highly optimized braid can have a very unstable  $Z_T$  during bending, twisting and/or pressing. An overbraided screen with a high filling factor or optical cover normally has a (pure) negative transfer impedance at high frequencies because of a large  $M''_{12}$  coupling through the mutual "space" between the left and right lays of the braid in comparison with a small leakage through the braid  $M'_{12}$ . Pressure on the jacket would improve the screening performance by diminishing the mutual "space" and decrease the  $Z_T$ .

The manufacture of a good stable optimized cable requires the control of braid parameters such as:

- braid angle, tension (and lubricant) of the strands;
- number of strand in a spindle;
- wire diameter;
- plating;
- pressure of the jacket on the braid in manufacturing.

## 8 Test possibilities

### 8.1 General

A number of test procedures are used to test cables for their screening properties, some of which will be found in IEC standards. Each procedure has benefits for some users which for historical reasons may not be widely appreciated. Table 2 summarizes the test procedures available, some of which will be discussed here, with special reference to their applicability to cables, cable assemblies and connectors.

### 8.2 Measuring the transfer impedance of coaxial cables

All tests listed in Table 2 can be used on coaxial cables, but if a single test is needed to cover frequencies above and below 100 MHz, tests 1, 4, 7, 9 and 10 can be dismissed. Of the others, those with 's' under 'grouping' (column 3) have better intrinsic isolation between measuring and injection circuits, while in those with 'o' under grouping the injection circuit is unscreened. The difference is the line interchange referred to in 4.5 above. One benefit of an unscreened injection line is that better access may be obtained for inspection of the cable under test, which may be useful if the sample is in any way flawed. The two test methods with unscreened injection lines are test 3 and test 8. The latter, with its wide frequency coverage is recommended for future testing.

### 8.3 Measuring the transfer impedance of cable assemblies

Even with a restricted frequency range, many of the tests listed in Table 2 are not suited to tests on cable assemblies. Tests 1, 4, and 6 are unsuitable because an electrically short sample may be needed to achieve the upper frequencies, while test 10 is still limited to frequencies above 100 MHz. Tests with screened injection wires (test 2 and test 5) are difficult to set up due to the varying cross section of the assembly, a difficulty which also applies to test 3. Such objections leave tests 7, 8 and 9. To set against its low (effective) upper frequency limit, with test 7 it is easy to distinguish between connector and cable contributions, so it is ideal in a diagnostic role. Test 9 works only above 30 MHz, which may be restrictive. Test 8 will require several measurements on each sample, as it is unreasonable to assume that a cable assembly has circular symmetry.

It is only fair to state that in any frequency domain test on cable assemblies where signal phase is not recorded, a test is only valid if the sample length is not varied (tests carried out on a sample of one length cannot be used to assess a sample of another length – whether it be longer or shorter). Of the transfer impedance tests being discussed, only test 7 can be used in this way.

Multi-conductor cable assemblies are more complex, because the 'core' cannot be considered to be coaxial. A test for such cable assemblies has not yet been addressed.

### 8.4 Measuring the transfer impedance of connectors

In principle, all the tests in Table 2 can be used on coaxial connectors.

As with tests on cable assemblies, there is much benefit to be gained from using a test with an unscreened injection circuit, though other tests will remain in the standard, because they have become accepted. If it is possible to distinguish the screening of a connector from that of the attached cable, this will considerably ease the test procedure.

Multi-pin connectors are far more numerous and varied than coaxial connectors. However, non-circular connectors cannot be tested by the means implied by the test procedures of Table 2, though by suitable variation test 7 and test 10 would become appropriate. This problem is under study.

NOTE These methods give only an outline for measurement of symmetrical multicore cables, multipin connectors and cable assemblies made with these components.

The problems to be addressed come from the fact that:

- a) a connector is electrically short, while the parameters of a cable are distributed, and it may be electrically long;
- b) multi-core cables rarely have circular symmetry. This applies both physically and to the signal paths on their conductors;
- c) most multi-pin connectors have no circular symmetry; nor are they equally spaced from other conductors, which might couple to them;
- d) economics will dictate that a cable assembly test should apply to other assemblies using the same components, even though of differing overall length.

### 8.5 Calculated maximum screening level

It is important to know the exact theoretical limitation of the test equipment. By knowing the limitations, it is possible to calculate the maximum measurable screening effectiveness. This should be calculated to check the strengths and weaknesses of the test setup or even to optimize the test setup.

The following test equipment specifications are required for the calculation:

- minimum input (noise floor);
- maximum input;



$$NL = (-173 + F + 10 \times \log_{10} \Delta f) \quad (29)$$

where

$NL$  is the noise floor level of receiving side of the measuring system in dBm;

$F$  is the noise figure of the pre amplifier in dB;

$\Delta f$  is the bandwidth of the receiver in Hz.

IECNORM.COM : Click to view the full PDF of IEC TS 62153-4-1:2014

**Table 2 – Screening effectiveness of cable test methods for surface transfer impedance  $Z_T$**

Short title	Reference	Grouping (see Note 1)	Frequency range		Injection N or F (see Note 2)	Advantages or shortcomings
			Possible	Actually used		
1 IEC triaxial	IEC 62153-4-3	kf s	d.c. to 50 MHz	10 kHz to 30 MHz	F	Rigid test rig or flexible (milked on braid) Flexible test jig relies on ferrites
2 Terminated triaxial (Simons)	Figure A5 of IEC 60096-1:1986 [32]	m s	10 kHz to 1 GHz	100 kHz to 500 MHz	N F	
3 Braid injection (Fowler)	[9]	m o	d.c. to 500 MHz	10 kHz to 500 MHz	N F	
4 Quadaxial	[10]	m s	100 kHz to 50 MHz	100 kHz to 1 GHz	N	Deep resonances make use above 50 MHz theoretically impossible. The test has been used for assessing screening at frequencies up to 1 GHz
5 Matched T triaxial (Staegar)	IEC 60169-1-3 [11]	m s	1 kHz to 12 GHz	100 MHz to 40 GHz 10 kHz to 100 MHz	N F	Rigid test jig needs good screening
6 ERA triaxial (Smithers)	[12]	kf s	d.c. to 400 MHz	10 kHz to 300 MHz	F	Very short CUT requires amplifier or phase locked loop
7 Line injection (time domain)	IEC 60096-4-1 [33] [13]	m o	d.c. to 100 MHz	1 kHz to 80 MHz (note 3)	N F	Very easy to use. Needs good screening in measuring amplifier
8 Line injection (frequency domain)	IEC 62153-4-6 [14]	m o	d.c. to 20 GHz	10 kHz to 3 GHz	N F	Flexible and cheap measuring set-up, equipment needs to be well shielded
9 Open screening attenuation test method (absorbing clamp)	IEC 62153-4-5	m o	30 MHz to 2,5 GHz	30 MHz to 1 GHz 300 MHz to 2,5 GHz	N F	Poor sensitivity. Measuring of $a_s$ is dependent on the surroundings
10 Reverberation chamber method	IEC 61726 [15]	kn kf	0,1 GHz →	0,3 GHz to 40 GHz	N & F	Flexible in use, but a complex and expensive computer controller with sophisticated test software needed
11 Shielded screening attenuation test method	IEC 62153-4-4 [16] (note 4)	m s	d.c. to 5 GHz	10 kHz to 3 GHz	F	High-sensitivity measurements can be made without a screened room. Transfer impedance and screening attenuation can be measured with one set-up
12 Open multipin connector screening test method	[17]	o	d.c. to 1 GHz	10 kHz to 700 MHz	N	Low cost and flexible

Short title	Reference	Grouping (see Note 1)	Frequency range		Injection N or F (see Note 2)	Advantages or shortcomings
			Possible	Actually used		
13 Coupling attenuation measurements of balanced cables, cable-assemblies, connecting hardware 13.1 Current clamp injection method 13.2 Shielded triaxial test method 13.3 Absorbing clamp method	IEC 62153-4-2 IEC 62153-4-9 [22] IEC 62153-4-5 IEC 62153-4-11 IEC 62153-4-12 IEC 62153-4-13 IEC 62153-4-7		50 MHz to 1 GHz d.c. to 3 GHz 50 MHz to 2,5 GHz	50 MHz to 1 GHz d.c. to 1 GHz 50 MHz to 2,5 GHz		High sensitivity but a screened room is recommended High-sensitivity measurements can be made without a screened room Poor sensitivity
14 Shielded screening attenuation, test method for measuring the transfer impedance $Z_T$ and the screening attenuation $a_S$ of RF connectors up to and above 3 GHz; tube in tube method		m s	d.c. to 20 GHz	d.c. to 3 GHz		High-sensitivity measurements can be made without a screened room Transfer impedance and Screening attenuation with one test set-up
15 Shielded screening attenuation test method for measuring the screening effectiveness of feedthroughs and electromagnetic gaskets – double coaxial method	IEC 62153-4-10	m s	d.c. to 4 GHz	d.c. to 3 GHz		High-sensitivity measurements can be made without a screened room

NOTE 1 Grouping by condition of 'primary circuit':  
kn = short circuit at near end;  
kf = short circuit at far end;  
m = matched with characteristic impedance;  
o = open on unscreened;  
s = screened or shielded.

NOTE 2 N denotes near end feeding of primary relative to secondary circuit. F denotes far end feeding of primary relative to secondary circuit.

NOTE 3 Effective frequencies tested. Actually pulse with  $T_R = 3,5$  ns and duration up to 160  $\mu$ s.

NOTE 4 Secondary circuit near end short circuited.

## 9 Comparison of the frequency response of different triaxial test set-ups to measure the transfer impedance of cable screens

### 9.1 General

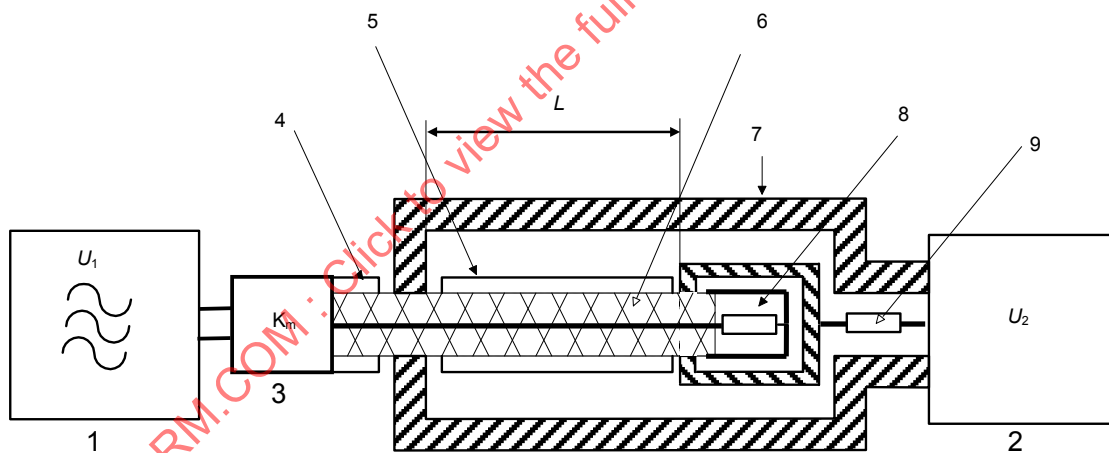
Different triaxial test set-ups for the measurement of the transfer impedance exist as described in EN 50289-1-6 and the IEC 62153-4 series. All of them are based on the same principle but are using different load conditions. In one method for example the cable under test is matched, while in the other the cable is short circuited at the far end. Furthermore, generator and receiver may be interchanged in the different set-ups. The following investigation analyses the frequency response of the different set-ups and their influence on the cut-off frequency up to which the transfer impedance could be measured.

### 9.2 Physical basics

#### 9.2.1 Triaxial set-up

##### 9.2.1.1 General

The triaxial set-up is of the “triple coaxial” form, see Figure 22 and Figure 23. A short length of the screen under test forms both, the inner conductor of the outer system and at the same time the outer conductor of the inner system. The coupling between the two coaxial systems is caused by the transfer impedance and the capacitive coupling admittance of the screen. The matching circuit, load resistor and series resistor are used to change the load conditions of the set-up. Also the generator and receiver may be interchanged between the different methods.

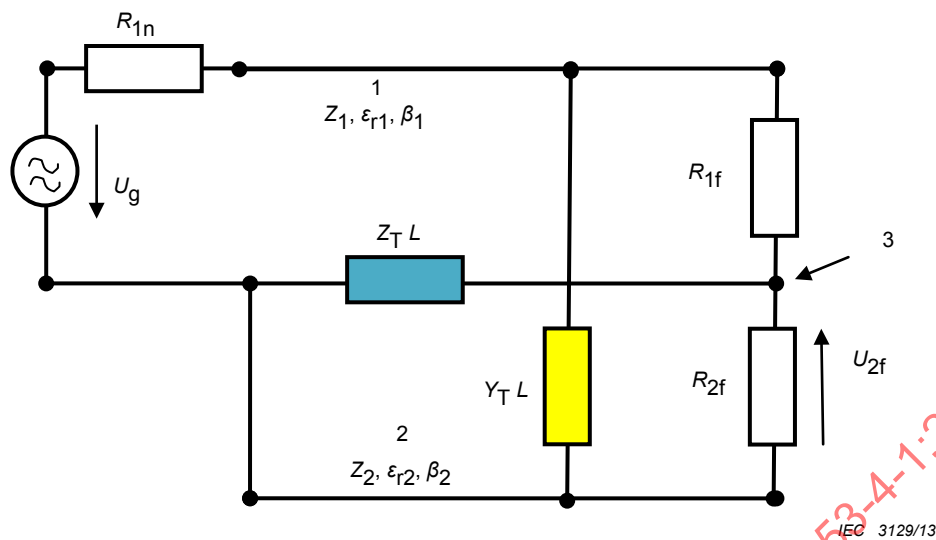


IEC 3128/13

#### Key

- |   |   |   |                      |
|---|---|---|----------------------|
| 1 | Signal generator                        | 6 | Cable screen         |
| 2 | Calibrated receiver or network analyzer | 7 | Tube                 |
| 3 | Matching circuit                        | 8 | Terminating resistor |
| 4 | Cable under test                        | 9 | Series resistor      |
| 5 | Cable sheath                            |   |                      |

Figure 22 – Triaxial set-up for the measurement of the transfer impedance  $Z_T$

**Key**

- 1 inner circuit, cable  
 2 outer circuit, tube  
 3 screen
- $Z_{1,2}$  characteristic impedance of the inner circuit, cable, respectively outer circuit, tube  
 $\epsilon_{1,2}$  dielectric permittivity of the inner circuit, cable, respectively outer circuit, tube  
 $\beta_{1,2}$  phase constant of the inner circuit, cable, respectively outer circuit, tube  
 $L$  coupling length  
 $Z_T$  transfer impedance  
 $Y_T$  capacitive coupling admittance  
 $R_{1n}$  load resistance at the near end of the inner circuit, cable. Equal to the output impedance of the generator respectively input impedance of the receiver including an eventually used feeding resistor  
 $R_{1f}$  load resistance at the far end of the inner circuit, cable. Depending on the used method either equal to the characteristic impedance of the cable or a short circuit.  
 $R_{2f}$  load resistance at the far end of the outer circuit, tube. Equal to the output impedance of the generator respectively input impedance of the receiver including an eventually used feeding resistor  
 $U_g$  EMF of the generator  
 $U_{2f}$  voltage at the far end of the outer circuit

**Figure 23 – Equivalent circuit of the triaxial set-up****9.2.1.2 Load conditions of the different set-ups**

EN 50289-1-6 is using a method, where the cable under test and the far end of the secondary circuit are matched. The signal is fed to the cable under test and the disturbing voltage is measured at the far end of the outer circuit. A simplified method is to neglect the matching resistor at the far end of the outer circuit, which results in a higher dynamic range.

IEC 61196-1 describes two methods:

Method 1: Feeding through a resistance, where the signal is fed via a resistance into the outer circuit and the disturbing voltage is measured at the far end of the cable under test.

Method 2: Direct feeding, where the signal power is fed directly into the outer circuit and the disturbing voltage is measured at the far end of the cable under test.

With the revision of IEC 61196-1, the standard IEC 62153-4-3 has been published which also describes several methods:

Method A “Matched-Short” is equal to EN 50289-1-6.

Method B “Short-Short” is the double short circuited method, where the load resistance of the cable is replaced by a short circuit, thus having two short circuits in the set-up. One is at the near end of the outer circuit (between the cable screen and the tube) and the other is at the far end of the cable. The advantage of this method is the simplification of the sample preparation. A short circuit is easier to make than to solder a resistor, especially if the sample is a multi-conductor cable. Furthermore, the measurement sensitivity is improved. Compared to the “matched-short” method, the dynamic range is improved by about 16 dB. In the “milked on braid” method, an additional braid, the measuring braid, is pulled over the cable sheath instead of using the measuring tube. The advantage is that the sample could be bent under test, however the preparation is more laborious than with the measuring tube.

The load conditions of the different methods are given in Table 3. The impedance of the outer circuit,  $Z_2$  is varying with the diameter of the screen under test. Using the measuring tube  $Z_2$  is in general higher, and in the “milked on braid” method  $Z_2$  is lower, than the input impedance of the receiver.

**Table 3 – Load conditions of the different set-ups**

Method	Generator	Receiver	$R_{in}/Z_1$	$R_{rf}/Z_1$	$Z_2/R_{2f}$
<b>EN 50289-1-6</b>					
Standard	IC	OC	1	1	0,71
simplified	IC	OC	1	1	1...5 depending on the tube diameter
<b>IEC 61196-1</b>					
Method 1: feeding through a resistance	OC	IC	1	1	0,71
Method 2: direct feeding	OC	IC	1	1	1...5 depending on the tube diameter
<b>IEC 62153-4-3 Double short circuit methods</b>					
With tube	OC	IC	1*	0	1...5 depending on tube diameter
With milked on braid	IC	OC	1*	0	0,1...0,4 depending on screen and sheath diameter of the cable
IC: inner circuit (cable under test)					
OC: outer circuit (tube)					
* only if the cable impedance is equal to the generator impedance. For other cable impedances, the value may vary, e.g. 0,67 for cables with an impedance of 75 Ω.					

### 9.2.2 Coupling equations

The equations for the coupling between the inner circuit and outer circuit for any load conditions are described in [18] and [19]. By taking into account the short circuit at the near end of the outer circuit (between the cable screen and the measuring tube), neglecting the attenuation of the disturbing and disturbed line, assuming non ferromagnetic materials and introducing further variables, the following equations are defined.

$$\frac{u_{2f}}{u_q} = \frac{L}{R_{1f} + R_{1n}} \cdot [Z_T \cdot g + Z_F \cdot h] \quad (30)$$

$$g = \frac{1}{N} \cdot \frac{1}{1-n^2} \cdot \frac{j}{x} \cdot \{ r \cdot [\cos x - \cos nx] - j \cdot n \cdot \sin nx + j \cdot \sin x \} \quad (31)$$

$$h = \frac{1}{N} \cdot \frac{1}{1-n^2} \cdot \frac{j}{x} \cdot \{ n \cdot r \cdot [\cos x - \cos nx] - j \cdot \sin nx + j \cdot n \cdot \sin x \} \quad (32)$$

$$N = \left\{ \cos x + \frac{j \cdot \sin x}{r+w} \cdot [1+r \cdot w] \right\} \cdot \{ \cos nx + j \cdot v \cdot \sin nx \} \quad (33)$$

$$x = \beta_1 \cdot L = 2\pi \cdot \frac{L}{\lambda_1} \quad (34)$$

$$n = \frac{\beta_2}{\beta_1} = \frac{\lambda_1}{\lambda_2} = \sqrt{\frac{\varepsilon_{r2}}{\varepsilon_{r1}}} \quad (35)$$

$$r = \frac{R_{1f}}{Z_1} \quad (36)$$

$$v = \frac{Z_2}{R_{2f}} \quad (37)$$

$$w = \frac{R_{1n}}{Z_1} \quad (38)$$

where

$Z_{1,2}$  is the characteristic impedance of the inner circuit (cable) respectively outer circuit (tube);

$\varepsilon_{1,2}$  is the dielectric permittivity of the inner circuit (cable) respectively outer circuit (tube);

$\beta_{1,2}$  is the phase constant of the inner circuit (cable) respectively outer circuit (tube);

$\lambda_{1,2}$  is the wave length in the inner circuit (cable) respectively outer circuit (tube);

$L$  is the coupling length;

$Z_T$  is the transfer impedance;

$Y_T$  is the capacitive coupling admittance;

$R_{1,n}$  is the load resistance at the near end of the inner circuit (cable). Equal to the output impedance of the generator respectively input impedance of the receiver including an eventually used feeding resistor;

$R_{1,f}$  load resistance at the far end of the inner circuit (cable). Depending on the used method either equal to the characteristic impedance of the cable or a short circuit.

The factors  $g$  and  $h$  (see Equations (31) and (32)) describe the frequency response of the test set-up. At low frequencies, when  $\lambda \gg L$ , the factors  $g$  and  $h$  are equal to 1. However, with increasing frequency, the factors  $g$  and  $h$  start to oscillate and thus also the measurement results. The maximum frequency to which the transfer impedance could be measured without oscillations, caused by the set-up, is defined as the 3 dB deviation from the linear interpolation of the measurement results. Or in other words, the maximum frequency is reached when the factor  $g$  respectively  $h$  becomes  $>\sqrt{2}$  respectively  $<1/\sqrt{2}$ .

### 9.3 Simulations

#### 9.3.1 General

For the following investigations, simulations have been chosen rather than a pure mathematical solution because they are easier to grasp and clearly illustrate the differences in the set-ups given in Table 4. In general, the capacitive coupling can be neglected compared to the magnetic coupling ( $Z_F \ll Z_T$ ). i.e. the cut-off frequency is mainly determined by the frequency behaviour of the factor  $g$ . Thus the following simulations are limited to the factor  $g$ .

Due to the reciprocity of the materials, it is possible to interchange the generator and receiver without changing the results. Thus the standard EN 50289-1-6 method gives the same results as IEC 61196-1, method 1: “feeding through a resistance” and the simplified EN 50289-1-6 method gives the same results as IEC 61196-1, method 2: “direct feeding”.

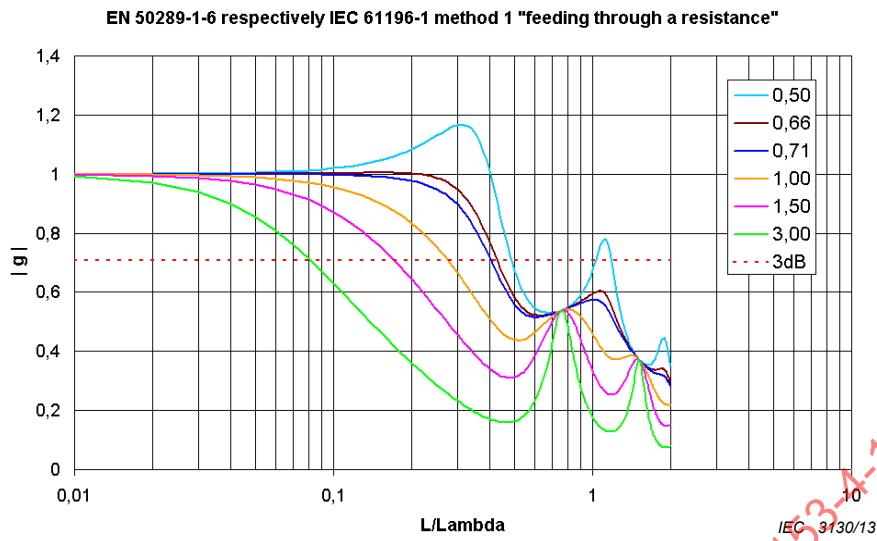
**Table 4 – Parameters of the different set-ups**

Method	$w=R_{1n}/Z_1$	$r=R_{1f}/Z_1$	$v=Z_2/R_{2f}$	$n=\sqrt{\epsilon_{r2}}/\sqrt{\epsilon_{r1}}$
<b>EN 50289-1-6, IEC 62153-4-3 method A</b>				
Standard	1	1	0,71	0,66 (0,45)...0,91
Simplified	1	1	1...5 depending on the tube diameter	
<b>IEC 61196-1</b>				
Method 1: feeding through a resistance	1	1	0,71	0,66 (0,45)...0,91
Method 2: direct feeding	1	1	1...5 depending on the tube diameter	
<b>IEC 62153-4-3 Double short circuit methods</b>				
With tube	1 <sup>a</sup>	0	1...5 depending on tube diameter	0,66 (0,45)...0,91
With milked on braid	1 <sup>a</sup>	0	0.1...0,4 depending on screen and sheath diameter of the cable	1,02...2,0
<sup>a</sup> only if the cable impedance is equal to the generator impedance. For other cable impedances, the value may vary, e.g. 0,67 for cables with an impedance of 75 Ω.				

In the tube methods, the factor  $n$  is given by the dielectric permittivity of the cable (inner circuit) as the dielectric permittivity of the outer circuit is nearly independent on the sheath material and can be assumed to be 1. However, in the “milked on braid method”, the factor  $n$  is dependent on both the dielectric permittivity of the cable insulation and the sheath, as the “measuring braid” is directly put on the sheath of the sample. The values for the factor  $n$  are given for typical insulation materials (PE, foam PE, PTFE ...). The values in brackets are given for an insulation material of PVC, which may be used in multi-pair/conductor cables. For the “milked on braid” method, typical combinations of insulation and sheath materials (PE/PVC, PE/LSZH, PTFE/FEP...) are taken into account, resulting in a value  $n > 1$ .

#### 9.3.2 Simulation of the standard and simplified methods according to EN 50289-1-6, IEC 61196-1 (method 1 and 2) and IEC 62153-4-3 (method A)

In EN 50289-1-6, IEC 61196-1 method 1: “feeding through a resistance” and IEC 62153-4-3 method A: “Matched-Short”, the factor  $v=Z_2/R_{2f}$  is specified at  $1/\sqrt{2}$ . The following simulations show that this factor is a good compromise with respect to the maximum frequency to which the transfer impedance could be measured.

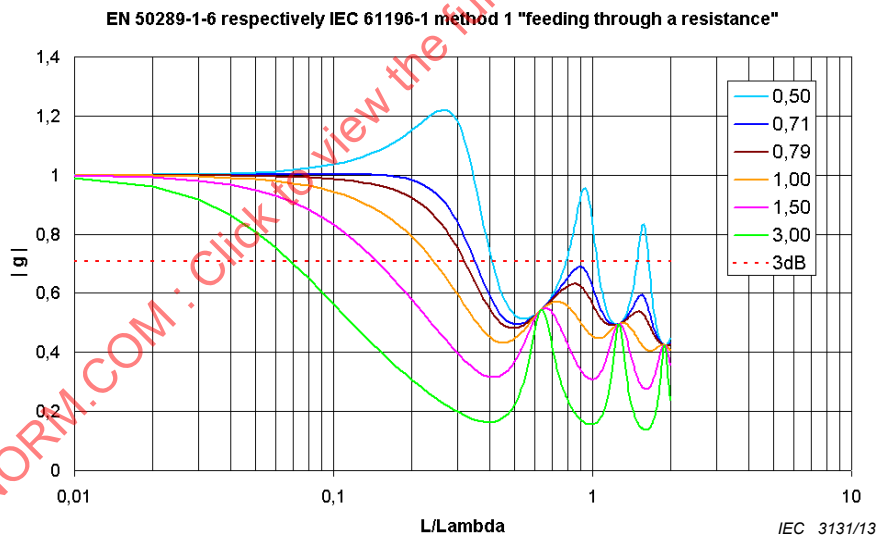


**Key**

Coloured lines correspond to indicated factors of  $v=Z_2/R_{2f}$ .

Simulation parameters		
$\epsilon_{r1}$	$\epsilon_{r2}$	$n$
2,3 (solid PE)	1,0	0,569

**Figure 24 – Simulation of the frequency response for g**

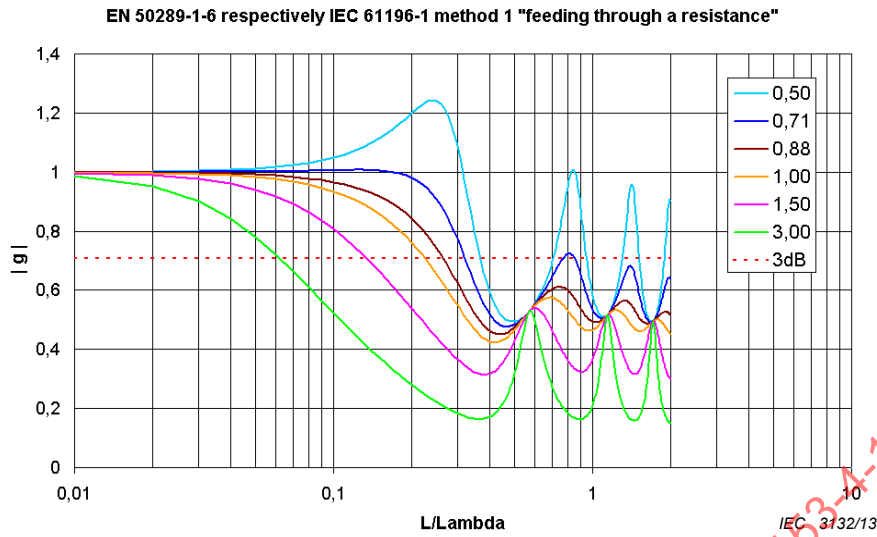


**Key**

Coloured lines correspond to indicated factors of  $v=Z_2/R_{2f}$ .

Simulation parameters		
$\epsilon_{r1}$	$\epsilon_{r2}$	$n$
1,6 (foam PE)	1,0	0,791

**Figure 25 – Simulation of the frequency response for g**

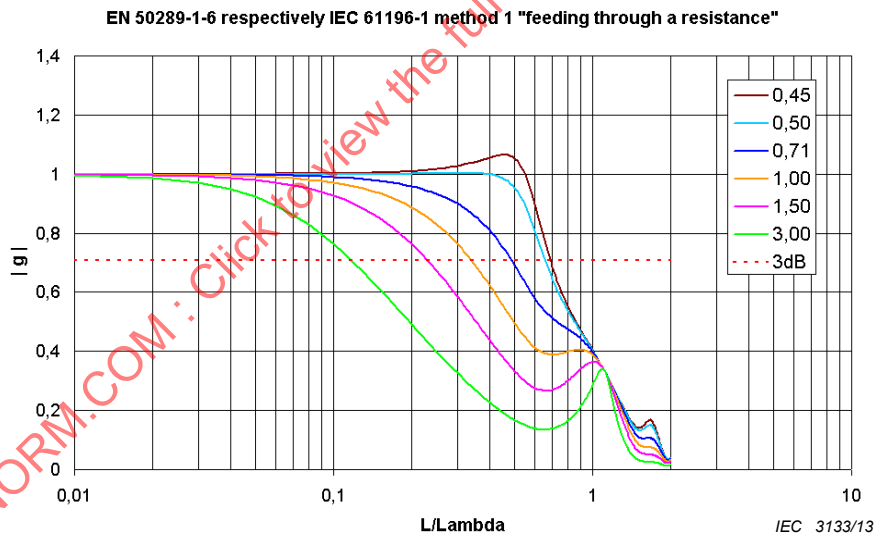


**Key**

Coloured lines correspond to indicated factors of  $v=Z_2/R_{2f}$ .

Simulation parameters		
$\epsilon_{r1}$	$\epsilon_{r2}$	$n$
1,3 (foam PE)	1,0	0,877

**Figure 26 – Simulation of the frequency response for  $g$**



**Key**

Coloured lines correspond to indicated factors of  $v=Z_2/R_{2f}$ .

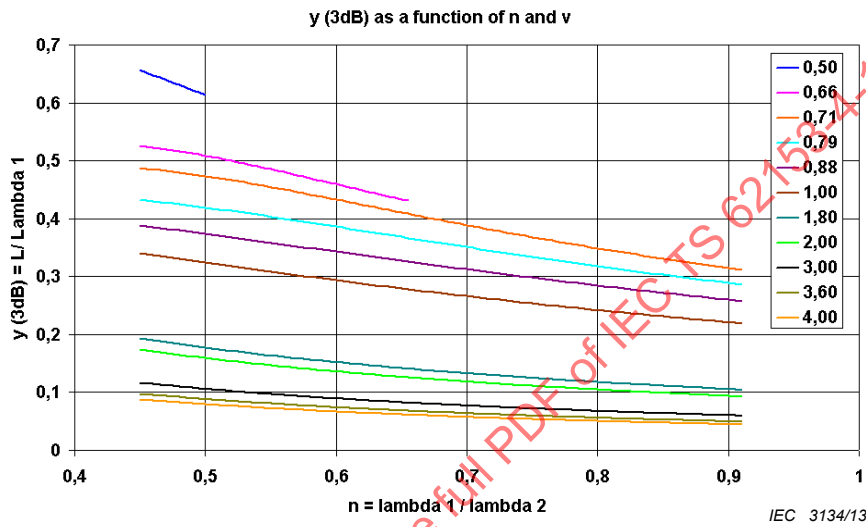
Simulation parameters		
$\epsilon_{r1}$	$\epsilon_{r2}$	$n$
5 (PVC)	1,0	0,447

**Figure 27 – Simulation of the frequency response for  $g$**

The highest frequencies (respectively shortest wavelengths) are obtained if the factor  $v=1/\sqrt{2}$  respectively  $v=n$ , whichever is smaller. In Figure 24 and Figure 27, the highest frequency is obtained for  $v=n$  ( $=0,659$  respectively  $0,447$ ). But in Figure 25 and Figure 26, the highest frequency is obtained for  $v=1/\sqrt{2}=0,71$ . Below that value, the factor  $g$  overshoots, i.e. becomes higher than one. Above that value, the cut-off frequency is decreasing.

Figure 28 gives the calculated, by iteration, 3 dB cut-off wavelength ( $L/\lambda_1$ ) at which the factor  $|g|$  becomes  $1/\sqrt{2}$ . The graph is given as a function of the factor  $n = \sqrt{\epsilon_{r2}}/\sqrt{\epsilon_{r1}}$  and for different factors  $v = Z_2/R_{2f}$ . The curves show a linear behaviour and could be interpolated by straight line.

This has been done in Figure 29 for  $v=1/\sqrt{2}$ ,  $v=1$ ,  $v=1,8$  and  $v=3,6$ . The factor  $v=1/\sqrt{2}$  corresponds to the set-up according to EN 50289-1-6, IEC 61196-1 method 1 "feeding through a resistance" and IEC 62153-4-3 method A "Matched-Short". The other values of the factor  $v$  correspond to the simplified set-up, i.e. direct feeding. For common diameters of the measuring tube (around 40 mm) and common cable screen diameter (2 mm to 9 mm), the impedance in the outer circuit is 90 Ω to 180 Ω and  $v=1,8...3,6$ .

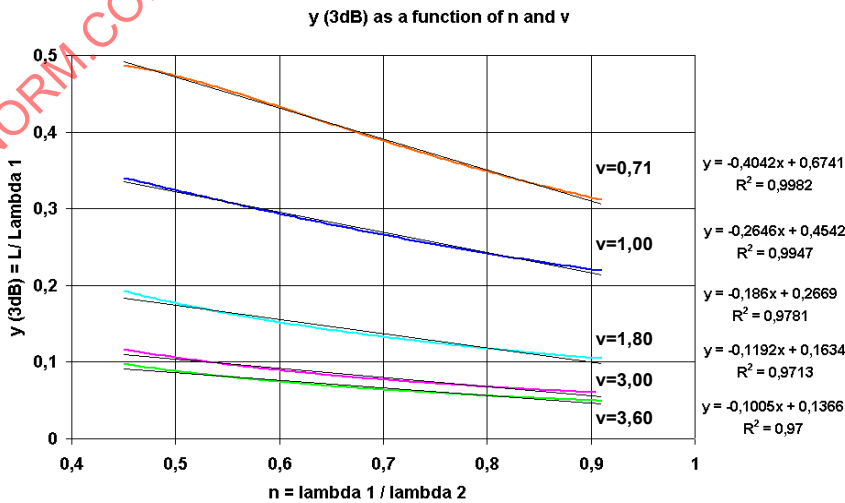


**Key**

Coloured lines correspond to indicated factors of  $v = Z_2/R_{2f}$ .

**Figure 28 – Simulation of the 3 dB cut off wavelength ( $L/\lambda_1$ )**

The graphs for  $v=0,5$  and  $v=0,66$  are only given for  $n$  up to 0,5 respectively 0,66 because otherwise the factor  $g$  overshoots as described above.



**Key**

Coloured lines correspond to indicated factors of  $v = Z_2/R_{2f}$ .

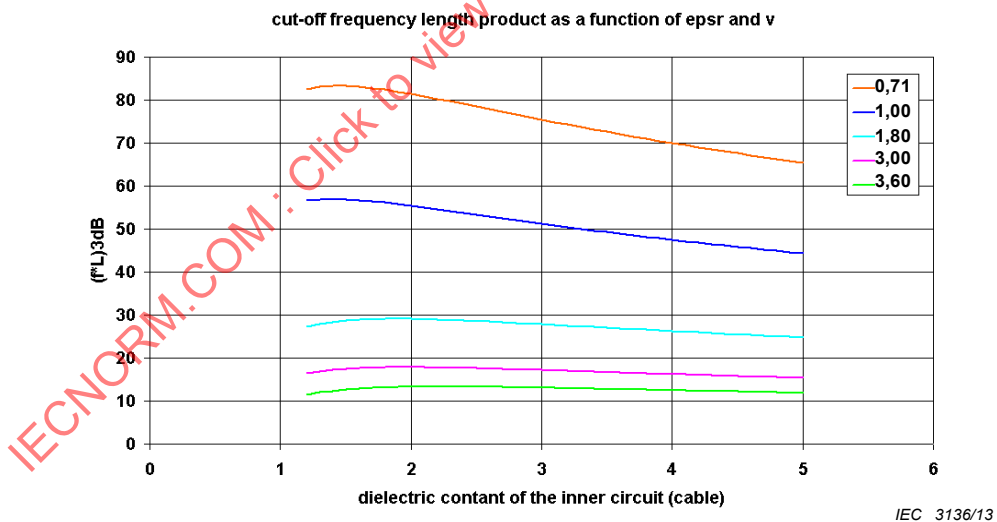
**Figure 29 – Interpolation of the simulated 3 dB cut off wavelength ( $L/\lambda_1$ )**

The linear interpolation equation is used to derive an equation to calculate the cut-off frequency length product up to which the transfer impedance could be measured in a given triaxial test set-up.

**Table 5 – Cut-off frequency length product**

Triaxial test set-up	$\nu$	Cut-off equation
EN 50289-1-6 IEC 61196-1 method 1 "feeding through a resistance" IEC 62153-4-3 method A "matched-short"	$\nu=1/\sqrt{2}$	$(f \cdot L)_{3 \text{ dB}} \approx \left[ \frac{200}{\sqrt{\epsilon_{r1}}} - \frac{120}{\epsilon_{r1}} \right] \cdot \text{MHz} \cdot \text{m}$
Simplified EN 50289-1-6 IEC 61196-1 method 2 "direct feeding"	$\nu=1$	$(f \cdot L)_{3 \text{ dB}} \approx \left[ \frac{135}{\sqrt{\epsilon_{r1}}} - \frac{80}{\epsilon_{r1}} \right] \cdot \text{MHz} \cdot \text{m}$
	$\nu=1,8$	$(f \cdot L)_{3 \text{ dB}} \approx \left[ \frac{80}{\sqrt{\epsilon_{r1}}} - \frac{55}{\epsilon_{r1}} \right] \cdot \text{MHz} \cdot \text{m}$
	$\nu=3$	$(f \cdot L)_{3 \text{ dB}} \approx \left[ \frac{50}{\sqrt{\epsilon_{r1}}} - \frac{35}{\epsilon_{r1}} \right] \cdot \text{MHz} \cdot \text{m}$
	$\nu=3,6$	$(f \cdot L)_{3 \text{ dB}} \approx \left[ \frac{40}{\sqrt{\epsilon_{r1}}} - \frac{30}{\epsilon_{r1}} \right] \cdot \text{MHz} \cdot \text{m}$

The equations given in Table 5 are drawn in the graphs of Figure 30.



**Key**

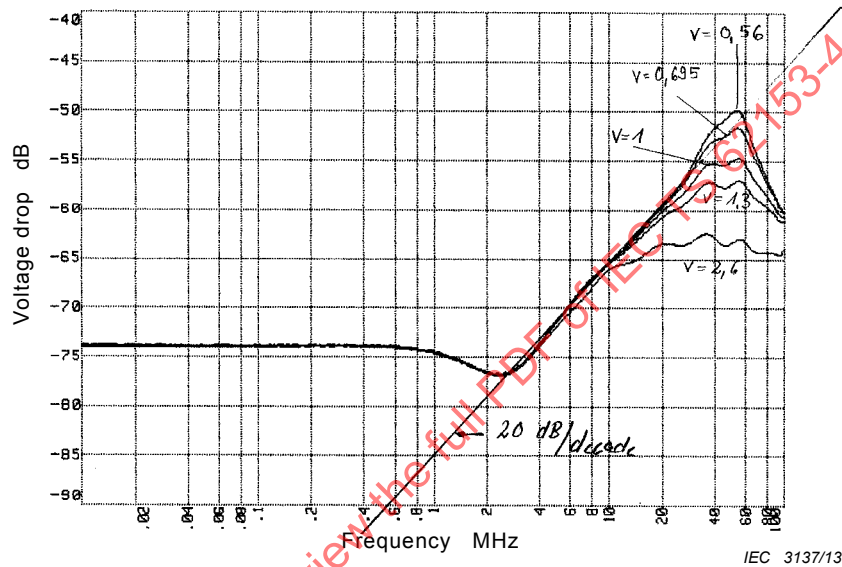
Coloured lines correspond to indicated factors of  $\nu=Z_2/R_{2f}$ .

**Figure 30 – 3 dB cut-off frequency length product as a function of the dielectric permittivity of the inner circuit (cable)**

For example, if a cable with a PE insulation – dielectric permittivity of,  $\epsilon_{r1} = 2,3$ , and a screen diameter of 3,5 mm is measured in a triaxial set-up according to EN 50289-1-6 or IEC 61196-1 method 1 "feeding through a resistance" with  $\nu=0,71$ , then the cut-off frequency length product is about 80 MHz·m. Therefore for a coupling length of 0,5 m, the maximum frequency to which the transfer impedance could be measured is around 160 MHz.

If the same cable is measured in a triaxial set-up according to IEC 61196-1 method 2 “direct feeding” or the simplified set-up according to EN 50289-1-6 where  $v=3$ , then the cut-off frequency length product is about 18 MHz·m. For a coupling length of 0,5 m, the maximum frequency to which the transfer impedance could be measured is around 36 MHz.

Figure 31 and Figure 32 show the measurement results of the normalised voltage drop – i.e. the attenuation caused by the series resistor has been taken into account – in the triaxial set-up for different factors of  $v$ . Both figures show the results of the same screen design, however one with a solid PE insulation ( $\epsilon_{r1}=2,3$ ), the other with a foam PE insulation ( $\epsilon_{r1}=1,6$ ). The measurement results confirm the simulations. From the equations given in Table 5 one obtains cut-off frequency length products for  $v=3$  of about 18 MHz·m and for  $v=1$  of about 55 MHz·m for both the solid PE and the foam PE. This is also found from the measurement results.

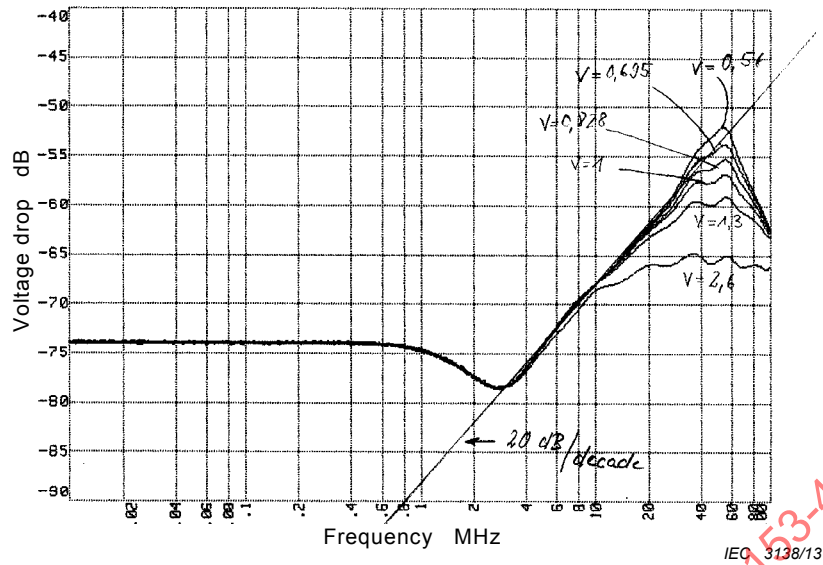


**Key**

Indicated lines correspond to factors of  $v=Z_2/R_{2f}$

Measurement set-up parameters				
$\epsilon_{r1}$	$\epsilon_{r2}$	$n$	$Z_2$	$L$
2,3 (PE)	1,0	0,659	130 $\Omega$	1 m

**Figure 31 – Measurement result of the normalised voltage drop of a single braid screen on a solid PE dielectric in the triaxial set-up**



**Key**

Indicated lines correspond to factors of  $v = Z_2/R_{2f}$

Measurement set-up parameters				
$\epsilon_{r1}$	$\epsilon_{r2}$	$n$	$Z_2$	$L$
1,6 (foam PE)	1,0	0,791	130 $\Omega$	1 m

**Figure 32 – Measurement result of the normalised voltage drop of a single braid screen on a foam PE dielectric in the triaxial set-up**

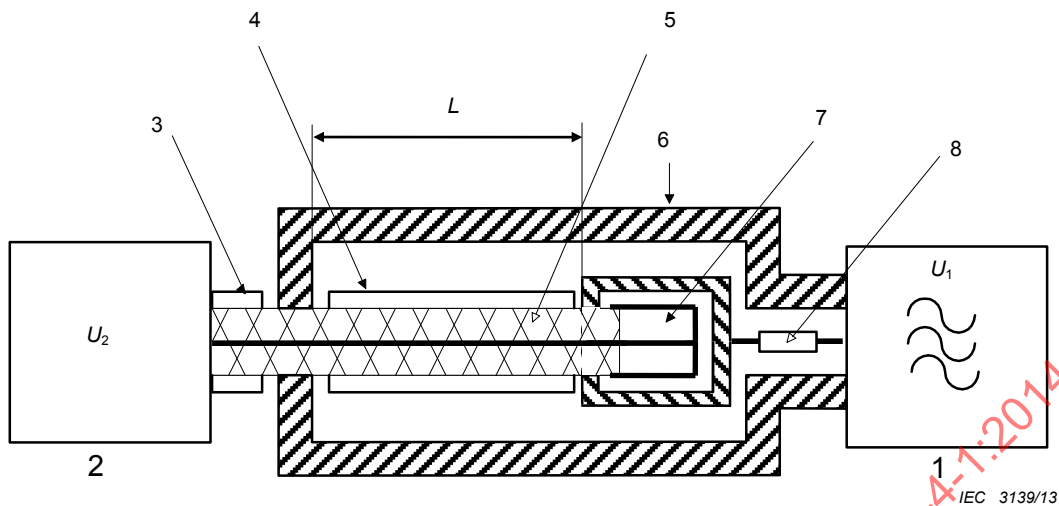
**9.3.3 Simulation of the double short circuited methods**

**9.3.3.1 General**

For the double short circuited methods, one has either a measuring tube or a “milked on braid”. When using a measuring tube, the dielectric permittivity of the outer circuit (tube) is nearly independent on the sheath material and could be assumed to be 1. However in the “milked on braid” method, the dielectric permittivity is given by the sheath material. Thus the factor  $n$  is different for both methods. Also the impedance of the outer circuit is different for both methods, first due to the different dimensions, second due to the different permittivities.

**9.3.3.2 Simulation of the double short circuited method using a measuring tube**

The double short circuited method using a measuring tube is shown in Figure 33. The outer circuit is fed over a fixed – i.e. the same value for all cable types – feeding resistor, the value of which is equal to the output impedance of the generator (e.g. 50  $\Omega$ ). Thus the load impedance of the outer circuit at the far end is equal to 2 times the output impedance of the generator. The factor  $v$  is then only dependent on the diameters of the screen and of the measuring tube.



**Key**

- 1 signal generator
- 2 calibrated receiver or network analyzer
- 3 cable under test
- 4 cable sheath
- 5 cable screen
- 6 tube
- 7 short circuit
- 8 series resistor (50 Ω)

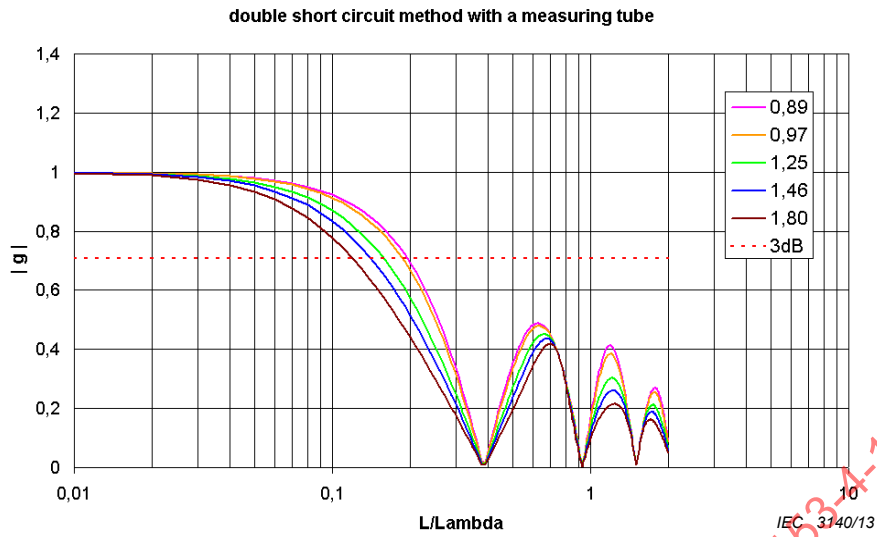
**Figure 33 – Triaxial set-up (measuring tube), double short circuited method**

**Table 6 – Typical values for the factor  $\nu$ , for an inner tube diameter of 40 mm and a generator output impedance of 50 Ω**

Screen diameter mm	$Z_2$ Ω	$\nu = Z_2/R_{2f}$
9	89	0,89
8	97	0,97
5	125	1,25
3,5	146	1,46
2	180	1,80

Those values have been used in the following simulations. The graphs in Figure 34 to Figure 37 show the simulated frequency response for different dielectric permittivities of the cable and for the different factors of  $\nu$  given in Table 6.

Figure 38 plots the results of calculation by iteration for the 3 dB cut-off wavelength ( $L/\lambda_1$ ) at which the factor  $|g|$  becomes  $1/\sqrt{2}$ . The curves have then been interpolated by straight lines.

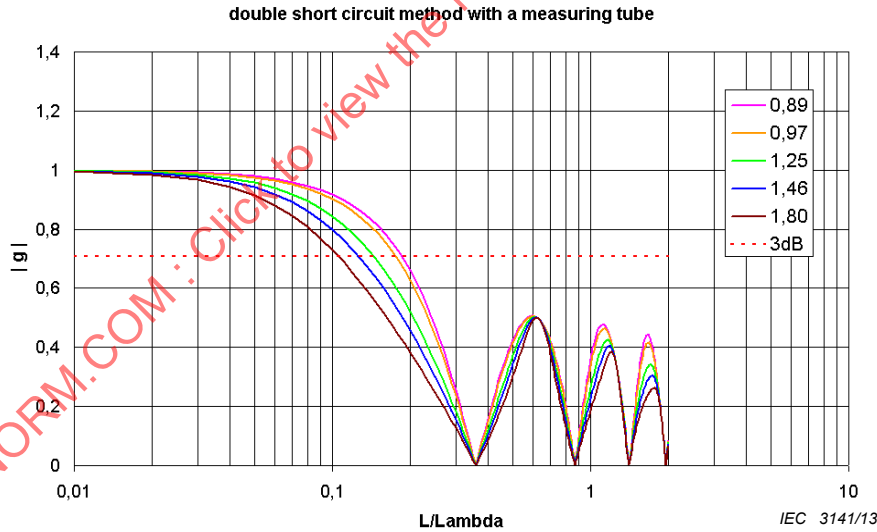


**Key**

Coloured lines correspond to indicated factors of  $v=Z_2/R_{2f}$ .

Simulation parameters		
$\epsilon_{r1}$	$\epsilon_{r2}$	$n$
2,3 (solid PE)	1,0	0,659

**Figure 34 – Simulation of the frequency response for  $g$  of a cable having solid PE dielectric ( $\epsilon_{r1}=2,3$ )**

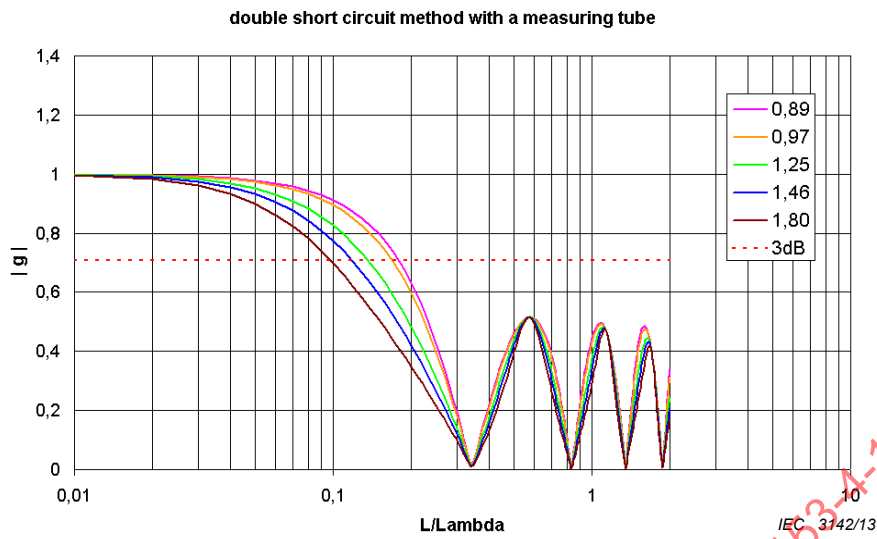


**Key**

Coloured lines correspond to indicated factors of  $v=Z_2/R_{2f}$ .

Simulation parameters		
$\epsilon_{r1}$	$\epsilon_{r2}$	$n$
1,6 (foam PE)	1,0	0,791

**Figure 35 – Simulation of the frequency response for  $g$  of a cable having foamed PE dielectric ( $\epsilon_{r1}=1,6$ )**

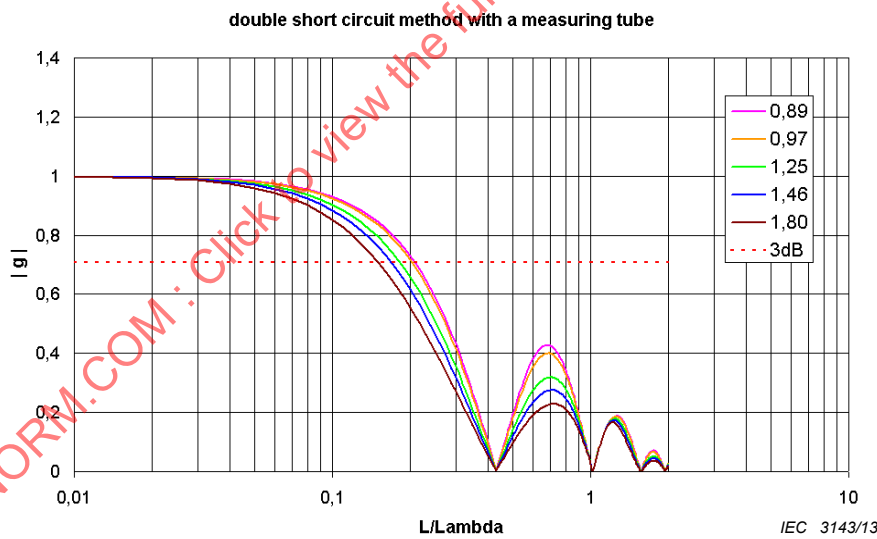


**Key**

Coloured lines correspond to indicated factors of  $v = Z_2/R_{2f}$ .

Simulation parameters		
$\epsilon_{r1}$	$\epsilon_{r2}$	$n$
1,3 (foam PE)	1,0	0,877

**Figure 36 – Simulation of the frequency response for  $g$  of a cable having foamed PE dielectric ( $\epsilon_{r1}=1,3$ )**

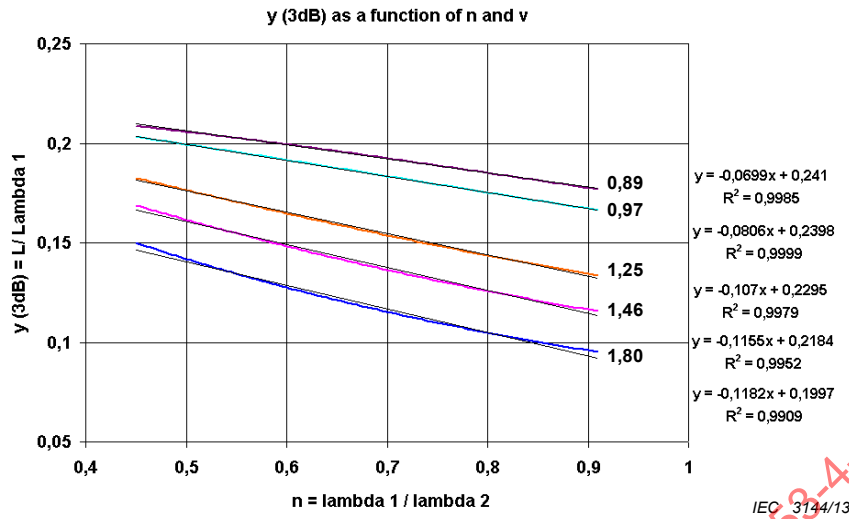


**Key**

Coloured lines correspond to indicated factors of  $v = Z_2/R_{2f}$ .

Simulation parameters		
$\epsilon_{r1}$	$\epsilon_{r2}$	$n$
5 (PVC)	1,0	0,447

**Figure 37 – Simulation of the frequency response for  $g$  of a cable having PVC dielectric ( $\epsilon_{r1}=5$ )**



**Key**

Coloured lines correspond to indicated factors of  $v=Z_2/R_{2f}$ .

**Figure 38 – Interpolation of the simulated 3 dB cut off wavelength ( $L/\lambda_1$ )**

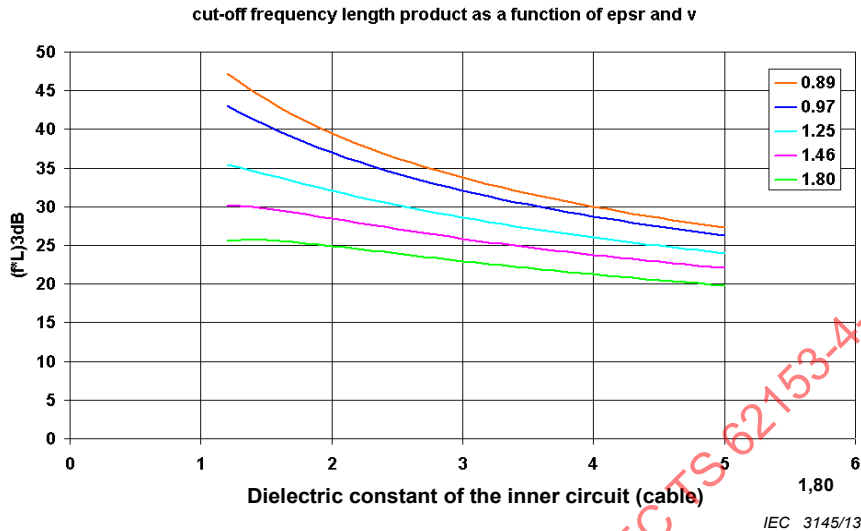
From the found linear interpolation, one can derive following equations to calculate the cut-off frequency length product, to which the transfer impedance could be measured in the “double short circuit” triaxial set-up using a measuring tube.

**Table 7 – Cut-off frequency length product**

$v=0,89$	$(f \cdot L)_{3 \text{ dB}} \approx \left[ \frac{70}{\sqrt{\epsilon_{r1}}} - \frac{20}{\epsilon_{r1}} \right] \cdot \text{MHz} \cdot \text{m}$
$v=0,97$	$(f \cdot L)_{3 \text{ dB}} \approx \left[ \frac{70}{\sqrt{\epsilon_{r1}}} - \frac{25}{\epsilon_{r1}} \right] \cdot \text{MHz} \cdot \text{m}$
$v=1,25$	$(f \cdot L)_{3 \text{ dB}} \approx \left[ \frac{68}{\sqrt{\epsilon_{r1}}} - \frac{32}{\epsilon_{r1}} \right] \cdot \text{MHz} \cdot \text{m}$
$v=1,46$	$(f \cdot L)_{3 \text{ dB}} \approx \left[ \frac{65}{\sqrt{\epsilon_{r1}}} - \frac{35}{\epsilon_{r1}} \right] \cdot \text{MHz} \cdot \text{m}$
$v=1,80$	$(f \cdot L)_{3 \text{ dB}} \approx \left[ \frac{60}{\sqrt{\epsilon_{r1}}} - \frac{35}{\epsilon_{r1}} \right] \cdot \text{MHz} \cdot \text{m}$

The equations given in Table 7 are plotted in the graphs of Figure 39. For example, if a cable with a PE insulation – dielectric permittivity of  $\epsilon_{r1}=2,3$  – is measured in a triaxial set-up with  $v=1,46$  (screen diameter=3,5 mm, tube diameter=40 mm), then the cut-off frequency length product is about 27 MHz·m.: i.e. for a coupling length of 0,5 m, the maximum frequency to which the transfer impedance could be measured is around 60 MHz. If the same cable is measured in a triaxial set-up according to IEC 61196-1 method 2 “direct feeding” or the simplified set-up according to EN 50289-1-6 where  $v=3$ , then the cut-off frequency length product is about 18 MHz·m: i.e. for a coupling length of 0,5 m, the maximum frequency to which the transfer impedance could be measured is around 36 MHz. That is to say, that the

double short circuit method (using a measuring tube) facilitates the sample preparation, has a 6 dB higher dynamic range and also allows to measure the transfer impedance up to higher frequencies, compared to the simplified EN 50289-1-6 or IEC 61196-1 method 2 “direct feeding”.



#### Key

Coloured lines correspond to indicated factors of  $v = Z_2 / R_{2f}$ .

**Figure 39 – 3 dB cut-off frequency length product as a function of the dielectric permittivity of the inner circuit (cable)**

#### 9.3.3.3 Simulation of the double short circuited method using a “milked on braid”

In the “milked on braid” method, a measuring braid is used instead of a measuring tube. The measuring braid is put directly over the sheath of the sample. Thus the dielectric permittivity of the outer circuit is given by the dielectric permittivity of the sheath ( $\epsilon_{r2} = 2 \dots 5$ ), and the impedance of the outer circuit is given by the dielectric constant and the diameter over the sheath of the sample.

In this method, the inner circuit is fed over a 10 dB attenuation pad instead of a 50  $\Omega$  feeding resistor while using a measuring tube. However, using a 10 dB attenuation pad instead of a feeding resistor doesn't affect the cut-off frequency, as described below.

For cable screen diameters between 1 mm to 10 mm, sheath thickness between 0,2 mm to 1 mm and  $\epsilon_{r2}$  between 2 and 5, the impedance in the outer circuit is between 5  $\Omega$  and 20  $\Omega$ , i.e.  $v$  between 0,1 and 0,4.

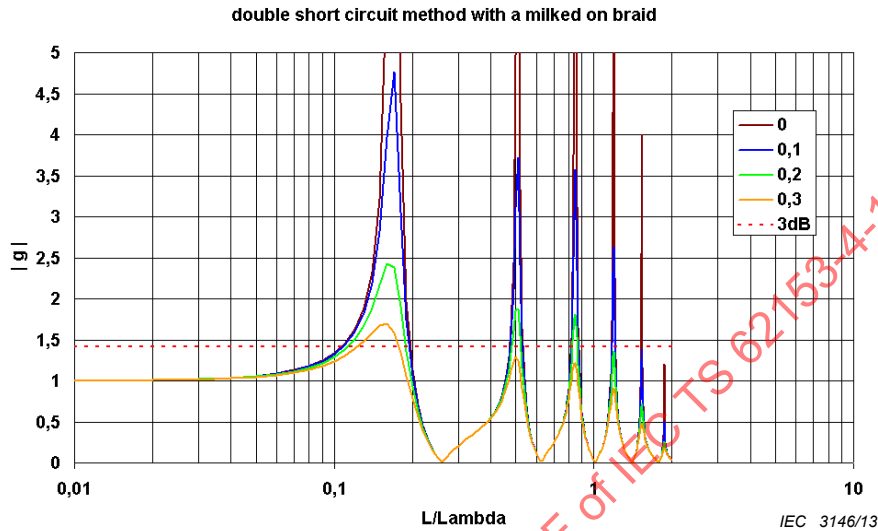
A closer look on the coupling equations (Equation (30) to Equation (38)) shows that for small values of the factor  $v$  and at low frequencies, the frequency response of the test set-up (factor  $g$ ) becomes nearly independent of it. The worst case with respect to the 3 dB cut-off is reached if  $v=0$ . This is drawn out in the equations below and in Figure 40. Thus, in the following, the simulations are done for  $v=0$ .

$$N = \left\{ \cos x + \frac{j \cdot \sin x}{r + w} \cdot [1 + r \cdot w] \right\} \cdot \{ \cos nx + j \cdot v \cdot \sin nx \} \quad (39)$$

for small values of  $v$ , i.e.  $v \ll 1$  and low frequencies, i.e.  $x \ll 1$  one gets

$$N = \left\{ \cos x + \frac{j \cdot \sin x}{r+w} \cdot [1+r \cdot w] \right\} \cdot \left\{ e^{j \cdot nx} - j \cdot (1-v \cdot \sin nx) \right\} \tag{40}$$

$$\approx \left\{ \cos x + \frac{j \cdot \sin x}{r+w} \cdot [1+r \cdot w] \right\} \cdot \left\{ e^{j \cdot nx} - j \right\}$$



**Key**

Coloured lines correspond to indicated factors of  $v=Z_2/R_{2f}$ .

Simulation parameters		
$\epsilon_{r1}$	$\epsilon_{r2}$	$n$
2,3 (PE)	5 (PVC)	1,474

**Figure 40 – Simulation of the frequency response for g**

Taking into account typical combinations of insulation and sheath materials (PE/PVC, PE/LSZH, PTFE/FEP...), one gets values for the factor  $n$  between 1,02 and 2. Those values in Table 8 have been used for the iteration of the 3 dB cut-off wavelength ( $L/\lambda_1$ ) shown in Figure 41.

**Table 8 – Material combinations and the factor  $n$**

$\epsilon_{r1}$	$\epsilon_{r2}$	$n = \sqrt{\epsilon_{r2}/\epsilon_{r1}}$
2,3 (PE)	5 (PVC)	1,47
	3 (LSZH)	1,14
1,6 (foam PE)	5 (PVC)	1,77
	3 (LSZH)	1,37
1,3 (foam PE)	5 (PVC)	1,96
	3 (LSZH)	1,52
2,0 (PTFE)	2,1 (FEP)	1,02
1,3 (expanded PTFE)	2,1 (FEP)	1,27



**Key**

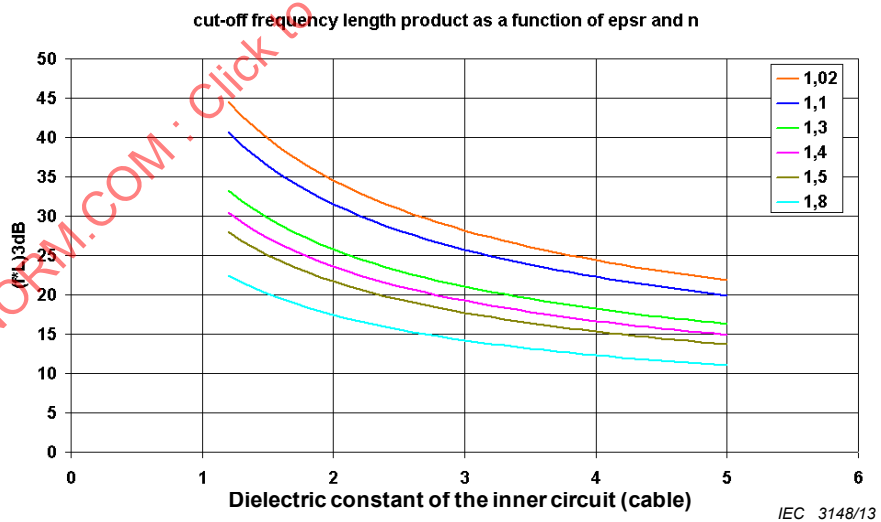
Plotted line is for  $v=Z_2/R_{2f} \ll 1$ .

**Figure 41 – Interpolation of the simulated 3 dB cut off wavelength ( $L/\lambda_1$ )**

From the interpolation, one can derive following equation given in Table 9 for the 3 dB cut-off frequency length product. The equation in Table 9 is plotted in Figure 42.

**Table 9 – Cut-off frequency length product**

$v \ll 1$	$(f \cdot L)_{3\text{dB}} \approx \left[ \frac{50 \times n^{-1,204}}{\sqrt{\epsilon_{r1}}} \right] \cdot \text{MHz} \cdot \text{m}$
-----------	---



**Key**

Coloured lines correspond to indicated factors of  $n = \sqrt{\epsilon_{r2}} / \sqrt{\epsilon_{r1}}$ , for  $v=Z_2/R_{2f} \ll 1$ .

**Figure 42 – 3 dB cut-off frequency length product as a function of the dielectric permittivity of the inner circuit (cable)**

For example, a cable with PE insulation and PVC sheath ( $n=1,47$ ) with the dimensions of a RG 58 (screen diameter around 3,5 mm) measured with the “milked on braid” method results in a cut-off frequency length product of 20 MHz·m. The same cable measured in the double

short circuit method with a measuring tube results in a cut-off length product of 27 MHz·m. If measured in the simplified EN 50289-1-6 method respectively one gets a cut-off frequency length product of 18 MHz·m. Thus the major advantage of the “milked on braid” method is that it allows for bending of the sample under test.

### 9.4 Conclusion

The best compromise between a simple test set-up and the cut-off frequency is given for the “double short circuit” method using a measuring tube. It covers the usually required frequency range of 100 MHz (see Table 10) for the transfer impedance measurement (using a 30 cm tube) and has the highest dynamic range of all triaxial methods.

The “milked on braid” method has a limited frequency range, requires a long sample preparation but allows for bending of the sample under test.

The matched method according to EN 50289-1-6, IEC 62153-4-3 method A “matched-short” respectively IEC 61196-1 method 1 “direct feeding” has the highest cut-off frequency but also the lowest dynamic range. An additional error source in that method is the accuracy of the series resistor which might have unknown frequency behaviour and thus an unknown attenuation.

**Table 10 – Cut-off frequency length product for some typical cables in the different set-ups**

Cable type	Sheath	EN 50289-1-6 IEC 61196-1 method 1 IEC 62153-4-3 method A	Double short circuit method using a tube	Double short method using a milked on braid
RG 58 ( $\epsilon_{r1}=2,3$ )	PVC	80 MHz·m ( $v=0,71$ )	28 MHz·m ( $v=1,46$ )	20 MHz·m ( $n=1,47$ )
	LSZH			28 MHz·m ( $n=1,14$ )
Thin Ethernet ( $\epsilon_{r1}=1,6$ )	PVC	83 MHz·m ( $v=0,71$ )	30 MHz·m ( $v=1,46$ )	20 MHz·m ( $n=1,77$ )
	LSZH			28 MHz·m ( $n=1,37$ )
RG 214 ( $\epsilon_{r1}=2,3$ )	PVC	80 MHz·m ( $v=0,71$ )	35 MHz·m ( $v=0,97$ )	20 MHz·m ( $n=1,47$ )
	LSZH			28 MHz·m ( $n=1,14$ )
RG 8 ( $\epsilon_{r1}=1,3$ )	PVC	83 MHz·m ( $v=0,71$ )	42 MHz·m ( $v=0,97$ )	20 MHz·m ( $n=1,96$ )
	LSZH			26 MHz·m ( $n=1,52$ )

## 10 Background of the shielded screening attenuation test method (IEC 62153-4-4)

### 10.1 General

In many cases, above all in the lower frequency range, the screening effectiveness of cables is described by the transfer impedance  $Z_T$ . It is, for an electrically short length of cable, defined (see Figure 43) as the quotient of the longitudinal voltage measured on the secondary side of the screen to the current in the screen, caused by a primary inducing circuit, related to unit length [23]. Although the transfer impedance  $Z_T$  covers only the galvanic and magnetic couplings, it is common practice to use it also as a quantity which includes the effect of the coupling capacitance  $C_T$  through the cable screen [24]. In this case, it is named equivalent

transfer impedance  $Z_{TE}$  which includes the effects of galvanic, magnetic and capacitive coupling.

For the determination of the proper coupling capacitance there is, as standardised quantity, the capacitance coupling admittance  $Y_T$ . The coupling admittance (see Figure 44) for an electrically short piece of cable is defined as the quotient of the current in the screen caused by the capacitive coupling in the secondary circuit to the voltage in the primary circuit related to unit length [23].

With electrically short cables, where wave propagation can be neglected, the screening quantities related to unit length can directly be used to calculate an induced disturbing voltage. In the higher frequency range, the implications get similar complicated as the transmission characteristics of a simple line, dependent on the impedance and admittance per unit length as well as on the terminating resistors.

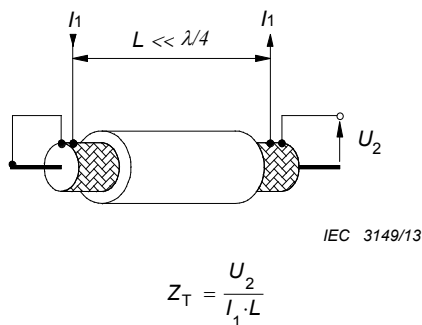


**Figure 43 – Definition of transfer impedance**

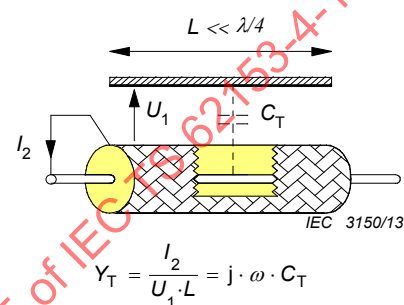


**Figure 44 – Definition of coupling admittance**

## 10.2 Objectives

It is desirable to measure and evaluate the screening efficiency of cable screens also in the wave propagation frequency range such that its characteristics can be directly applied. This requires a closer examination of the conditions of such applications.

In general, a system of electromagnetic induction consists of a transmission circuit in the cable, which is assumed to be fully defined, and of a surrounding transmission system, which is assumed to be universal with respect to the definition of cable screening. The screening effectiveness may be universally described by the maximum power output into the surroundings of the cable related to the power propagating in the cable. The power ratio is best expressed logarithmically as screening attenuation.

An often used procedure to determine the screening attenuation is the well-known “absorbing clamp method” given in IEC 62153-4-5. The drawback of this method is that the set-up requires relatively much space, does not exclude environmental effects – unless the measuring area is enclosed in a shielded cabin –, and that the available absorbing clamp transformers considerably limit the measurement sensitivity.

It suggests itself to limit the free space such that the said problems don't occur but wave propagation near the cable surface is not significantly changed. A triaxial measuring set-up is the solution. It has a one-sided short circuit between the metal tube and the cable screen. Power is fed into the terminated inner circuit of the cable and the disturbing power is measured at the opposite end of the outer circuit.

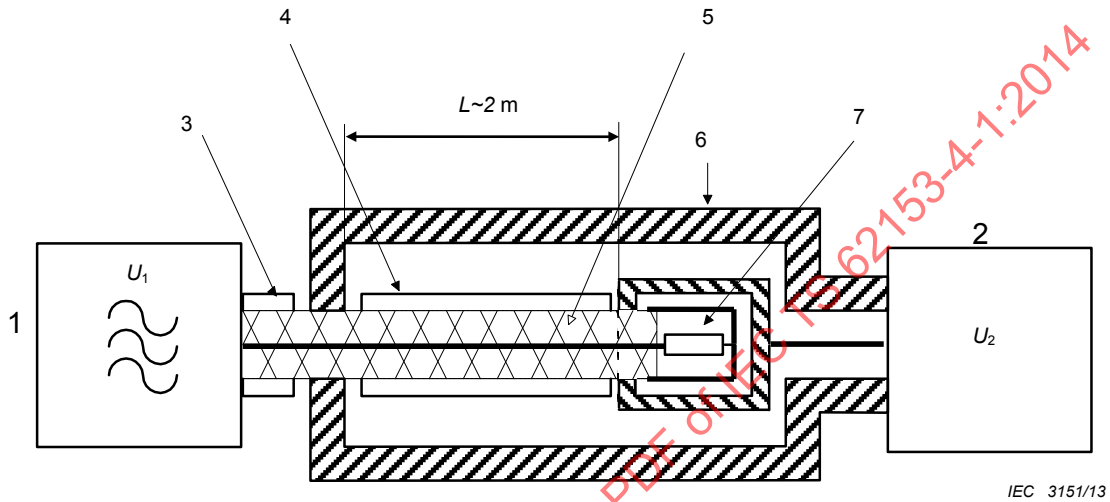
## 10.3 Theory of the triaxial measuring method

On the basis of the known reversibility of primary and secondary measuring circuits, the proposed measuring set-up, presented in Figure 45, is similar to the triaxial set-up for measuring the transfer impedance. The benefits of feeding the inner system, which is

terminated by its characteristic impedance, are the matching of the generator and reflection free wave propagation over the cable length.

The characteristic impedance of the outer circuit depends on the diameter of the measuring tube and the cable design. The effect of the mismatch in the outer circuit is discussed later on.

The equivalent circuit using lumped circuit elements (shown in Figure 46) facilitates the understanding of the theoretical relationships.



**Key**

- |   |                                  |
|---|----------------------------------|
| 1 signal generator                        | 5 cable screen                   |
| 2 calibrated receiver or network analyzer | 6 tube                           |
| 3 input voltage to cable under test       | 7 terminating resistor $R_1=Z_1$ |
| 4 cable sheath                            |                                  |

**Figure 45 – Triaxial measuring set-up for screening attenuation**

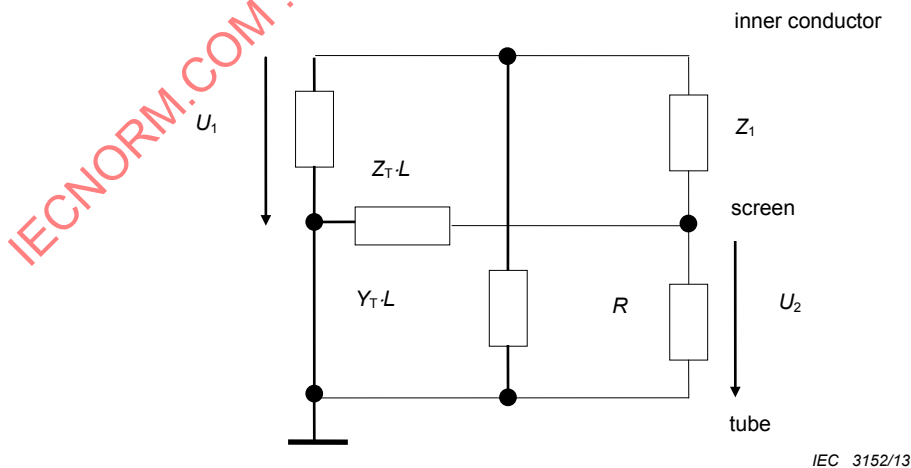


**Figure 46 – Equivalent circuit of the triaxial measuring set-up**

Based on the conditions of the objects to be measured, it is assumed that the transfer impedance  $Z_T$  is low and the reciprocal quantity of the coupling admittance  $Y_T$  is high in comparison with the characteristic impedances  $Z_1$  and  $Z_2$  and the load resistance  $R$ . Therefore, the feedback of the secondary circuit on primary circuit can be neglected.

When the frequency is low, one may consider the primary circuit shown in Figure 46 as a voltage divider and read the disturbing voltage ratio directly. The one-sided short circuit in the measuring circuit prevents the efficiency of the capacitance coupling admittance  $Y_T$ .

$$\frac{U_2}{U_1} \approx \frac{Z_T \cdot L}{Z_1} \quad (41)$$

In the high frequency range, where wave propagation has to be considered, one may expect the transfer impedance to be proportional to the frequency in most cases. Therefore it is expedient to use the following equation:

$$Z_T = R_T + j \cdot \omega M_T \approx j \cdot \omega M_T \quad (42)$$

and consider the effective mutual inductance per unit length  $M_T$  at high frequencies as an approximated constant quantity as it is usually done with the through capacitance  $C_T$ .

It is common practice to describe the capacitive coupling in the form of the capacitive coupling impedance  $Z_F$ , which is nearly invariant with respect to the geometry of the outer circuit (tube). [24], [27].

$$Z_F = Z_1 Z_2 Y_T = Z_1 Z_2 \cdot j \cdot \omega C_T \quad (43)$$

Furthermore, the attenuation constants  $\alpha_1$  and  $\alpha_2$  of the circuits may generally be neglected as, for example, the value of nearly 1 dB/m of the common cable type RG 58 at 3 GHz is relatively small compared to the usual measuring uncertainty.

In the relevant literature it is common practice to describe wave propagation in the form of phase constant [24], [25]. If the ratio between effective length and wave length is used instead of the phase constant, the periodic phenomena become clearer. With wave length  $\lambda_0$  in free space or  $\lambda_1, \lambda_2$  in the circuits 1 and 2, the following relation exists:

$$\beta_{1,2} \cdot L = 2\pi \cdot \sqrt{\varepsilon_{r1,2}} \cdot \frac{L}{\lambda_0} = 2\pi \frac{L}{\lambda_{1,2}} \quad (44)$$

According to the theory of wave propagation [25] and line crosstalk [26], a wave propagates in the matched inner circuit towards the matched end. In the outer circuit, a part of the induced wave propagates forwards to the measuring receiver and the other part is moving backwards to the short circuit. The total reflection at the short circuit reverses this backward wave and superposes it to the original forward wave, i.e. the sum can be obtained as measured value.

If the second circuit is matched at both ends, the backward wave would be measured at the generator end (near end) and the forward wave at the opposite end (far end) separately.

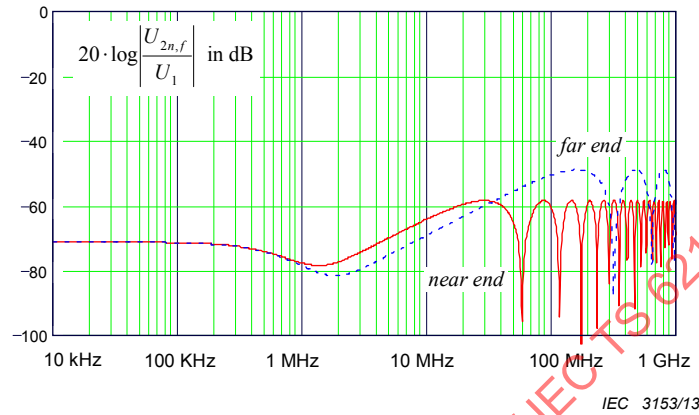
Hence equations for the near end are derived from [24]:

$$\frac{U_{2n}}{U_1} = \frac{Z_T + Z_F}{2Z_1} \frac{c_0}{j \cdot \omega (\sqrt{\varepsilon_{r1}} + \sqrt{\varepsilon_{r2}})} \left\{ 1 - e^{-j2\pi (\sqrt{\varepsilon_{r1}} + \sqrt{\varepsilon_{r2}}) \frac{L}{\lambda_0}} \right\} \quad (45)$$

and for the far end:

$$\frac{U_{2f}}{U_1} = \frac{Z_F - Z_T}{2Z_1} \frac{c_0}{j \cdot \omega (\sqrt{\epsilon_{r1}} - \sqrt{\epsilon_{r2}})} \cdot \left\{ 1 - e^{-j \cdot 2\pi (\sqrt{\epsilon_{r1}} - \sqrt{\epsilon_{r2}}) \frac{L}{\lambda_0}} \right\} \cdot e^{-j \cdot 2\pi \frac{L}{\lambda_2}} \quad (46)$$

Equations (47) and (48) are depicted in Figure 47 with the indicated parameters.



Calculation parameters

$C_T$	=	0,02	pF/m	$M_T$	=	0,4	nH/m
$R$	=	50	$\Omega$	$L$	=	2	m
$Z_1$	=	50	$\Omega$	$\epsilon_{r1}$	=	2,3	
$Z_2$	=	120	$\Omega$	$\epsilon_{r2}$	=	1,1	

Figure 47 – Calculated voltage ratio for a typical braided cable screen

With a short circuit and an unmatched measuring receiver, these original voltage waves cause additional voltage portions. The sum of all voltage portions is zero at the shorted end (near end) and  $U_2$  at the receiver end (far end). By use of the wave parameter and reflection factors or terminating resistors, it is possible to calculate all voltage portions and the voltage  $U_2$  from the primary induced voltage waves, see Equation (45) and Equation (46):

$$\left| \frac{U_2}{U_1} \right| \approx \left| \frac{Z_T - Z_F}{\sqrt{\epsilon_{r1}} - \sqrt{\epsilon_{r2}}} \cdot \left[ 1 - e^{-j \cdot \varphi_1} \right] + \frac{Z_T + Z_F}{\sqrt{\epsilon_{r1}} + \sqrt{\epsilon_{r2}}} \cdot \left[ 1 - e^{-j \cdot \varphi_2} \right] \right| \cdot \left| \frac{1}{\omega \cdot Z_1} \right| \cdot \left| \frac{c_0}{2 + (Z_2 / R - 1) \cdot (1 - e^{-j \cdot \varphi_3})} \right| \quad (47)$$

or in consideration of Equations (42) and Equation (43)

$$\left| \frac{U_2}{U_1} \right| \approx \left| \frac{M_T / Z_1 - C_T Z_2}{\sqrt{\epsilon_{r1}} - \sqrt{\epsilon_{r2}}} \left[ 1 - e^{-j \cdot \varphi_1} \right] + \frac{M_T / Z_1 + C_T Z_2}{\sqrt{\epsilon_{r1}} + \sqrt{\epsilon_{r2}}} \left[ 1 - e^{-j \cdot \varphi_2} \right] \right| \cdot \left| \frac{c_0}{2 + (Z_2 / R - 1) \cdot (1 - e^{-j \cdot \varphi_3})} \right| \quad (48)$$

where

$$\varphi_1 = 2\pi (\sqrt{\epsilon_{r1}} - \sqrt{\epsilon_{r2}}) \frac{L}{\lambda_0} \quad \varphi_2 = 2\pi (\sqrt{\epsilon_{r1}} + \sqrt{\epsilon_{r2}}) \frac{L}{\lambda_0} \quad \varphi_3 = \varphi_2 - \varphi_1 = 4\pi \sqrt{\epsilon_{r2}} \frac{L}{\lambda_0}$$

Calculated results for a typical braided cable screen are given in Figure 49. Another way to obtain the related induced voltage is given in [21].

The functional equation (see Figure 48)

$$|1 - e^{-j\varphi}| = |2 \times \sin(\varphi/2)| \quad \text{with } \varphi = \varphi_1, \varphi_2, \varphi_3 \quad (49)$$

shows that the equation of the voltage ratio contains three periodic partial functions of the ratio effective length  $L$  to wave length  $\lambda_0$ :

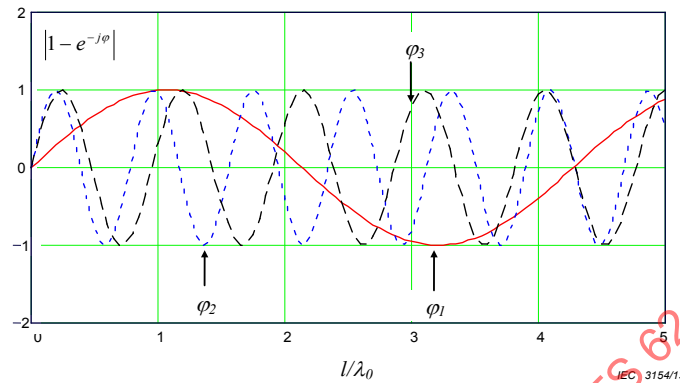
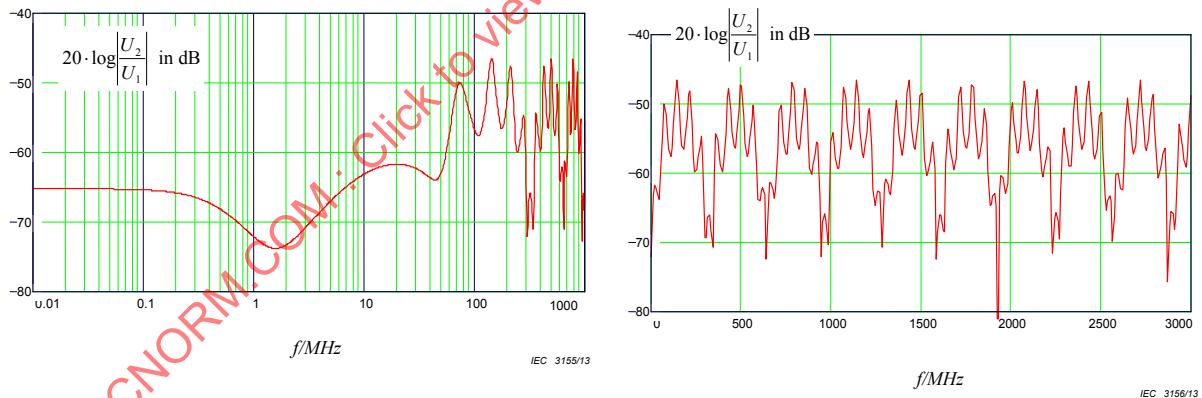


Figure 48 – Calculated periodic functions for  $\epsilon_{r1} = 2,3$  and  $\epsilon_{r2} = 1,1$

For low frequencies, when  $L \ll \lambda_0$  and, consequently,  $\sin(\varphi) \approx \varphi$ , Equation (48) changes into Equation (42), the result of the common measuring method for the transfer impedance.

An example of the theoretical curve of the voltage ratio is shown in Figure 49 in two diagrams: The left one, a) with a logarithmic scale to extend the lower frequency range and the right one b) with a linear scale up to very high frequencies.



a) Logarithmic frequency scale

b) Linear frequency scale

Calculation parameters

$C_T$	=	0,02	pF/m	$M_T$	=	0,4	nH/m
$R$	=	50	$\Omega$	$L$	=	2	m
$Z_1$	=	50	$\Omega$	$\epsilon_{r1}$	=	2,3	
$Z_2$	=	120	$\Omega$	$\epsilon_{r2}$	=	1,1	

Figure 49 – Calculated voltage ratio-typical braided cable screen

It is not useful to specify the induced power for an exact length of cable at a single frequency, anywhere between a minimum and maximum of the function. Only the periodic maximum voltage is important for the evaluation of the screening effectiveness. In the outer circuit, the wave propagation shall be nearly the same as in free space. Therefore, the characteristic

impedance  $Z_2$  is higher than the common input resistance  $R$  of the measuring receiver, i.e. 50  $\Omega$  or sometimes 75  $\Omega$ .

Consequently, periodic maximum values of the voltage ratio are obtained from Equation (47) and Equation (48), which are independent of the input resistance of the receiver  $R$  and of effective cable length  $L$ :

$$\left| \frac{U_2}{U_1} \right|_{\max} \approx \frac{C_0}{\omega Z_1} \cdot \left| \frac{Z_T - Z_F}{\sqrt{\varepsilon_{r1}} - \sqrt{\varepsilon_{r2}}} + \frac{Z_T + Z_F}{\sqrt{\varepsilon_{r1}} + \sqrt{\varepsilon_{r2}}} \right| \quad (50)$$

or in consideration of Equation (42) and Equation (43):

$$\left| \frac{U_2}{U_1} \right|_{\max} \approx \left| \frac{M_T/Z_1 - C_T Z_2}{\sqrt{\varepsilon_{r1}} - \sqrt{\varepsilon_{r2}}} + \frac{M_T/Z_1 + C_T Z_2}{\sqrt{\varepsilon_{r1}} + \sqrt{\varepsilon_{r2}}} \right| \cdot C_0 \quad (51)$$

At first sight,  $C_T$ ,  $Z_2$ ,  $\varepsilon_{r2}$  and  $Z_F$  appear as random quantities which depend on freely chosen dimensions of the measuring tube. In reality, however, the voltage ratio is independent of the characteristic impedance of the outer circuit since  $C_T Z_2$  and  $Z_F$  are practically invariant with respect to the dimensions of the measuring tube [24], [27]. Furthermore, the influence of the cable sheath on the resulting relative permittivity  $\varepsilon_{r2}$  is negligible if the design of the measuring tube takes into account the requirement for a wave propagation which is approximately the same as in the free space; in consequence  $\varepsilon_{r2} \approx 1,0$ .

The periodic maximum value is independent of the effective length  $L$  and frequency  $f$  or wave length  $\lambda$ . A measured frequency response would hint at a frequency-related quantity rather than the pure mutual inductance  $M_T$ .

As it is seen from Figure 48 and Figure 49, the envelope rise is reached with the first maximum of the wide period at:

$$\frac{\lambda_0}{L} \leq 2 \cdot \left| \sqrt{\varepsilon_{r1}} - \sqrt{\varepsilon_{r2}} \right| \quad \text{or} \quad f > \frac{C_0}{2 \cdot L \cdot \left| \sqrt{\varepsilon_{r1}} - \sqrt{\varepsilon_{r2}} \right|} \quad (52)$$

In this frequency range,  $Z_T$  can be calculated if  $Z_F$  is negligible:

$$\left| Z_T \right| \approx \frac{\omega \cdot Z_1 \cdot \left| \varepsilon_{r1} - \varepsilon_{r2} \right|}{2 \cdot C_0 \cdot \sqrt{\varepsilon_{r1}}} \cdot \left| \frac{U_2}{U_1} \right|_{\max} \quad (53)$$

#### 10.4 Screening attenuation

The screening attenuation is defined as the logarithmical ratio of the maximum power in the secondary (outer) circuit to the power propagating in the primary (inner) circuit.

$$a_s = -10 \times \log_{10} \left( \text{Env} \left| \frac{P_{r,\max}}{P_1} \right| \right) \quad (54)$$

The power coupled into the outer circuit depends on  $Z_2$  although the peak voltage is independent of it. Thus a normalised value of the characteristic impedance of the outer circuit  $Z_s$  must be defined. It is common practice to define  $Z_s = 150 \Omega$  [24].

In the standardised "absorbing clamp method" (see IEC 62153-4-5), the outer circuit is matched with  $Z_2$ , and the radiated power is the sum of the near end and far end crosstalk. From the comparison of that measuring circuit with the measuring circuit of the triaxial method results the relation of the measured power to the radiated power.

The equivalent circuit for an electrical short part of the length  $\Delta L$  and for a negligible capacitive coupling illustrates the circumstances in Figure 50.

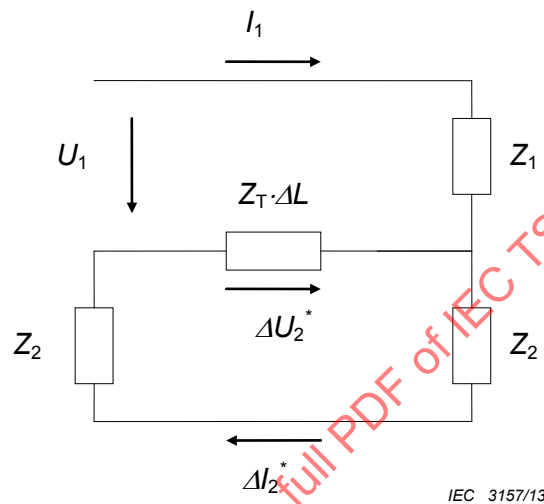


**Figure 50 – Equivalent circuit for an electrical short part of the length  $\Delta L$  and negligible capacitive coupling**

The power in the primary circuit is:

$$P_1 = U_1 \cdot I_1 = \frac{U_1^2}{Z_1} = I_1^2 \cdot Z_1 \quad (55)$$

The power in the secondary circuit, which is coupled by the transfer impedance  $Z_T$  is

$$P_2^* = \Delta U_{2^*} \cdot \Delta I_{2^*} \quad \Delta U_{2^*} = I_1 \cdot Z_T \cdot \Delta L \quad (56)$$

$$\Delta I_{2^*} = \frac{\Delta U_{2^*}}{2 \cdot Z_2} \quad (57)$$

Thus

$$\frac{P_2^*}{P_1} = \frac{(\Delta U_{2^*})^2}{2 \cdot Z_2} \cdot \frac{1}{I_1^2 \cdot Z_1} = \frac{(Z_T \cdot \Delta L)^2}{2 \cdot Z_1 \cdot Z_2} \quad (58)$$

If the secondary circuit is short circuited at one end and terminated by  $R$  at the other end, the power measured at  $R$  is

$$\frac{P_2}{P_1} = \frac{(Z_T \cdot \Delta L)^2}{Z_1 \cdot R} \quad (59)$$

Thus

$$\frac{P_2^*}{P_2} = \frac{R}{2Z_2} \quad (60)$$

or in the case of radiation due to the normalised characteristic impedance of the environment

$$\frac{P_r}{P_2} = \frac{P_{r,max}}{P_{2,max}} = \frac{R}{2Z_s} \quad (61)$$

Thus the screening attenuation is calculated by:

$$\begin{aligned} a_s &= 10 \times \log_{10} \left| \frac{P_1}{P_{r,max}} \right| = 10 \times \log_{10} \left| \frac{P_1}{P_{2,max}} \frac{2Z_s}{R} \right| \\ &= 10 \times \log_{10} \left| \left( \frac{U_1}{U_{2,max}} \right)^2 \frac{2Z_s}{Z_1} \right| \\ &= 20 \times \log_{10} \left| \frac{U_1}{U_{2,max}} \right| + 10 \times \log_{10} \left| \frac{300}{Z_1} \right| \end{aligned} \quad (62)$$

### 10.5 Normalised screening attenuation

From Equation (50), it is seen that the maximum voltage ratio and therefore the screening attenuation is a function of the velocity difference between the primary and secondary circuit. Therefore the test results may also be presented for normalised conditions where  $Z_s = 150 \Omega$  and the velocity difference  $|\Delta v/v_1| = 10 \%$  or  $\epsilon_{r1}/\epsilon_{r2,n} = 1,21$ .

The normalised screening attenuation is calculated by:

$$a_{s,n} = 20 \times \log_{10} \left| \frac{\omega \cdot \sqrt{Z_1 \cdot Z_s} \cdot \left| \sqrt{\epsilon_{r1}} - \sqrt{\epsilon_{r2,n}} \right|}{Z_T \cdot c_0} \right| \quad (63)$$

With respect to Equation (50), Equation (62) and Equation (63) and assuming negligible  $Z_F$ , the difference  $\Delta a$  of the normalised and the measured screening attenuation is given by:

$$\Delta a = a_{sn} - a_s = 20 \times \log_{10} \left( \sqrt{2} \cdot \frac{\left| 1 - \sqrt{\frac{\epsilon_{r2,n}}{\epsilon_{r1}}} \right|}{\left| 1 - \frac{\epsilon_{r2,t}}{\epsilon_{r1}} \right|} \right) \quad (64)$$

where  $\epsilon_{r2,t} \approx 1,1$  is the relative dielectric permittivity of the outer circuit (tube) during measurement.

Table 11 shows the difference  $\Delta a$  for typical cable dielectric.

**Table 11 –  $\Delta a$  in dB for typical cable dielectrics**

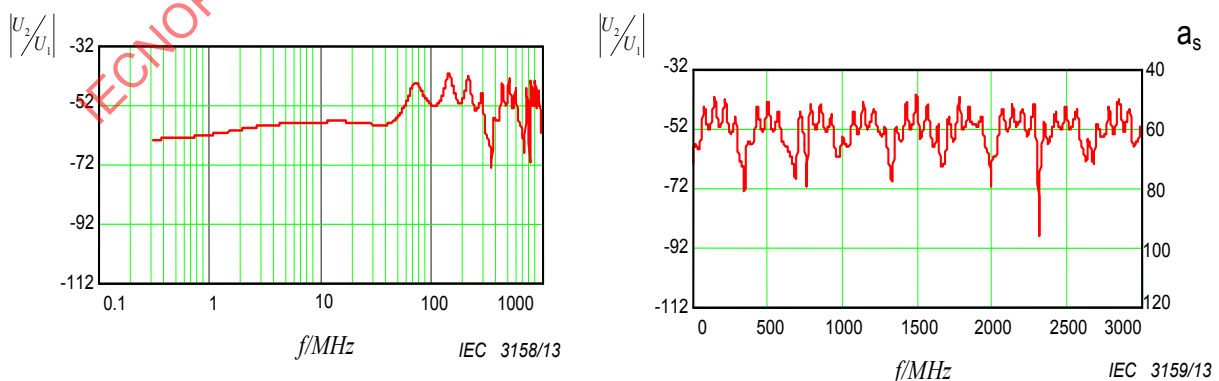
Outer circuit (tube) $\epsilon_{r2,n}$	Cable dielectric $\epsilon_{r1}$	$\Delta a$ in dB
1,9	2,3	-12
1,7	2,1	-11
1,3	1,6	-8
1,1	1,3	-2

**10.6 Measured results**

The measured screening attenuation of common types of cables shows the validity of the theoretical basis. The voltage ratio  $U_2/U_1$  is measured by means of a network analyser having an internal resistance of  $50 \Omega$ . The screening attenuation  $a_s$  is presented in Figures 51 to Figure 55 for three types of cables as a function of frequency.

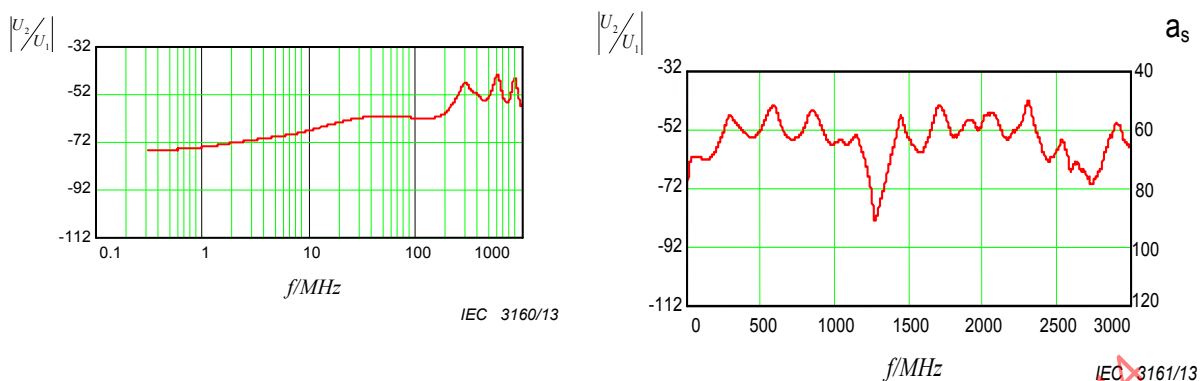
- RG 58 according to MIL-C-17 with single copper braid;
- HF 75 0,7/4,8 2YCY with a dielectric of solid PE and a single copper braid;
- HF 75 1,0/4,8 02YCY with a dielectric of foamed PE and a single copper braid;
- RG 223 according to MIL-C-17 with double copper braid.

The theoretical relations of the transitions from low to medium and high frequencies – appearing in the calculated curve in Figure 47 – become most evident with the single copper braid (see Figure 51). Here the voltage ratio is independent of the frequency up to approximately 0,4 MHz but proportional to the effective length of the measuring tube like the transfer impedance. At high frequencies, higher than about 100 MHz, super-positioned periodic functions occur showing maximum values of approximately equal magnitude independent of frequency and effective length. The frequency at which the superposition appears is reciprocal to the effective length just as the frequency spacing of the peak values (see Figure 51 and Figure 52). In contrast to the effective length of 2 m, the effective length of 0,5 m does not allow to plot the screening envelope curve with sufficient accuracy any more, due to the wide spacing of the long period maximum values.



Logarithmic voltage ratio  $|U_2/U_1|$  in dB (left hand scale) and screening attenuation  $a_s$  (right hand scale) Coupling length  $L = 2$  m.

**Figure 51 –  $a_s$  of single braid screen, cable type RG 58,  $L = 2$  m**

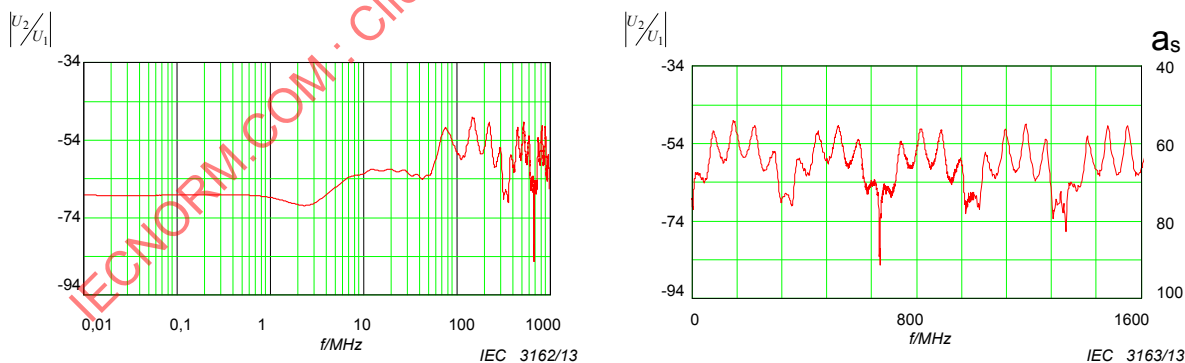


Logarithmic voltage ratio  $|U_2/U_1|$  in dB (left hand scale) and screening attenuation  $a_s$  (right hand scale)  
Coupling length  $L = 0,5$  m.

**Figure 52 –  $a_s$  of single braid screen, cable type RG 58,  $L = 0,5$  m**

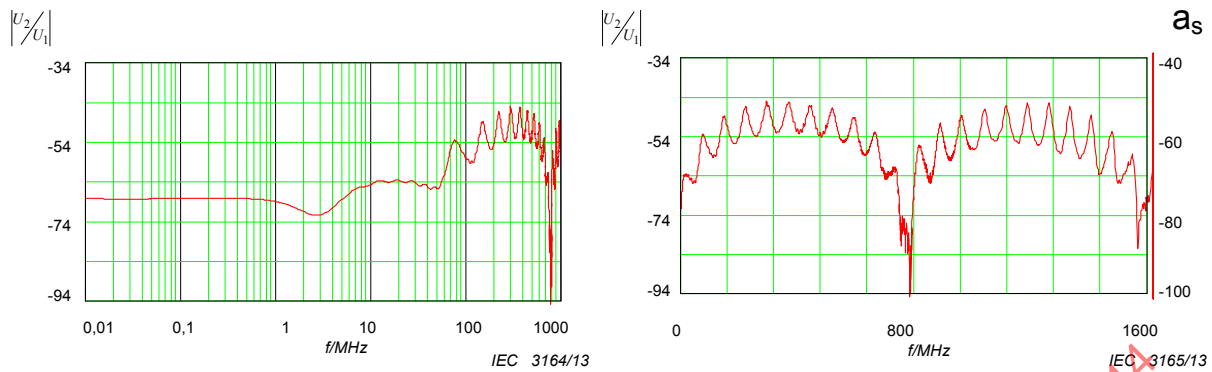
The periodic frequency spacing in the measured curve and the screening attenuation are dependent on the velocity difference between primary and secondary circuit (Equation (47) and Equation (50)). This theoretical relation becomes most evident in Figure 53 and Figure 54 where the cable screens of both cables are equal, but the relative permittivities of the cable dielectric  $\epsilon_{r1}$  and thus the velocity difference in the test set-up differ. In Figure 53 we have  $\epsilon_{r1}=2,3$  and a velocity difference  $|\Delta v/v_1| \approx 45$  whereas in Figure 54  $\epsilon_{r2}=1,7$  and  $|\Delta v/v_1| \approx 24$  %. Thus, in Figure 54, we have a larger frequency spacing of the wide period and also a lower screening attenuation. But the normalised screening attenuation of both cable screens is equal,  $a_s \approx 43$  dB.

For the cable with double copper braid (see Figure 55), the theoretical relations become apparent only if the measurement is very accurate and the receiver is sensitive enough for low induced voltage. Apart from its level and distinct function of frequency, the screening attenuation of the double copper braid is obviously similar to that of the single copper braid.



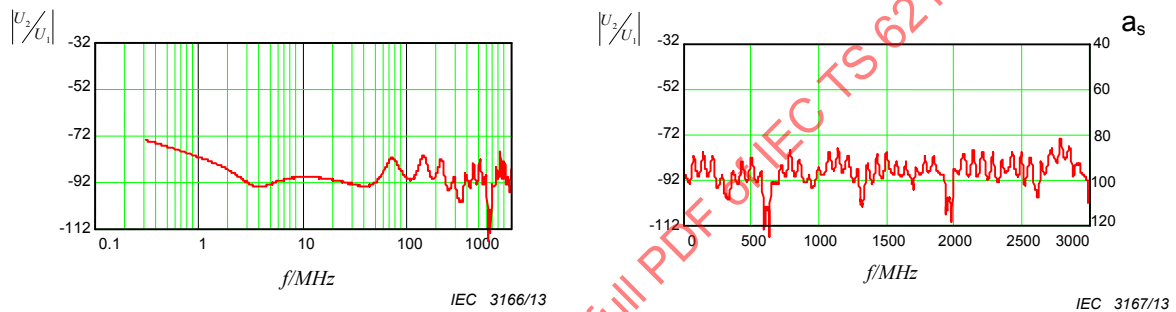
Logarithmic voltage ratio  $|U_2/U_1|$  in dB (left hand scale) and screening attenuation  $a_s$  (right hand scale)  
 $\epsilon_{r1}=2,3$ ,  $|\Delta v/v_1|=45$  %, coupling length  $L = 2$  m.

**Figure 53 –  $a_s$  of cable type HF 75 0,7/4,8 2YCY (solid PE dielectric)**



Logarithmic voltage ratio  $|U_2/U_1|$  in dB (left hand scale) and screening attenuation as (right hand scale),  $\epsilon_{r1}=1,7$ ,  $|\Delta v/v_1|=24\%$ , coupling length  $L = 2$  m.

**Figure 54 –  $a_s$  of cable type HF 75 1,0/4,8 02YCY (foam PE dielectric)**



Logarithmic voltage ratio  $|U_2/U_1|$  in dB (left hand scale) and screening attenuation as (right hand scale)  
Coupling length  $L = 2$  m.

**Figure 55 –  $a_s$  of double braid screen, cable type RG 223**

### 10.7 Comparison with absorbing clamp method

In the absorbing clamp method according to IEC 62153-4-5, in principle, the current on the outside of the cable under test is measured. The matched outer circuit is directly induced by the inner circuit. The power in the outer circuit is related to the current by calibration.

Table 12 gives a comparison of results of some coaxial cables with different screen designs. They show a maximum difference of 3 dB.

**Table 12 – Comparison of results of some coaxial cables**

Cable type, screen	Screening attenuation $a_s$ in dB		
	Frequency GHz	Absorbing clamp method	Triaxial method
RG 58, single braid	0,2	51	48
	0,8	52	50
	3,0	-	50
RG 214, braided	0,2	51	50
	0,8	54	51
	3,0	-	53
RG 214, double braid	0,2	79	79
	0,8	82	81
	3,0	-	83
RG 223, double braid	0,2	86	88
	0,8	90	90
	3,0	-	83

### 10.8 Practical design of the test set-up

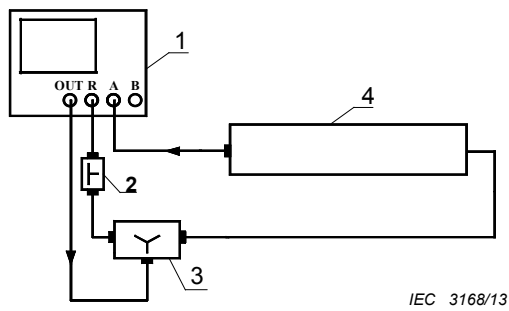
The set-up to measure the screening attenuation  $a_s$  is in principle the set-up to measure the attenuation of RF devices, where the voltage ratio  $U_2/U_1$  is measured. The cable under test is connected to the output of a RF-generator, the output of the coupling tube is connected to the measuring input of a RF-receiver. Generator and receiver may be included in a sensitive network analyser (see Figure 45 and Figure 56).

The measuring tube shall be of a material, which is not ferromagnetic and good conductive (for example brass), with an inner diameter of about 40 mm to 50 mm and a length of 2 m to 4 m or more, where the total length of 2 m or more may be achieved by screwing together single parts of tubes (RF-tight).

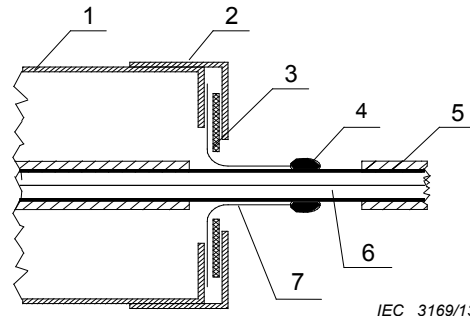
One way to realise the short circuit at the near end of the CUT is to solder a braid of silvered copper wires to a punched disk of copper. This "contacting braid" is fixed on the outer conductor of the cable sample where the sheath is removed, e.g. with cable clamps. The electrical contact between this contacting braid and the measuring tube may then be achieved by a jam-disk, which is fixed by the clasp cap, which is screwed to the tube (see Figure 57).

The contacting braid, which is prepared once, may be used several times. Soldering of the screen of the cable sample to the tube – as usual at the classic triaxial – set-up is no longer required and the time to prepare the CUT is minimised.

The termination at the far end of the CUT is achieved by a resistor of the same value as the characteristic impedance of the CUT. Experience has shown that the best results are obtained with SMD resistors, respectively so called "mini-melf-resistors" with low mechanical dimensions and good RF-characteristics, which are soldered directly between the inner and the outer conductor of the CUT. To avoid radiation and to contact the outer conductor of the CUT, this termination is shielded by a case, which is well conductive (see Figure 45).



IEC 3168/13



IEC 3169/13

**Key**

- 1 Network analyser
- 2 Attenuator 20 dB
- 3 Power divider
- 4 Measuring tube

**Key**

- 1 tube of brass
- 2 clasp cap
- 3 jam disk
- 4 contact to the cable screen of CUT
- 5 sheath of cable sample
- 6 cable under test (CUT)
- 7 contacting braid

**Figure 56 – Schematic for the measurement of the screening attenuation  $a_s$**

**Figure 57 – Short circuit between tube and cable screen of the CUT**

To obtain clear and reproducible results, the sample must be well centered in the measuring tube. A slackly mounted cable under test in the measuring tube will lead to deviations of the characteristic impedance  $Z_2$  of the outer system over the coupling length and thus to additional reflections. Centering may be achieved by mounting the sample in punched polyethylene disks which are placed in the measuring tube, or better by stretching the sample under test, e.g. with a desk vice. Also, vertical mounting of the measuring tube is useful.

**10.9 Influence of mismatches**

**10.9.1 Mismatch in the outer circuit**

Mismatches in the outer circuit may result in significant errors. With the screening case of the terminating resistor, a mismatch is inserted into the outer circuit, which affect the results significantly depending on the mechanical dimensions [28]. The mean characteristic impedance of the outer circuit, formed by the cable screen and the measuring tube, respectively in the outer circuit at the screening case is given by:

$$Z_2 \approx \frac{60}{\sqrt{\epsilon_{r2}}} \cdot \ln\left(\frac{D_m}{D_a}\right) \tag{65}$$

$$Z_3 \approx \frac{60}{\sqrt{\epsilon_{r2}}} \cdot \ln\left(\frac{D_m}{D_{case}}\right) \tag{66}$$

where

- $D_a$  is the outer diameter of cable screen;
- $D_{case}$  is the outer diameter of screening case;
- $D_m$  is the inner diameter of measuring tube.

A deviation between  $D_{case}$  and  $D_a$  thus results in different impedances and therefore in additional reflections in the outer circuit. For example, a screening case with an outer diameter of  $D_{case} = 1,2 \cdot D_a$  results in a impedance  $Z_3$  which is  $11 \Omega$  less than  $Z_2$  ( $\epsilon_{r2}=1,0$ ).

Figure 58 facilitates the understanding of the theoretical relationships.

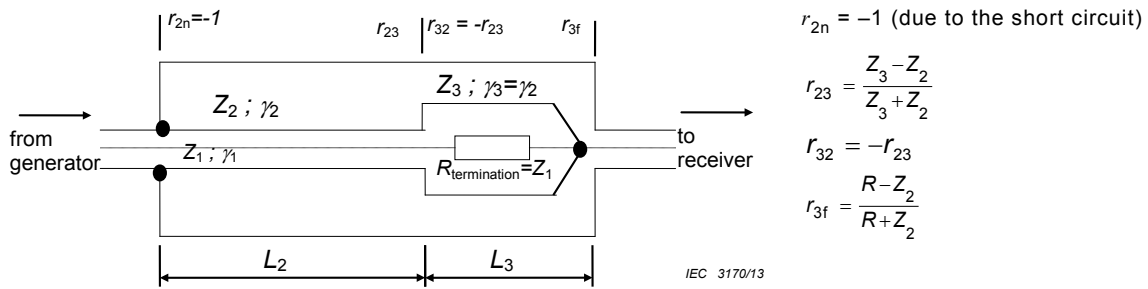


Figure 58 – Triaxial set-up, impedance mismatches

The outer circuit thus consists of two lines with different characteristic impedances. To calculate the voltage at the receiver, some additional variables have to be defined.

$U_h$  is the voltage, which is coupled from the cable under test into the outer circuit ( $Z_2, \gamma_2, L_2$ ), propagation to the far end, including the total reflection at the near end.

$$\frac{U_h}{U_1} = \frac{U_{2f}}{U_1} + \frac{U_{2n}}{U_1} \cdot r_{2n} \cdot e^{-\gamma_2 \cdot L_2} \quad (67)$$

Where  $U_{2f}, U_{2n}$  are the voltages in a matched outer circuit according to Equation (42) and Equation (44).

Multiple reflections of this wave between the short circuit at the near end of the outer circuit and the transition from  $Z_2$  to  $Z_3$  are described by  $T_{2f}$ .

$$T_{2f} = \frac{1 + r_{23}}{1 - r_{2n} \cdot r_{23} \cdot e^{-2 \cdot \gamma_2 \cdot L_2}} \quad (68)$$

The superposition of the wave which is propagating from the line  $Z_2, \gamma_2, L_2$  to the far end (receiver) of the line  $Z_3, \gamma_3, L_3$  – including the multiple reflections between the transitions from  $Z_3$  to  $Z_2$  and  $Z_3$  to  $R$  (receiver input) – is described by  $T_{3f}$ .

$$T_{3f} = \frac{1 + r_{3f}}{1 - r_{32} \cdot r_{3f} \cdot e^{-2 \cdot \gamma_3 \cdot L_3}} \cdot e^{-\gamma_3 \cdot L_3} \quad (69)$$

The superposition of the wave which is propagating from line  $Z_3, \gamma_3, L_3$  to line  $Z_2, \gamma_2, L_2$  is described by  $T_{32}$ .

$$T_{32} = \frac{1 + r_{32}}{1 - r_{32} \cdot r_{3f} \cdot e^{-2 \cdot \gamma_3 \cdot L_3}} \cdot r_{3f} \cdot e^{-2 \cdot \gamma_3 \cdot L_3} \quad (70)$$

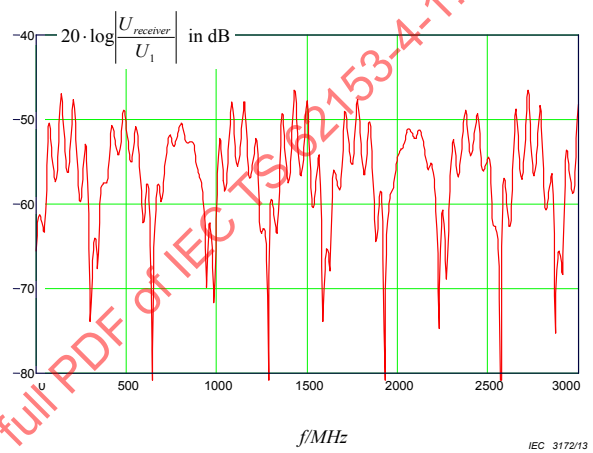
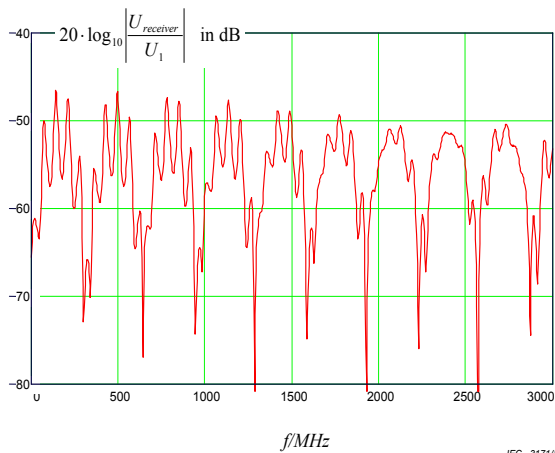
The superposition of the wave which is propagating from line  $Z_2, \gamma_2, L_2$  to line  $Z_3, \gamma_3, L_3$  is described by  $T_{23}$ .

$$T_{23} = \frac{1 + r_{23}}{1 - r_{2n} \cdot r_{23} \cdot e^{-2 \cdot \gamma_2 \cdot L_2}} \cdot r_{2n} \cdot e^{-2 \cdot \gamma_2 \cdot L_2} \quad (71)$$

In consideration of all these reflections, the voltage at the receiver is calculated by:

$$\frac{U_{\text{receiver}}}{U_1} = \frac{U_h}{U_1} \cdot \frac{T_{2f} \cdot T_{3f}}{1 - T_{32} \cdot T_{23}} \quad (72)$$

Figure 59 and Figure 60 show the calculated voltage ratio for a cable screen with the same characteristics as in Figure 49 but with different dimensions of the screening case.



quantities used:

$$C_T = 0,02 \text{ pF/m}$$

$$M_T = 0,4 \text{ nH/m}$$

$$R = 50 \text{ } \Omega \quad Z_1 = 50 \text{ } \Omega \quad \epsilon_{r1} = 2,3$$

$$Z_2 = 120 \text{ } \Omega \quad \epsilon_{r2} = 1,1 \quad L_2 = 2 \text{ m}$$

$$Z_3 = 90 \text{ } \Omega \quad \epsilon_{r2} = 1,1 \quad L_3 = 0,03 \text{ m}$$

**Figure 59 – Calculated voltage ratio including multiple reflections caused by the screening case**

quantities used:

$$C_T = 0,02 \text{ pF/m}$$

$$M_T = 0,4 \text{ nH/m}$$

$$R = 50 \text{ } \Omega \quad Z_1 = 50 \text{ } \Omega \quad \epsilon_{r1} = 2,3$$

$$Z_2 = 120 \text{ } \Omega \quad \epsilon_{r2} = 1,1 \quad L_2 = 2 \text{ m}$$

$$Z_3 = 90 \text{ } \Omega \quad \epsilon_{r2} = 1,1 \quad L_3 = 0,1 \text{ m}$$

**Figure 60 – Calculated voltage ratio including multiple reflections caused by the screening case**

To avoid the disturbing reflections at the screening case, the reflection factor  $r_{23}$  or (and)  $r_{3f}$  must be minimized. A worthwhile solution in practice is to design the screening case in a way that the characteristic impedance  $Z_3$  is approximately of the same value as the input resistance of the receiver. In this case, the reflection factor  $r_{3f} \approx 0$  and thus  $T_{3f}=1$ ,  $T_{32}=0$ . This results in a voltage ratio which is equal to the ideal frequency response of Equation (48).

## 10.9.2 Mismatch in the inner circuit

### 10.9.2.1 General

A mismatch in the inner circuit, i.e. between the generator and the DUT or between the DUT and the load resistor, may result in significant errors.

The mismatch between the DUT and the load resistor can be reduced by choosing an appropriate load resistor. Theoretical and practical investigations [28] show that a mismatch of the terminating resistor in the inner circuit is of low influence as long as:

$$\frac{|R_{\text{termination}} - Z_1|}{Z_1} \cdot 100 \% \leq 10 \%$$

However, when measuring cables, especially multi-conductor cables having a “coaxial” impedance significantly different from the generator impedance, one has either to use impedance matching adapters or to take into account the reflection loss of the mismatch between generator and DUT.

Impedance matching adapters are only available for standard impedances like 60 Ω or 75 Ω. For other impedances, one would have to build homemade adapters. However, those adapters only work for frequencies up to some 10 MHz. This is illustrated in Figure 61. It shows the attenuation and return loss of a 50 Ω to 5 Ω impedance matching adapter. A DUT impedance of 5 Ω is typical when measuring multi-pair cables with individually screened pairs or when measuring high voltage cables for electrical vehicles.

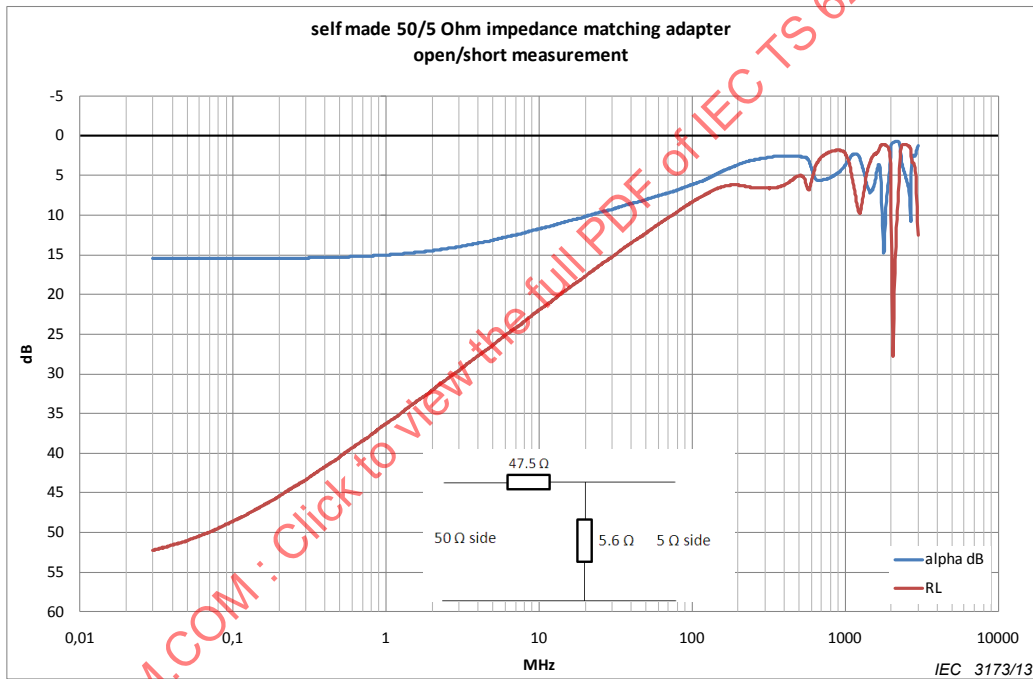


**Figure 61 – Attenuation and return loss of a self-made 50 Ω to 5 Ω impedance matching adapter**

Therefore it is recommended not to use self-made impedance matching adapters but to measure with mismatch between generator and DUT and to take into account the reflection loss of the mismatch:

$$a_s = 10 \times \log_{10} \left| \frac{P_1}{P_{S_{\text{max}}}} \right| = 10 \times \log_{10} \left| \frac{P_1}{P_{2_{\text{max}}}} \times \frac{2 \times Z_s}{R} \right| \tag{73}$$

$$a_s = \text{Env} \left\{ -20 \times \log_{10} |S_{21}| + |\Gamma_s| + 10 \times \log_{10} \left| \frac{300}{Z_1} \right| \right\} \tag{74}$$

where

$a_s$  is the screening attenuation related to the radiating impedance  $Z_s$  of 150  $\Omega$  in dB;

$Env$  is the minimum envelope curve of the measured values in dB;

$S_{21}$  is the scattering parameter  $S_{21}$  (complex quantity) of the set-up where the primary side of the two port is the DUT and the secondary side is the tube, i.e. the operational attenuation of the set-up;

$\Gamma_s$  is the reflection loss of the junction between the generator and DUT.

The junction loss is obtained from the reflection coefficient (scattering parameter  $S_{11}$ ) as described in 10.9.2.2. Where  $S_{11}$  could either be measured or calculated using the mean characteristic impedances for the purpose of simplification:

$$S_{11} = \frac{Z_1 - Z_0}{Z_1 + Z_0} \quad (75)$$

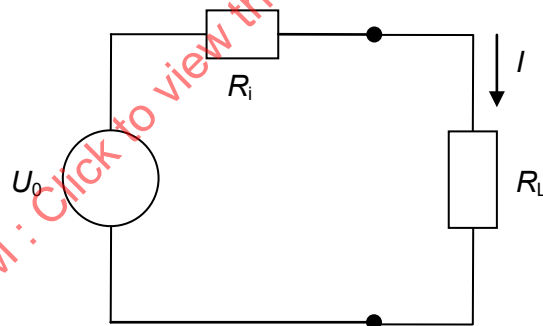
where

$Z_1$  is the nominal characteristic impedance of the cable under test in  $\Omega$ ;

$Z_0$  is the output impedance of the generator, i.e. system impedance of the network analyser, in  $\Omega$ .

### 10.9.2.2 Reflection loss of a junction

In case a source with an inner resistance  $R_i$  feeds a load with a different resistance  $R_L$ , power is lost compared to the matched case due to the mismatch. If the source is connected to the junction by a transmission line with a characteristic impedance  $Z_1=R_i$  and the load is connected to the junction by a transmission line with a characteristic impedance  $Z_2=R_L$ , the equivalent circuit is as shown in Figure 62:



IEC 3174/13

Figure 62 – equivalent circuit of a load resistance connected to a source

The power in the load resistance  $R_L$  is given by

$$P = I^2 R_L = \left( \frac{U_0}{R_i + R_L} \right)^2 R_L = U_0^2 \frac{R_L}{(R_i + R_L)^2} \quad (76)$$

In case of impedance matching  $R_L=R_i$ , the maximum power  $P_0$  is fed:

$$P_0 = U_0^2 \frac{R_i}{4R_i^2} = \frac{1}{4} U_0^2 \frac{1}{R_i} \quad (77)$$

The ratio of Equations (76) and (77) describes the loss:

$$\frac{P}{P_0} = \frac{U_0^2 R_L}{(R_i + R_L)^2} \frac{4R_i}{U_0^2} = \frac{4R_L R_i}{(R_i + R_L)^2} \tag{78}$$

The following auxiliary calculation introduces the reflection coefficient  $r$  :

$$1 - r^2 = 1 - \left( \frac{R_L - R_i}{R_L + R_i} \right)^2 = \frac{(R_L + R_i)^2}{(R_L + R_i)^2} - \frac{(R_L - R_i)^2}{(R_L + R_i)^2} = \frac{R_L^2 + 2R_L R_i + R_i^2 - R_L^2 + 2R_L R_i - R_i^2}{(R_L + R_i)^2} = \frac{4R_L R_i}{(R_L + R_i)^2} \tag{79}$$

Using Equation (79), the power ratio (Equation (78)) becomes:

$$\frac{P}{P_0} = 1 - r^2 \tag{80}$$

The magnitude in dB therefore is (see also IEC/TR 62152 Equation C.67)

$$\Gamma_s = -10 \log_{10} |1 - r^2| \tag{81}$$

## 11 Background of the shielded screening attenuation test method for measuring the screening effectiveness of feed-throughs and electromagnetic gaskets (IEC 62153-4-10)

### 11.1 General

The proper function of modern communication equipment is strongly influenced by the proper EMI shielding of electrical components. Feed-through configurations with poor ground connections can contribute significantly to the overall EMI level of communication equipment [1]. Electromagnetic gaskets like contact springs or conducting polymers can dramatically reduce conducted and radiated emissions, respectively. A cross-sectional sketch of the typical configuration of a feed-through is shown in Figure 63. The connector body is soldered onto the circuit board and thus electrically connected to the ground potential or equipotential of the electronic circuitry.

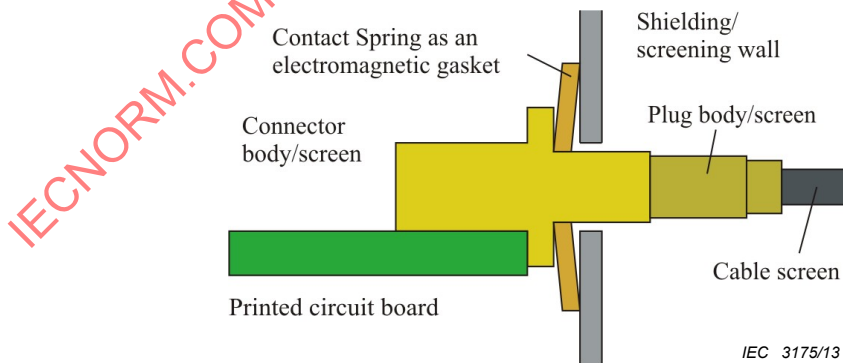


**Figure 63 – Cross-sectional sketch of a typical feed-through configuration**

At higher frequencies, the potential of the circuit board’s ground plane is usually not equal to that of the shielding box. A contact spring short circuits this potential difference. If the contact spring were not present in the setup of Figure 63, excessive radiation of electromagnetic waves along the cable’s outer conductor will be the result.

It is usually a very time-consuming task to evaluate the shielding or screening effectiveness of a feed-through or electromagnetic gasket (EMI or EMC gasket) in a test configuration as e.g.

is recommended in CISPR 25. The measurement setups that are described there are generally based on some kind of free space measurement, which requires an anechoic chamber.

The introduction of well-defined electrically conducting boundaries in a test fixture would greatly simplify the measurement procedure. This is possible by application of a coaxial test setup based on the experience in measuring shielding effectiveness of cables, cable assemblies and connectors with the standardized shielded triaxial screening effectiveness test methods [5], [7] and [10] by IEC and CENELEC.

## 11.2 Theoretical background of the test Fixtures and their equivalent circuit

A cross-sectional view of the test fixture is shown in Figure 64. The left section represents the inner area of a shielding box. A signal is fed to the outer conductor of the connector under test by means of the coaxial line's inner and outer conductor. The amount of RF leakage that can be detected on the opposite side of the shielding wall is picked up by the coaxial line to the right. A separate EMI gasket can be tested with the configuration in Figure 64a).

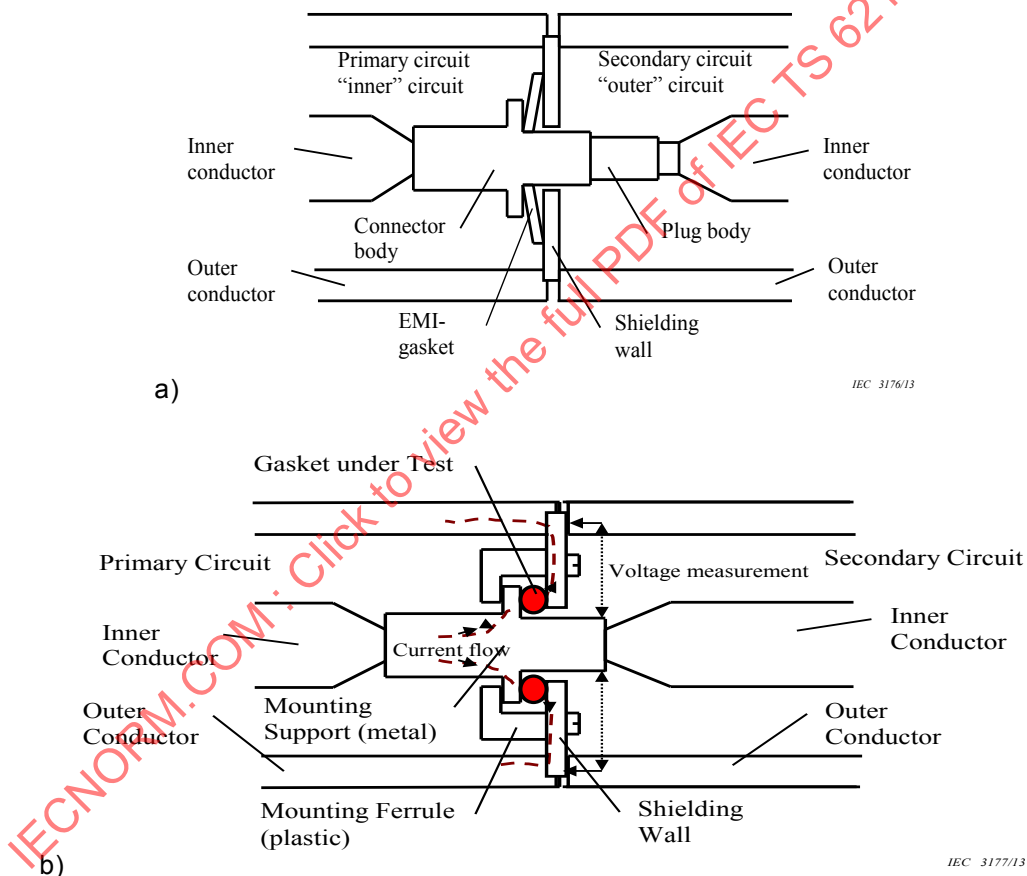
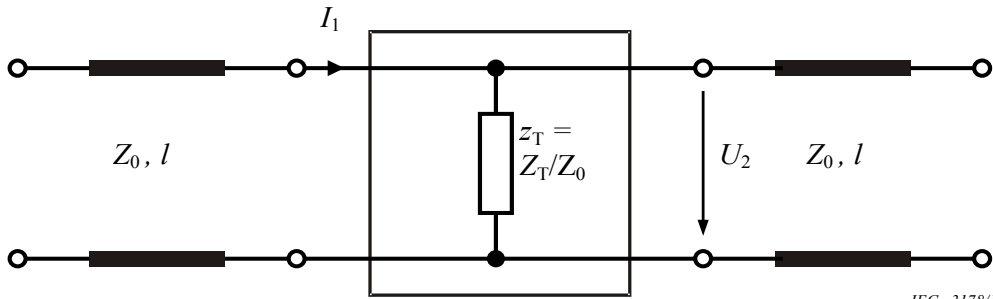


**Figure 64 – Cross-sectional sketch of the test fixture with a feed-through connector (a) and EMI gasket (b) under test**

The test fixture consists of cascaded two-ports formed by a primary and a secondary transmission line separated with an isolating metallic plate to mount the test objects. The equivalent circuit of the test fixtures is shown in Figure 65.



**Key**

- $z_T = Z_T/Z_0$     normalised transfer impedance
- $Z_T$             transfer impedance of the device under test
- $Z_0$             reference impedance (generator and receiver impedance)
- $I_1$             current in the primary transmission line
- $U_2$             coupled voltage to the secondary circuit
- $l$               length of the coaxial line section

**Figure 65 – Equivalent circuit of the test fixture**

In the case of a two-port scattering parameter  $S_{21}$  or forward transfer function measurement, where the two ports of the network analyzer are connected to both coaxial line sections,  $S_{21}$  is a direct measure for the shielding efficiency of a feed-through or EMI gasket tested in well-defined circumstances that make repeatable and comparable tests possible.

In an equivalent circuit of the measurement of a feed-through or gasket, the transfer impedance is shunt impedance  $Z_T$  between the primary and secondary circuit.

The transfer impedance of an electrically short screen is defined as the quotient of the open circuit voltage  $U_2$  induced to the secondary circuit by the current  $I_1$  fed into the primary circuit or vice versa.  $Z_T$  of an electrically short screen is expressed in ohms [ $\Omega$ ] or decibels in relation to 1  $\Omega$ .

Operational (Betriebs) transfer function in the forward direction  $H_{B21}$  or the forward Operational (Betriebs) scattering parameter  $S_{21}$  of a two-port (see Figure 66) is defined as

$$S_{21} = \left. \frac{V_{r2}}{V_{i1}} \right|_{V_{i2}=0} = \frac{2U_2}{E_1} \sqrt{\frac{Z_A}{Z_B}} = H_{B21} \tag{82}$$

where  $V_{i1}$  and  $V_{r1}$  are the square roots of incident (unreflected) and reflected complex power waves at port 1, and  $V_{i2}$  and  $V_{r2}$  are those at port 2. See Annex C of IEC TR 62152:2009.

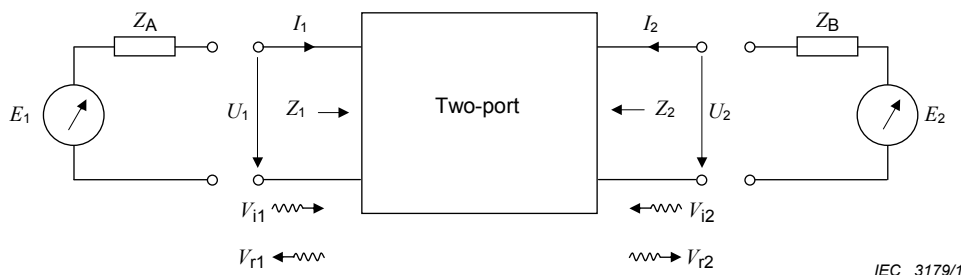


**Figure 66 – Two-port network**